GAS-PHASE DISSOCIATION PATTERNS OF ALIPHATIC HYDROXYCARBOXYLIC ACIDS

A Thesis

Presented to

The Faculty of Graduate Studies

of

The University of Guelph

by

LISA RABSON

In partial fulfilment of requirements

for the degree of

Master of Science

July, 2009

Your file Votre référence
ISBN: 978-0-494-56971-9
Our file Notre référence
ISBN: 978-0-494-56971-9

ABSTRACT

GAS-PHASE DISSOCIATION PATTERNS OF ALIPHATIC HYDROXYCARBOXYLIC ACIDS

Lisa Rabson
University of Guelph, 2009

Advisor:
Dr. Wojciech Gabryelski

This thesis is an investigation of the gas-phase dissociation patterns of aliphatic hydroxycarboxylic acids (HAs). Tandem mass spectrometry analysis, on a quadrupole ion trap mass spectrometer, along with hydrogen-deuterium exchange studies, were carried out on linear and branched (2- or 3-) HAs to determine their collision induced dissociation (CID) patterns. The complexity of the CID behaviour was greater when the hydroxyl group was positioned on carbon-2, rather than carbon-3. The 3-HAs examined generated one fragment ion (*m/z* 59) and higher order fragmentation (MS^n) on this ion could not be achieved.

2-HA CID typically resulted in a prominent loss of H_2CO_2 (elemental composition), and minor losses of H_2O and H_2. However, methyl branching along the aliphatic chain can directly inhibit these characteristic CID pathways. MS^n analysis of these product ions (and their fragments) show fragmentation patterns that can be used to distinguish between isomers, identify methyl branching and indicate the carbon-chain length of the corresponding 2-HA parent ion.

Acknowledgments

I would like to thank my supervisor, Dr. Wojciech Gabryelski, for giving me the opportunity to challenge myself and grow as a scientist. I will always be grateful for the continual support and encouragement you gave me. Appreciated help must also be noted from Dr. Nigel Bunce. I am truly grateful for all the advice and guidance you gave to me, stretching far beyond this research project.

I owe many thanks to Natalia Kulikova, Michael Baker and Sandeep Sagoo. Being part of a research group with all of you truly enhanced my research experience. Thank you for lending an ear, offering new perspectives, being optimistic and of course your friendship.

To my family and friends, thank you. Thank you for all the humour and much needed sarcasm that had an efficient way of turning any doubts into confidence. And to James Bisch, where do I start? All software tricks and conversion assistance; clarification of the vastly misused *font* versus *typeface*; always finding a way to make me laugh or believing in me despite the challenges I faced. Regardless, you are my #1 and #2, for that I thank you.

Finally, I would like to thank GWC^2 for the opportunity to conduct this research and NSERC for funding it.

Table of Contents

List of Figures

List of Schemes

List of Abbreviations

ac – Alternating current

CID – Collision induced dissociation

CR – Negative charge redistribution

DBP – Disinfection byproducts

DC – Direct current

EI – Electron ionization

ESI – Electrospray ionization

GC/MS – Gas chromatography mass spectrometry

HA – Hydroxycarboxylic acid

HA^- - Hydroxycarboxylate

HAs – Hydroxycarboxylic acids

HAs^- - Hydroxycarboxylates

HDX – Hydrogen-deuterium exchange

LC/MS – Liquid chromatography mass spectrometry

MS^2 – Tandem mass spectrometry

MS^n – Tandem mass spectrometry to the n^{th} stage

m/z – Mass to charge ratio

NA – Nucleophilic attack

NCE – Normalized collision energy

PT – Proton transfer

Q1 – The first quadrupole cell in a *QqQ*

Q3 – The third quadrupole cell in a *QqQ*

q – The second quadrupole cell in a *QqQ*, also referred to as the collision cell

QqQ – Triple quadrupole mass spectrometer

QIT MS – Quadrupole ion trap mass spectrometry

rf. – Radio frequency

RI – Relative intensity

CHAPTER 1: INTRODUCTION

1.1 Hydroxycarboxylic acids

1.1.1 General structure of hydroxycarboxylic acids

Hydroxycarboxylic acids (HAs) are a class of organic acids that contain both a carboxylic group and a hydroxyl group. The HAs examined within this study were 2-hydroxycarboxylic acids and 3-hydroxycarboxylic acids. Therefore, the hydroxyl group is on either carbon-2 or carbon-3, respectively (refer to figure 1.1).

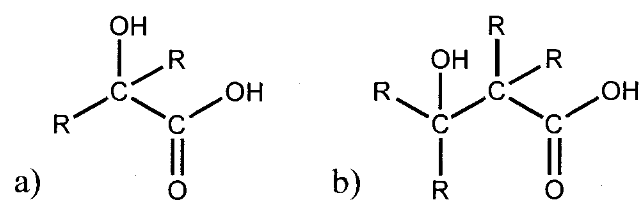

Figure 1.1: The general structure of **a**) 2-hydroxycarboxylic acids and **b**) 3-hydroxycarboxylic acids. R= alkyl group or hydrogen.

1.1.2 Industrial uses and natural occurrences of hydroxycarboxylic acids

2-Hydroxypropanoic acid (commonly referred to as lactic acid) is the most widely occurring HA in the natural environment and the industrial world. [1] It is naturally found in foods and as microbial fermentation byproducts (e.g. yogurt and sauerkraut). Previously, it had been widely used in leather tanning but its current applications have shifted towards the pharmaceutical industry (e.g. time-released drugs) and polymer synthesis. Currently, the worldwide yearly production of lactic acid is 120 000 tons. [1]

The smallest 2-HA, 2-hydroxyacetic acid (commonly referred to as glycolic acid), is considered a lucrative compound in the aesthetic industry. In the past decade, it has been widely used in chemical facial peels, designed to reduce the appearance of wrinkles and fine lines.[2] Aside from aesthetics, glycolic acid also has medical benefits in the area of skin tumor inhibition, for tumors developed from UVB exposures.[3,4]

HAs can also be found in distilled alcohol spirits,[5,6] such as cognac and whisky, as they are formed through the fermentation and distillation processes. Profiling these byproducts is beneficial as it can differentiate between the types, brands and maturation of the spirits based on mono, di, hydroxy and phenolic acid compositions.[5] Other uses of HAs, particulary 2-hydroxycarboxylic acids, are in the formation of silver complexes.[7-9] These silver complexes have been shown to exhibit antibacterial properties[10] and are now used in drug development for tuberculosis.[9,10]

HAs can also be found in biological systems. For example, 3-hydroxybutanoate (deprotonated 3-hydroxybutanoic acid) is classified as one of the three ketone bodies (the other two being acetoacetate and acetone).[11] Ketone bodies are produced through a biochemical pathway called ketogenesis. Ketogenesis is a catabolic pathway that breaks down acetyl-CoA into ketone bodies, when acetyl-CoA accumulates in liver cells.[11] HAs can also be found in the form of fatty acids. Hydroxy fatty acids (such as 2-hydroxy fatty acids) can have a number of functions within biological systems. Their roles can include, but not limited to, brain mylination[12] and mediation of inflammatory responses.[13]

1.1.3 Hydroxycarboxylic acids and the environment

Recently, a study on chlorinated drinking water contaminants discovered the presence of a number of HAs.[14] The most abundant compound in the water sample, 2-hydroxyacetic acid, was observed at high parts per million concentrations. It has been suggested that HAs are disinfection byproducts (DBP),[14] but no experimental evidence was provided to establish a source of these abundant contaminants. The decomposition of humic substances in natural water or during disinfection leads to the formation of polysaccharides and monosaccharides (such as glucose). In tap, natural and waste-water, two to ten percent of the organic carbon is present as sugars. [15] Ozonation disinfection, for example, degrades polysaccharides to monosaccharides, and monosaccharides to ozonation byproducts through advanced oxidations processes involving hydroxyl radicals. The major ozonation byproduct of glucose is gluconic acid, but glycolic acid (2-hydroxyacetic acid) is also generated, in a 20:3 ratio (glucose to glycolic acid). [15] Similar processes may be feasible when drinking water is subjected to other disinfection processes, such as chlorination.

1.1.4 Typical analysis of hydroxycarboxylic acids

GC/MS provides high-resolution separation and mass detection of compounds in a complex mixture. This technique is also excellent at identifying a variety of compounds as there are spectral libraries containing a vast number of compounds. [16] GC/MS methods for the analysis of HAs require liquid-liquid extraction from the aqueous mixture to an organic solvent (such as dichloromethane), solvent evaporation, and derivatization of the nonvolatile and thermally unstable acids in order to achieve efficient separation and mass detection of the modified HAs. [17] These analytical steps are time-consuming and labor-intensive. More importantly, there are additional problems faced when using these analytical steps.

Derivatization of HAs prevents hydrogen bonding by the polar functional groups therefore increasing their volatility. [17] Unfortunately, it also creates qualitative and quantitative uncertainty during their analysis if, i) derivatization is incomplete [18] or, ii) the number of derivatization sites is unknown. [17] Derivatization of HAs typically involves additional reactions that generate derivatization side-products. This was well documented in a study implementing methyl or ethyl chloroformate to form O-alkoxycarbonylalkyl esters (R'OCOO-CHR-COOR') of HAs. [19] The main derivatization product was always accompanied by a number of side-reaction products. Figure 1.2 shows the structure and yield of the expected derivatization product of 2-hydroxypropanoic acid (Figure. 1.2**a**) and the main side-reaction products: a dimer inter-ester derivative (Figure 1.2**b**) and a trimer inter-ester derivative (Figure 1.2**c**). The authors concluded that complete elimination of side-products with these two reagents did not appear to be possible. [19]

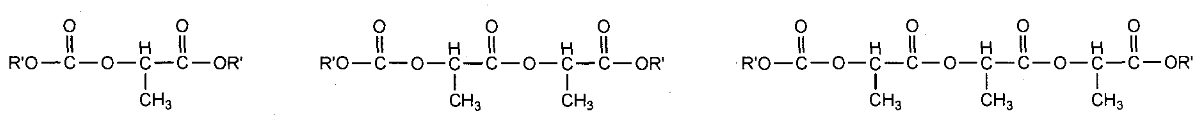

(a) 65% (b) 33% (c) 2%

Figure 1.2: Structures and yield of the derivatization products of lactic acid when derivatized with methyl or ethyl chloroformate. Figure **a)** is the major derivative containing one 2-hydroxypropanoic acid molecule, **b)** the major side-reaction products (inter-ester derivative) containing two 2-hydroxypropanoic acid molecules and **c)** the minor side-reaction products (inter-ester derivative) containing three 2-hydroxypropanoic acid molecules. [19]

A relatively successful example of the derivatization of HAs (2-hydroxypropanoic acid and 3-hydroxybutanoic acid) is esterification with phenyldiazomethane (to form benzyl ester derivatives), or with N,N'-dicyclohexyl-O-benzylisourea (to form benzyl ester O-benzyl ether derivatives). [20] These methods were almost quantitative without the formation of byproducts, provided the reactions occurred at zero degrees Celsius. Unfortunately, poor separation and tailing peaks were observed in gas chromatogram for these derivatives. [20]

1.2 Purpose of the study

The work presented in this study investigated the gas-phase dissociation patterns of commercially available HAs. The purpose of this study was to establish the general collision induced dissociation patterns of non-halogenated 2- or 3-hydroxycarboxylic acids. The patterns established for these organic acids, which contain biologically relevant functional groups, generated fragmentation profiles that may be used in the future for their identification in complex mixtures, such as drinking water or distilled spirits. By taking a fragmentation profile approach over the traditional GC/MS spectral library, identification and/or structural information can be obtained for these organic acids without facing the analytical problems described above. In addition, tandem mass spectrometry analysis on these organic acids will reveal fragmentation patterns capable of distinguishing between isomers.

1.3 Ionization methods used for MS analysis

Successful ionization of HAs is essential for their analysis using mass spectrometry techniques. The following are two examples of ionization techniques. The first technique described is electron ionization and it is commonly used for GC/MS analysis. The later example, electrospray ionization, is the ionization technique used in this current investigation of HA fragmentation patterns.

1.3.1 Electron Ionization (EI)

Electron ionization (EI) is most often used for producing molecular ions from thermally stable, volatile, nonpolar analytes with molecular weights ranging up to 1000 u.

Molecular ions are generated when electrons (e^-) are accelerated (70 electron volts (eV)) at the neutral analyte (M). [16] Collisions between the neutral and an electron transfers the energy to the neutral compound causing one electron to be ejected from the neutral forming a radical cation species ($M^{\bullet+}$) (refer to figure 1.3 for the ionization reaction). Most molecules have ionization energies ranging from 7-15 eV and therefore, the excess energy leads to several consecutive bond cleavages of the $M^{\bullet+}$ ion. [16] EI generates highly reproducible mass spectra and as a result, EI spectral libraries/databases are available and used as a tool for chemical identification of detected species. [17] In the case of HA derivatives, any excess energy that is deposited to a molecular ion would lead to its spontaneous dissociation, resulting in minimal or no detection of the molecular ion. [19] Although the EI dissociation products could provide spectral fingerprints, the limitations of GC/MS analysis indicate that this technique is not a method of choice for the comprehensive characterization of these highly polar compounds.

$$M + e^-_{(70\ eV)} \longrightarrow M^{\bullet+} + 2e^-$$

Figure 1.3: The typical electron ionization reaction of a neutral compound. M = neutral analyte, $M^{\bullet+}$ = radical cation of the neutral analyte and e^- = electron. [16]

1.3.2 Electrospray ionization (ESI)

Electrospray ionization (ESI) is the ideal ionization method for tandem mass spectrometry analysis of HAs. ESI is capable of generating protonated ($[M+H]^+$) or deprotonated parent ions ($[M-H]^-$) from a wide range of analytes that are nonvolatile, [21] thermally unstable and contain polar groups (such as carboxyl groups) with molecular weights ranging up to 100,000 Da. [22, 23] Unlike electron ionization (EI), ESI is considered a "*soft ionization technique*" as gas-phase ions are successfully formed without causing extensive fragmentation of the parent ion. [24] Therefore, this particular ionization technique is appropriate for generating deprotonated HAs for tandem mass spectrometry analysis.

The formation of ions in ESI occurs when the analyte (in a volatile buffer solution) is pumped (μL/min) to the tip of a metal capillary where a high electrical field disperses the liquid sample into small charged droplets. [25] Nitrogen assisted desolvation facilitates the evaporation of the solvent from the emerging droplets. As the solvent evaporates, the charge density increases on the surface of the droplets, ultimately leading to the formation of gas phase ions through one of two previously proposed mechanisms.[26] In the first, the increased charge density causes the droplets to repeatedly divide into smaller charged droplets until gas phase ions are liberated (*Coulomb fission*). [27]

Alternatively, the increased charge density on the surface of the droplet causes the coulomb repulsions to increase until they overcome the surface tension of the droplet. This would result in the release of gas phase ions from the droplet (*Ion evaporation*). [27] Whether gas phase ions are generated through *Ion evaporation* or *Coulomb fission* is still debated. Regardless, the gas phase ions that are generated enter the mass analyzer of the mass spectrometer. [17]

1.4 Mass analyzers

There is a variety of mass analyzers available on the market, each with its own advantageous properties and performance characteristics. Essentially, the mass analyzer is the part of the mass spectrometer that separates ions, typically by electric forces. [28] Quadrupole mass analyzers will first be discussed because they have been used in a limited number of studies looking at HA fragmentation. In the latter part of section *1.4*, the structure and function of the quadrupole ion trap mass spectrometer (QIT MS) will be summarized. Because the QIT MS was used in this fragmentation study, its performance capabilities will be addressed and compared to those of quadrupole mass analyzers.

1.4.1 Quadrupole mass analyzers

Quadrupole mass analyzers are the typical mass analyzers used in GC/MS and LC/MS instrumentation. They consist of four hyperbolic shaped electrodes that extend in the *z*-direction (refer to figure 1.4).[29, 16] Electrodes opposite one another are considered pairs and these pairs create an electric field by the application of *rf (radio frequency)* and DC (direct current) potentials.[30] When ions (generated in the ionization source) enter the electric field of the quadrupole, they begin to oscillate in the *x*, *y* and *z* directions. The overall trajectory of the ion's oscillation is directly related to its mass to charge ratio (*m/z*) and the trajectory is considered to be either *stable* or *unstable*.[16]

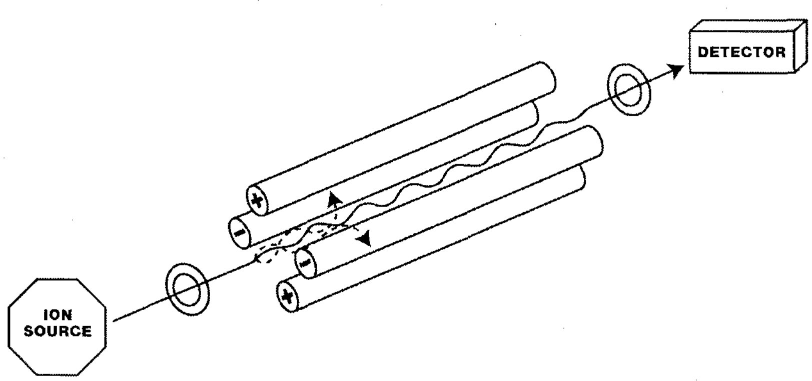

Figure 1.4: Structure of the quadrupole mass analyzer. As ions enter the quadrupole they oscillate in three dimensions. The trajectory of the oscillations may be unstable and the ion is lost when it collides with an electrode (dashed lines). Ions oscillating in a stable trajectory (solid line) will transmit through the quadrupole and reach the detector. (Modified from [28]).

Unstable trajectories will result in an overall drift away from the center of the quadrupole and towards the electrodes (see figure 1.4). Eventually the ion will collide with an electrode and thus not reach the detector. [16, 30] Alternatively, stable trajectories will allow the ion to travel along the *z*-direction, without an overall drift in the *x* and *y*-directions, and reach the detector (see figure 1.4). Adjusting the DC potential applied to the quadrupole electrodes will only allow ions of a single *m/z* ratio to oscillate at a stable trajectory, essentially having the quadrupole act as a mass filter. [16] Scanning the DC potential (ramping the DC and *rf* magnitude at a constant ratio) allows the quadrupole to scan the ions it contains in order of increasing *m/z* values and thus generate a mass spectrum. [16] Alternatively, by setting the DC potential to zero the quadrupole will be operating in an *rf* only mode. The application of an *rf* only mode allows for a wide range of *m/z* values to have stable trajectories and transverse the quadrupole. This type of function allows the mass analyzer to act as an ion guide or collision cell [16] (advantages of the *rf* only mode will be discussed below).

1.4.2 Tandem MS with quadrupole mass analyzers

Controlled tandem mass spectrometry can't be achieved with a single quadrupole mass analyzer. [28] Figure 1.5**a** illustrates single stage mass spectrometry where the ions formed from the ion source (through EI for example) enter the quadrupole. The quadrupole, operating in the DC scanning mode, allows the parent ion and its fragments to transverse the mass analyzer according to increasing *m/z* values and be detected, generating a mass spectrum. [28]

Only by combining mass analyzers can controlled tandem mass spectrometry can be achieved. [16] A common example is the *triple quadrupole* (*QqQ*) mass spectrometer. This instrument combines three quadrupole mass analyzers. This first quadrupole (*Q1*) acts a mass filter where a specific *m/z* ion can be isolated. [16] This isolated ion enters the second quadrupole (*q*) that is operating in the *rf* only mode. This allows *q* to act as a collision cell where the ions are fragmented through *collision induced dissociation* (CID). [29] In this cell, the selected ions will undergo collisions with an inert gas (such as helium) and some of the kinetic energy is transferred to internal energy, resulting in controlled ion fragmentation. [28] The remaining parent ions and their fragments then enter the third quadrupole (*Q3*) that is operating in the scanning mode. The parent ions and their fragments transverse *Q3* (according to increasing *m/z* values) to the detector and an MS^2 spectrum is generated [16, 29] (see figure 1.5**b**). This type of operation on a *QqQ* is called a *product ion scan.* [29] This type of tandem mass spectrometry is referred to as "*tandem in space*" because the analysis occurs in different mass analyzers. [28, 31]

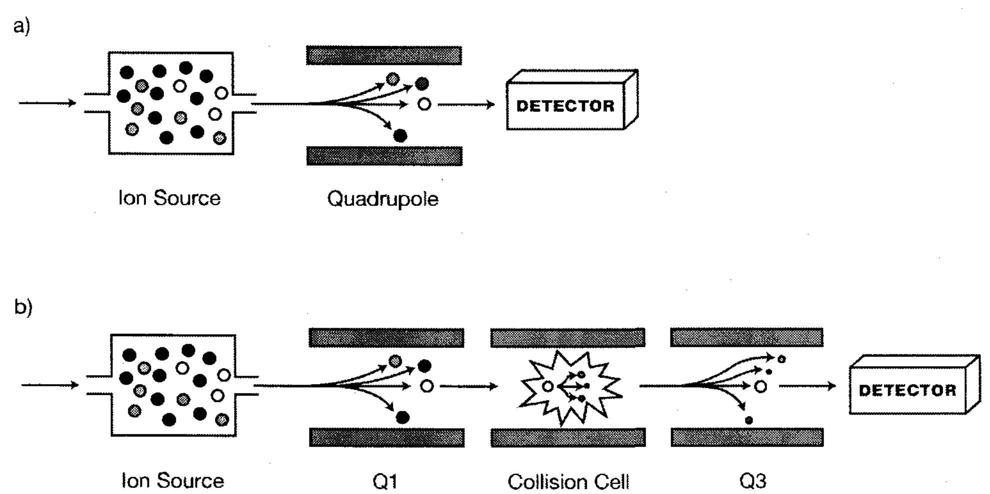

Figure 1.5: Comparison of **a**) single-stage mass spectrometry and **b**) tandem mass spectrometry with quadrupole mass analyzers. Panel **a)** depicts a quadrupole MS where individual ions can't be isolated and fragmented. Panel **b)** depicts a *QqQ* MS where *Q1* is operating as a mass filter to isolate a specific ion based on its *m/z*, the collision cell is operating in the *rf* only mode and *Q3* is operating in a full scan mode (DC and *rf* ramping) to detect the generated fragments. (Diagram modified from [28]).

The performance of the *QqQ*, in comparison to the *quadrupole ion trap MS* (QIT MS) (discussed below), is relatively similar. Both MS instruments offer unit mass resolution [16, 31] (distinguishes between ions with *m/z* 131 and 132 for example) and comparable mass accuracy. [31] However, within day analytical variations on *QqQ* instruments range from 10-15% whereas the variation in QIT instruments is 30%. [32] Another advantage of the *QqQ* over the QIT is its linear dynamic range: three orders of magnitude (in comparison to two orders for the QIT [33]), so it is therefore an ideal instrument for quantitative studies. [32-34] However, the main disadvantage of *QqQ* MS is its limited tandem mass spectrometry capabilities. *QqQ* are only capable of MS^2 analysis where QIT MS is capable of MS^n analysis (where $n \leq 9$). [16] For this reason, the QIT MS is the preferred MS instrument when distinguishing between isomeric compounds and establishing fragmentation patterns/profiles. [31-33, 35] Details regarding the operation of the QIT MS are presented below.

1.4.3 Quadrupole Ion Trap MS

The appropriate choice of mass analyzer is critical for obtaining the desired CID information. The quadrupole ion trap mass spectrometer (QIT MS) is capable of performing tandem mass spectrometry experiments through controlled dissociation and detection of fragment ions. The QIT MS also offers higher order tandem mass spectrometry (MS^n) capabilities. [36] This means that each dissociation product from MS^2 analysis can be investigated further in sequential MS^3 experiments. The quadrupole ion trap typically allows for sequential MS^9 or MS^{10} analysis, provided the ion population in the trap remains high enough for ion detection. [17] With these capabilities, the quadrupole ion trap is the ideal mass analyzer for characterizing structures of dissociation products and establishing gas-phase CID patterns of larger HAs.

1.4.3.1 The Theory behind the QIT MS

The ion trap of the QIT MS consists of three electrodes, two end cap electrodes and one ring electrode (refer to figure 1.6).[37] The ions enter the trap through the inlet at the entrance end cap electrode in packets of ions, rather than a continuous beam of ions (as with the *QqQ*). The packet of ions is contained within the trap by the application of a radio frequency (*rf*) applied to the ring electrode, while both end cap electrodes are grounded. This is referred to as the *trapping potential*, which generates a 'potential well' where the contained ions oscillate (secular oscillations) in stable trajectories.[37] The oscillation stability is directly related to the ions' *m/z*, frequency of oscillation and amplitude of the *rf* potential. Unlike the detection of ions in a *QqQ*, detection of the trapped ions in a QIT MS is based on creating unstable oscillating trajectories. Therefore, their detection is achieved by increasing the *rf* amplitude (referred to as *rf ramping*) causing the ions in the trap to have unstable oscillations. The instability causes the ions to be ejected from the potential well, exiting the trap through the exit end cap electrode to the electron multiplier (detector). The ejection of the ions occurs in ascending order, with respect to their *m/z*, thus generating an MS scan.[37]

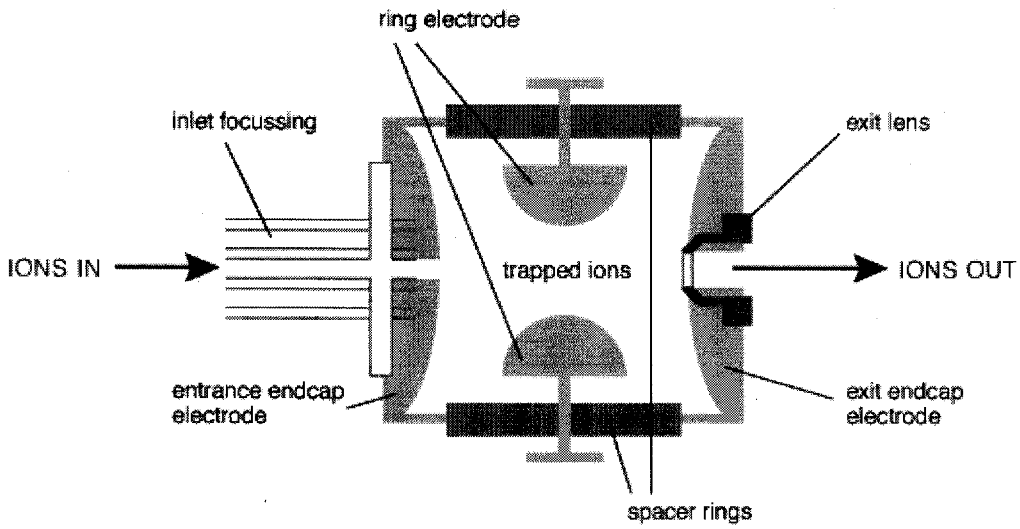

Figure 1.6: Representation of a QIT MS. This illustration shows the entrance end cap electrode, ring electrode, trapped ions (in the potential well) and exit end cap electrode (positioned in front of the detector). Diagram modified from [38].

1.4.3.2 Isolation and CID with a QIT MS

Isolation of a particular ion in a QIT MS can be achieved once the ions enter the potential well in the ion trap. An *rf* potential is applied to the ring electrode to generate this potential well and trap the ions. [37] Isolation of a desired *m/z* ion requires the application of a supplementary voltage (referred to as *broadband waveforms*) to the end caps. [39] The broadband waveforms contain a wide frequency band with a 1 kHz frequency notch that corresponds to the oscillation frequency of the desired *m/z* ion to be isolated. The result of this notched waveform is the ejection of all ions with a mass to charge ratio different than that of the desired ion. [37]

Once the ion of interest is isolated in the trap, collision induced dissociation (CID) can be conducted to obtain MS^2 data. [37] During CID a small alternating current (*ac*) voltage, at a frequency corresponding to the frequency of the oscillating target ions, is applied to the end-cap electrode (referred to as *a normalized collision energy* (NCE)) to increase the kinetic energy of the oscillating target ions. By increasing their kinetic energy, their amplitude of oscillation and number of activating collisions with the buffer gas (helium) increases. Successive collisions cause the target ions' internal energy to increase, leading to their dissociation. [16, 37, 40] The fragment ions generated via CID are also confined within the trap and are detected once they are ejected from the trap, through *rf* ramping. Detection of the fragment ions is also in ascending *m/z* order to generate a MS^2 spectrum. [37] The process of isolation and CID can be repeated to generate MS^n spectra because ion isolation, collision activation and acquisition of fragment ion spectra are conducted within the same space (the trap). This is why the QIT MS is termed a "*tandem in time*" instrument. [16] The ability to carryout MS^n functions is advantageous when performing structural elucidation and fragmentation behaviour studies [40] and thus was used in this study.

1.5 Analytical approach

1.5.1 Instrumentation

Eleven of commercially available HAs were analyzed by tandem mass spectrometry on a Finnigan LCQ^{Deca} Ion Trap MS using negative mode ESI. Therefore the ions generated were deprotonated HAs (hydroxycarboxylates) and are denoted as $[M-H]^-$ ions.

1.5.2 Compounds studied

The reaction mechanisms of 2-hydroxyacetic acid have been established through the use of isotopically-labeled compounds (see section *1.6.2*). Such isotopically-labeled compounds are not available for larger HAs. Dissociation reactions of 2-hydroxyacetate can be applied only to some extent to larger homologues to gain insight into the gas-phase reactivity. Comprehensive tandem mass spectrometry investigations were conducted on a group of selected commercially available HAs (see figure 1.7). The tandem mass spectrometry examination of 2-hydroxypropanoic acid, as well as larger, linear 2-HAs, was conducted to determine general trends in gas-phase chemistry for this class of compounds. The linear 2-HAs analyzed range from three to eight carbons in length (see figure 1.7**a-d**).

Following the investigation of linear 2-HAs, branched 2-HAs were analyzed via tandem MS analysis in order to determine how branching along the aliphatic chain can affect the gas-phase chemistry of 2-HAs. The branched 2-HAs analyzed contain either a four or five-carbon chain with methyl or dimethyl branching at carbon-2, 3 or 4 (see figure 1.7**e-h**). In addition to the studies on linear and branched 2-HAs, selected 3-HAs have been analyzed to determine the effect of different hydroxyl group positioning. One linear, one methyl branched and one phenyl branched 3-HAs have been studied to determine their fragmentation behaviour (figure 1.7**i-k**).

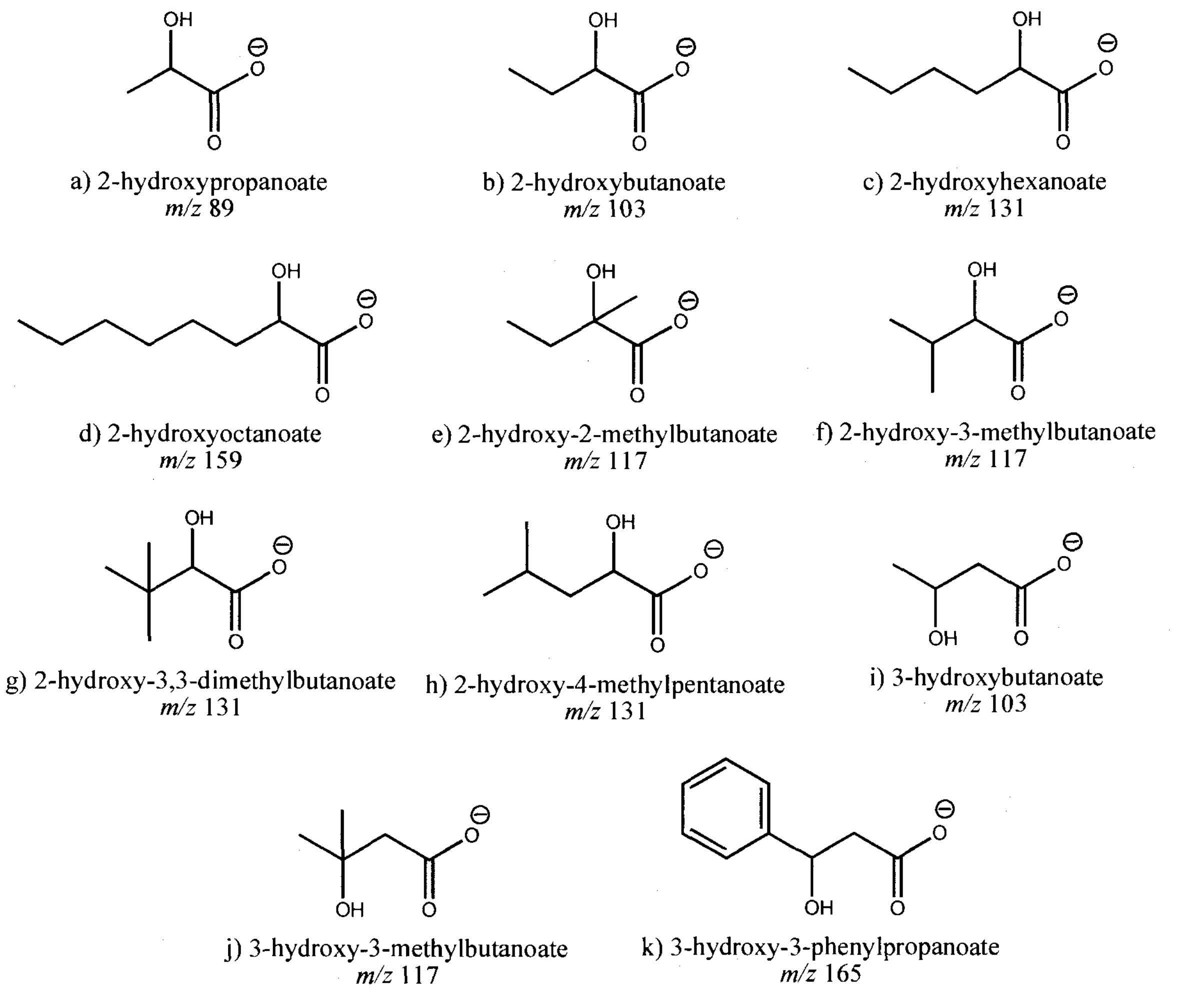

Figure 1.7: Structures of the hydroxycarboxylates examined through tandem MS methods.

1.5.3 Complementary hydrogen-deuterium exchange (HDX) studies

The combination of hydrogen-deuterium exchange (HDX) procedures and tandem mass spectrometry analysis is an excellent source of complementary information regarding the atoms involved in the neutral mass eliminations. This technique has been widely used [31] for a range of compounds including, but not limited to, biomolecules [41, 43] and inorganic compounds. [42] Solution HDX procedures (see section *2.4*) were carried out on some of the compounds presented in figure 1.7 (**a**, **b**, **c**, **e**, **g**, **i-k**), followed by tandem mass spectrometry to elucidate which hydrogen atoms were involved in the observed neutral eliminations. Additional information pertaining to the DHX studies is presented in *chapter 6.*

1.6 Collision induced dissociation of HAs

The studies regarding the fragmentation behaviour of hydroxycarboxylates (HA^-) have been limited. Prior to discussing the current literature, the general types of fragmentation for even electron negative ions will be summarized in brief.

1.6.1 Fragmentation of even electron negative ions

In general, there are four basic fragmentation types for even electron anions. [44] Ion dissociation can be, i) facilitated by an initial proton transfer, ii) homolytic cleavage to form stable radical anions, iii) formation of an anion complex (with a neutral for example) or iv) rearrangement reactions prior to a mass loss. These rearrangements may include skeletal rearrangements or redistribution of the negative charge in unsaturated compounds. [44] Fragmentation reactions have been studied on some organic compounds. One well documented example of characteristic fragmentation is the loss of CO_2 from carboxylates.[12,45,46] Unlike the carboxylates, HAs^- do not show the loss of CO_2. An overview on the gas-phase reactions of the smallest 2-HA^- (2-hydroxyacetate) will be described first.

1.6.2 MS^2 CID behaviour of 2-hydroxyacetate ($[M-H]^-$ m/z 75)

The gas phase chemistry of 2-hydroxyacetate was extensively studied after it was detected at high parts per million (ppm) concentrations in drinking water. [14] This particular study was carried out on a quadrupole ion trap (QIT) mass spectrometer to determine the sequential fragmentation behaviour through tandem MS. [47] In addition to the analysis of 2-hydroxyacetate, the study incorporated tandem MS analysis on commercially available, isotopically labeled analogues to gain insight and conformation on the proposed fragmentation pathways. The isotopically labeled analogues included ^{13}C at carbon-1 and ^{13}C at both carbon atoms. In the same study, another isotopically labeled analogue used had two deuterium atoms bonded to carbon-2. [47]

Through tandem MS analysis on 2-hydroxyacetate and its isotopically labeled analogues, it was determined that its major fragmentation pathways were initiated by a nucleophilic attack on the α-carbon by the negatively charged carboxyl oxygen. [47] As a result of the nucleophilic attack, all following dissociation reactions occurred through an alpha-lactone (three-membered ring) intermediate (refer to figure 1.8) leading to the loss of H_2 (*m/z* 73 as the major fragment ion) (figure 1.8**a**), CO (intense peak at *m/z* 45) (figure 1.8**b**) and H_2CO (low intensity peak at *m/z* 43) (figure 1.8**c**). Other low intensity peaks observed in the MS^2 spectrum were correlated to the formation of a hydroxyl ion. However, the hydroxyl ions were not detected at a mass to charge ratio (*m/z*) of 17. Instead, they formed non-covalent adducts with a water or methanol molecule that are introduced (and present) to the ion trap, with either the helium buffer gas or electrospray solvents. [48-50] The complexes of hydroxyl ions were detected at *m/z* 35 (with water) and *m/z* 49 (with methanol) (refer to figure 1.8**d**). [47]

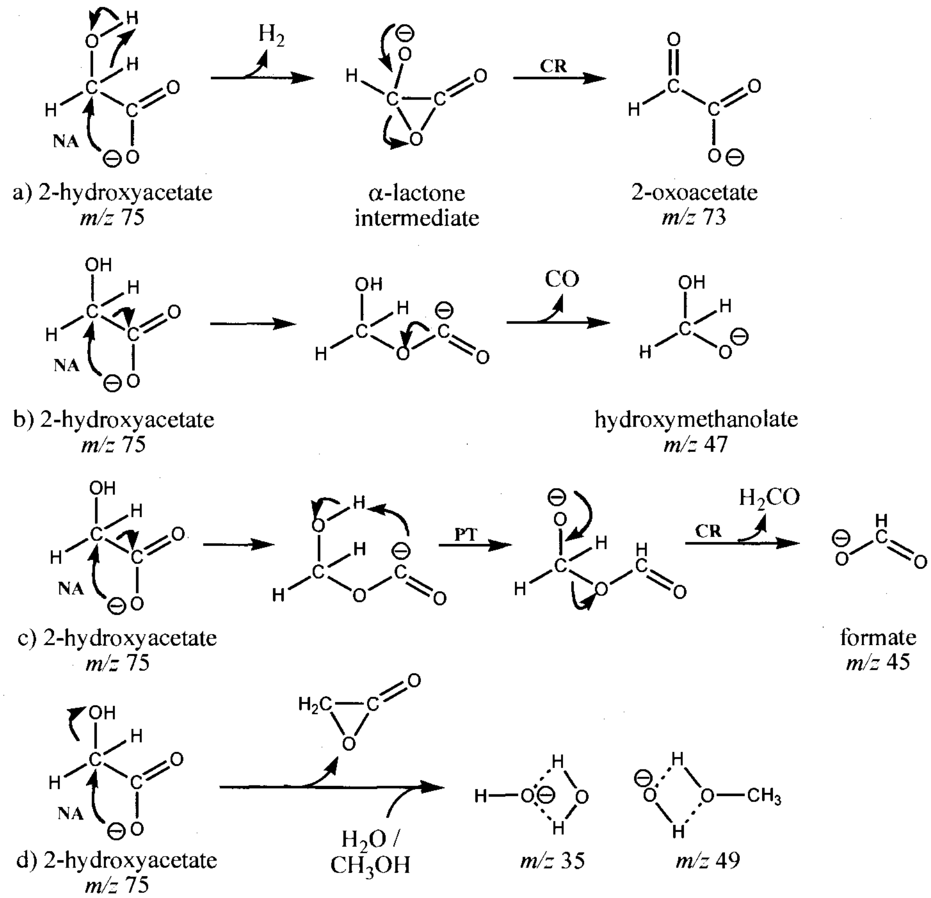

Figure 1.8: The MS^2 CID pathways of 2-hydroxyacetate (*m/z* 75). A nucleophilic attack (NA) on the α-carbon forms α-lactone like intermediate that leads to the loss of **a)** H_2 (*m/z* 73), **b)** CO (*m/z* 47), **c)** H_2CO (*m/z* 45) as well as **d)** the formation of hydroxyl ion complexes with water (*m/z* 35) and methanol (*m/z* 49). Proton transfer (PT) and negative charge redistributions (CR) involved in the formation of these fragments are indicated in the corresponding schemes. [47]

1.6.3 MS^3 CID behaviour of 2-hydroxyacetate

Higher order tandem MS^3 analysis was carried out on the fragment ions generated from 2-hydroxyacetate (*m/z* 75) and its isotopically labeled analogues. Further dissociation of the *m/z* 73 ions ($[M\text{-}H\text{-}H_2]^-$) revealed the loss of CO (*m/z* 45) and the formation of the hydroxyl:water complex (*m/z* 35) in MS^3 spectrum. [47] The loss of CO was initiated by a nucleophilic attack of the negatively charged carboxylic oxygen on the alpha-carbon and proceeded through an α-lactone-like transition state (Figure 1.9**a**). The formation of the hydroxyl ion and its solvent complex was initiated by the proton transfer from the beta-carbon to the negatively charged carboxylic oxygen with subsequent elimination of C_2O_2 (figure 1.9**b**). [47]

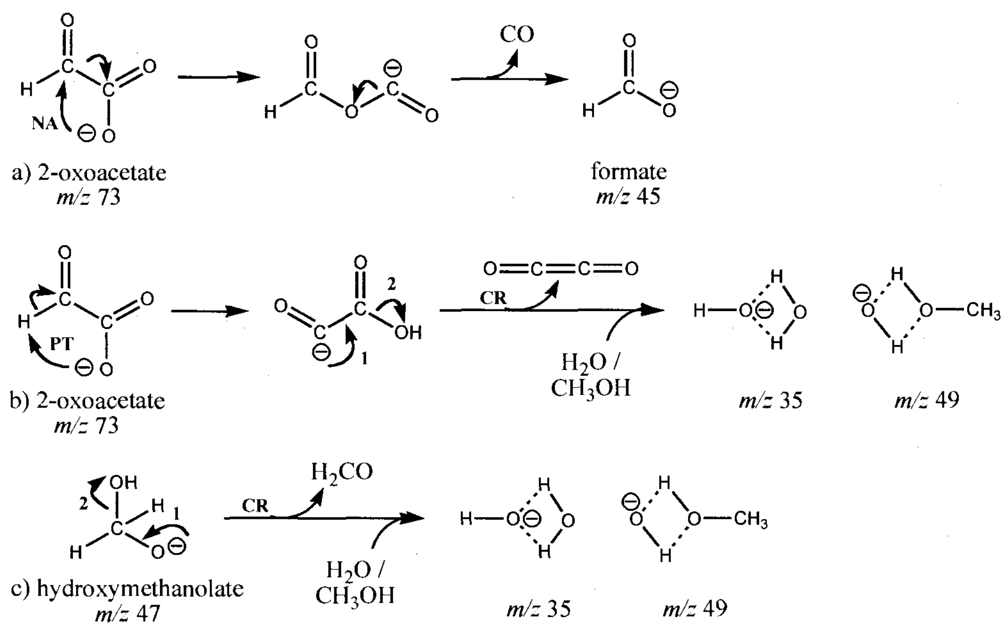

Figure 1.9: The MS^3 CID pathways for 2-hydroxyacetate fragment ions. The $[M\text{-}H\text{-}H_2]^-$ fragment ion (m/z 73) dissociates through **a)** a nucleophilic attack (NA) (leading to the loss of CO) or **b)** initiated through a proton transfer (PT) (leading to the formation of hydroxyl ion complexes). The MS^3 CID pathway of the $[M\text{-}H\text{-}CO]^-$ fragment (m/z 47) is initiated via **c)** redistribution of the negative charge (CR) to result in the formation of hydroxyl ion complexes with a solvent molecule. [47]

The other fragment $[M\text{-}H\text{-}CO]^-$ ions (*m/z* 47), generated from 2-hydroxyacetate (*m/z* 75), dissociated in MS^3 analysis to form only hydroxyl ion complexes with water (*m/z* 35) and methanol (*m/z* 49). The complexes were formed through a simple redistribution of the negative charge, from the negatively charged oxygen to the oxygen of the leaving group (refer to figure 1.9**c**). [47]

The tandem mass spectrometry study of the smallest $2\text{-}HA^-$ (2-hydroxyacetate) had identified three different ways to initiate its CID pathways. The predominant initiation is via nucleophilic attack, whereas redistribution of the negative charge and a proton transfer drive some higher order fragmentation pathways. Similar reactions can be expected during dissociation of larger 2-HAs$^-$.

1.6.4 Previous studies on the loss of 46 mass units from 2-hydroxycarboxylates

There has been a limited number of studies looking at the fragmentation of 2-HAs$^-$. In these studies, the loss of 46 mass units was the only fragmentation pathway examined. [12, 45] This particular pathway was studied using a *QqQ* MS and it was determined that the loss of 46 was the elimination of H_2CO_2. Through the use of deuterated analogues, the hydrogen atoms involved in this elimination were identified as the hydroxyl hydrogen and the hydrogen on the β-carbon. A pathway was proposed (presented in figure 1.10) that is initiated by a proton transfer off the hydroxyl group onto the negatively charged hydrogen.[12,45] Redistribution of the charge releases a formic acid carboanion (*m/z* 45) that forms a neutral ion complex with the remaining aldehyde (see figure 1.10). The carboanion is thought to abstract a proton from the β-carbon. Redistribution of the charge leads to the formation of an enolate as the $[M\text{-}H\text{-}H_2CO_2]^-$ product ion. [12, 45]

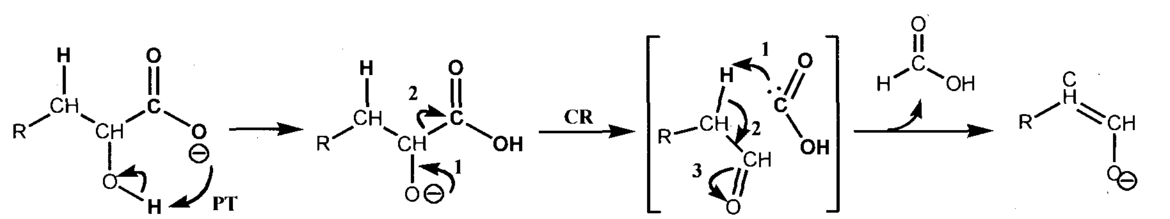

Figure 1.10: The proposed CID pathway for the loss of H_2CO_2 from 2-hydroxycarboxylates via neutral ion complex. The pathway is initiated with a proton transfer off the hydroxyl group. The atoms in bold font indicate those involved in the neutral mass loss. R= alkyl group, PT = proton transfer and CR = negative charge redistribution. [12, 45]

The pathway presented above was based on the presence of a moderately intense *m/z* 45 peak in the MS^2 spectrum. [12, 45] Again, the data was obtained using a *QqQ* MS. There have been examples in literature where compounds subjected to MS^2 analysis on different mass analyzer will generate spectral variation regarding the relative peak intensities and even observed peaks. [51] It is important to note that the time ions experience in the collision cell of a *QqQ* is 10^{-5} seconds, which is significantly shorter than the time ions are activated in a QIT MS (10^{-2} seconds). [31] As one will see throughout chapter *3* the MS^2 spectra generated on the QIT MS do not show a peak pertaining to the *m/z* 45 formic acid carboanion. The spectral data obtained on the QIT MS also show the presence of a $[M\text{-}H\text{-}18]^-$ fragment, which was absent in the spectra generated on the *QqQ*. [12, 45] These variations will be considered in chapter *7* when a few selected fragmentation pathways will be proposed.

CHAPTER 2: METHODOLOGY

2.1 HAs chosen for mass and tandem mass spectrometry analysis

The linear 2-HAs examined were 2-hydroxypropanoic acid, 2-hydroxybutanoic acid and 2-hydroxyhexanoic acid and were purchased from Aldrich (Oakville, ON), whereas 2-hydroxyoctanoic acid was purchased from Alfa Aesar (Ward Hill, MA, USA). The branched 2-HAs examined were 2-hydroxy-4-methylpentanoic acid, 2-hydroxy-3,3-dimethylbutanoic acid, 2-hydroxy-3-methylbutanoic acid, and 2-hydroxy-2-methylbutanoic acid and were obtained from Aldrich (Oakville, ON). 3-hydroxybutanoic acid, 3-hydroxy-3-methylbutanoic acid and 3-hydroxy-3-phenylpropanoic acid, were also obtained from Alfa Aesar (Ward Hill, MA, USA) and used to investigate the CID behaviour of 3-HAs.

2.2 HA sample preparation

Stock solutions of HAs were individually prepared at a concentration of 10 mM in HPLC grade H_2O. Working solutions of the HAs were prepared at 10 μM by diluting the stock solutions in a 0.1 mM ammonium acetate buffer solution (90:10 v/v methanol/water). Water, methanol, and ammonium acetate were HPLC grade and were purchased from Fisher Scientific (Nepean, ON).

2.3 Mass spectrometry: Negative mode ESI-QIT-MS^n

The tandem mass spectrometry analysis of HAs was carried out on a Finnigan LCQ^{Deca} Ion Trap mass spectrometer. The working solutions (10 μM) were directly infused to the electrospray ionization source operating in negative ion mode (-4000 V), at a flow rate of 5 μL/min via syringe pump. The CID MS^n spectra were obtained by isolating each target ion and activating the ion via CID (applying a normalized collision energy (NCE) voltage to the end-cap electrode). The NCE voltage varied from 19 V to 24 V and was optimized for each investigated HA. The NCE voltages used are given in the figure captions of reported spectra (throughout chapters *3* and *6*). The nitrogen gas (ESI desolvation gas) and the helium gas (ion trap buffer gas) were obtained from Linde (Guelph, ON).

2.4 Hydrogen-deuterium exchange (HDX) studies

Three of the linear 2-HAs (2-hydroxypropanoic acid, 2-hydroxybutanoic acid and 2-hydroxyhexanoic acid), two of the branched 2-HAs (2-hydroxy-2-methylbutanoic acid and 2-hydroxy-3,3-dimethylbutanoic acid) and all three 3-HA compounds were selected for HDX. All these compounds have been effectively D-labeled through hydrogen-deuterium exchange (HDX) in solution containing methanol/deuterated water; a presence of 0.1 mM ammonium acetate buffer was critical for effective labeling. A simple labeling procedure of HAs involved diluting 2 μL of 10 mM stock solution (prepared in HPLC grade H_2O) in 1 mL of an exchange-buffer solution (80:20 v/v methanol/D_2O containing 0.1 mM ammonium acetate). The H/D buffer solutions, with total concentration of HA at 20 μM, were left to exchange for ~20 hours at room temperature, prior to tandem MS analysis (refer to *section 2.3*). The D_2O used in the HDX studies was purchased from Cambridge Isotope Laboratories Inc.(Andover, MA, USA).

CHAPTER 3: MASS SPECTRA OF HYDROXYCARBOXYLATE ANIONS

This chapter displays the mass spectra of 2-HAs$^-$. The spectra were generated on a LCQ Ion Trap MS operating in negative ion mode. The first series of spectra (figure 3.1) is the MS^n analysis of 2-hydroxypropanoate. Panel **a** is the MS^2 spectrum and the MS^3 spectra is displayed in panels **b** through **d**. Following 2-hydroxypropanoate are the MS^n spectra of larger, linear, 2-HAs$^-$ (figures 3.2-3.4), again showing the MS^2 spectra in panel **a** and the MS^3 and MS^4 spectra in the subsequent panels. The MS^n spectra of branched 2-HAs$^-$ follow the linear compounds and are displayed in figures 3.5-3.8. The 3-HAs$^-$ could only generate MS^2 spectra and therefore the spectrum from 3-hydroxybutanoate (panel **a**), 3-hydroxy-3-methylbutanoate (panel **b**) and 3-hydroxy-3-phenylpropanoate (panel **c**) are all shown in figure 3.9. Within the individual spectra, ions denoted by square brackets indicate the anion that was selected and fragmented. The round brackets found in the spectrum indicate the difference in mass between the fragment ions and the ion selected for fragmentation. This spectral data was used to construct fragmentation trees for each HA^-, which are presented in the following chapter.

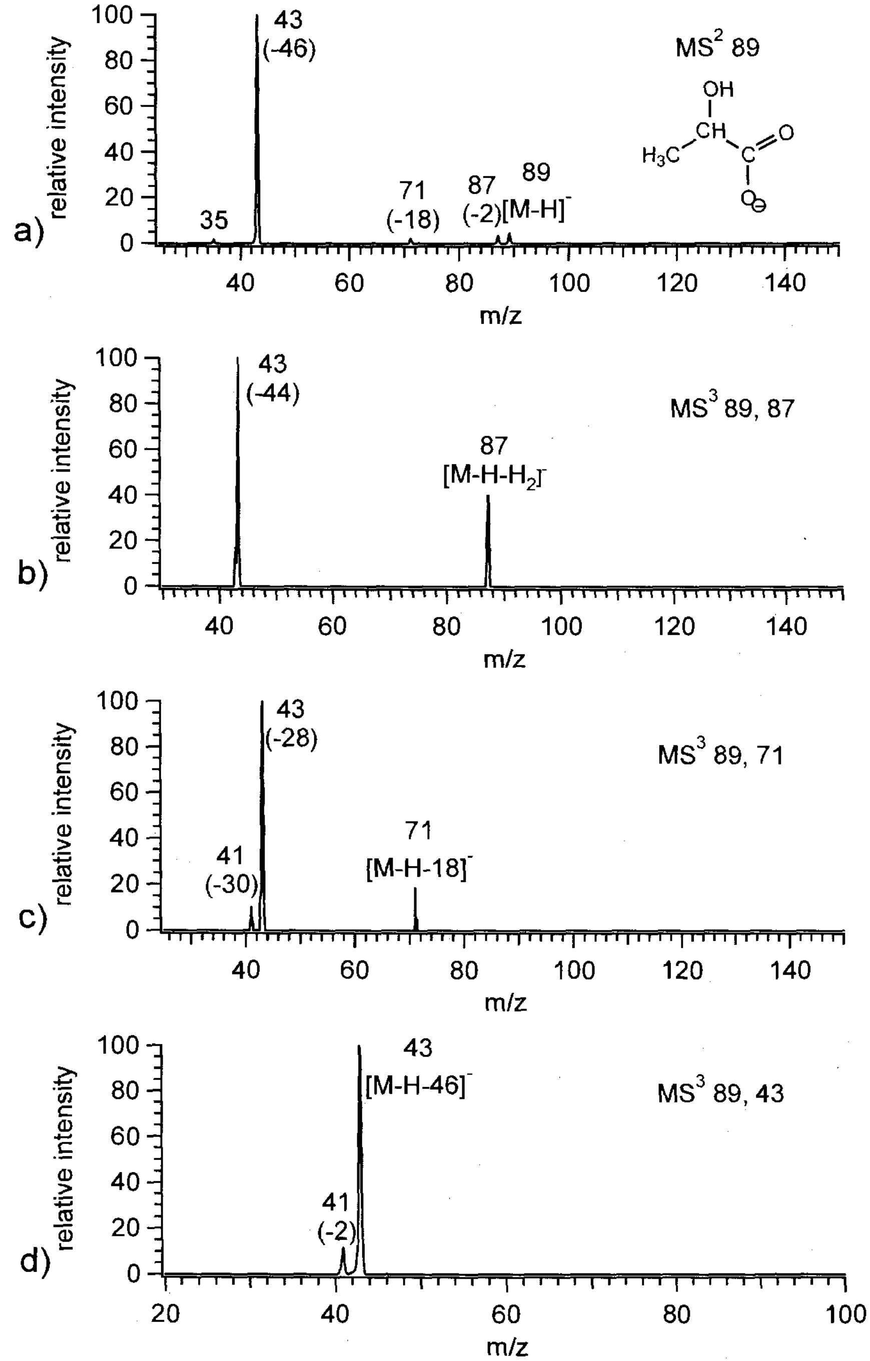

Figure 3.1: The mass spectra generated from MS^n analysis of 2-hydroxypropanoate (*m/z* 89). Panel **a** is the MS^2 analysis of the parent ion ($[M-H]^-$), **b** the MS^3 analysis of the $[M-H-H_2]^-$ ion (*m/z* 87), **c** the MS^3 analysis of the $[M-H-18]^-$ ion (*m/z* 71) and **d** the MS^3 analysis of the $[M-H-46]^-$ ion (*m/z* 43). The spectra were generated on a LCQ Ion Trap MS, operating in negative ion mode. NCE = 24 V.

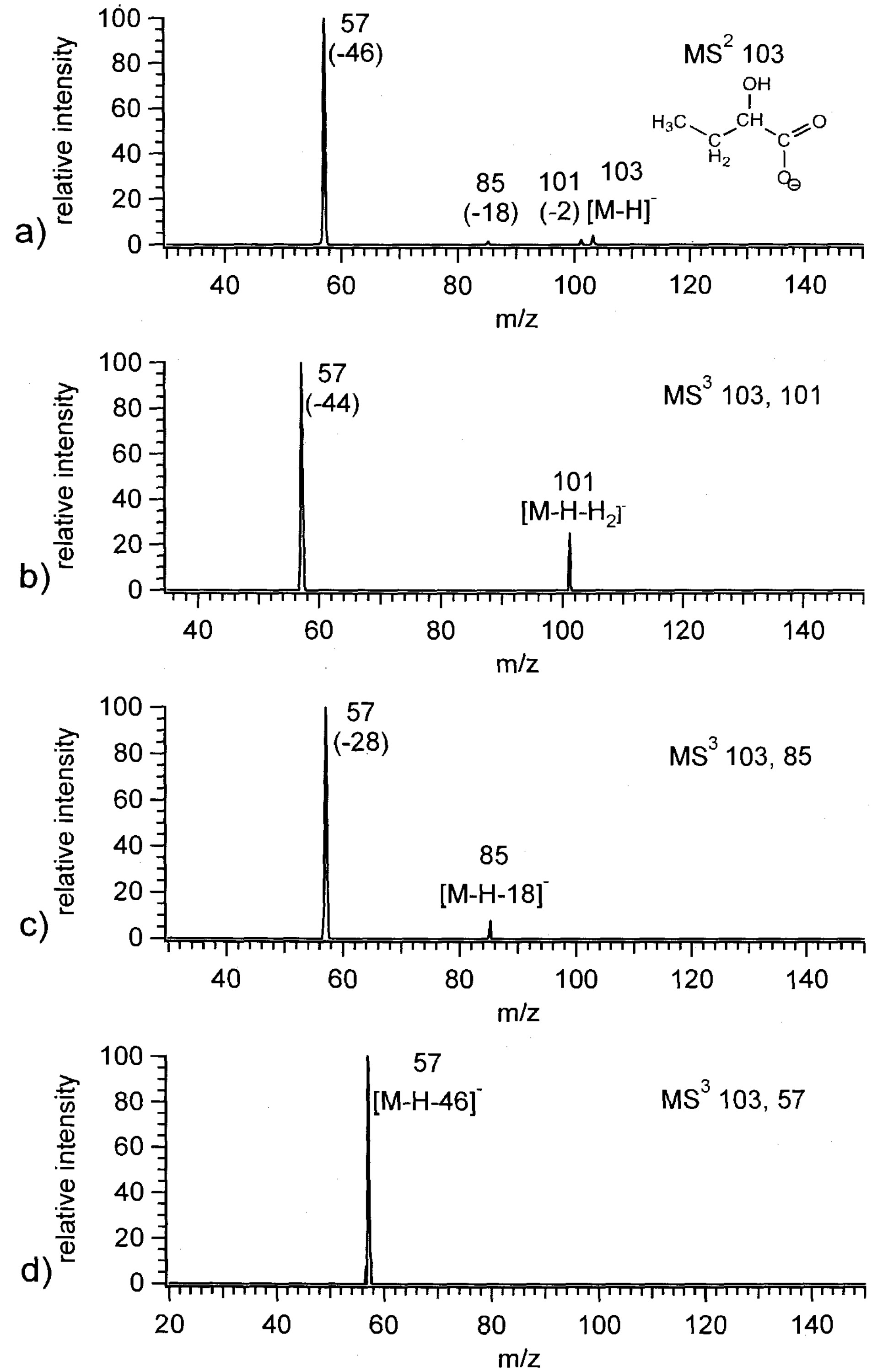

Figure 3.2: The mass spectra generated from MS^n analysis of 2-hydroxybutanoate (*m/z* 103). Panel **a** is the MS^2 analysis of the parent ion ([M-H]$^-$), **b** the MS^3 analysis of the [M-H-H_2]$^-$ ion (*m/z* 101), **c** the MS^3 analysis of the [M-H-18]$^-$ ion (*m/z* 85) and **d** the MS^3 analysis of the [M-H-46]$^-$ ion (*m/z* 57). The spectra were generated on a LCQ Ion Trap MS, operating in negative ion mode. NCE = 24 V.

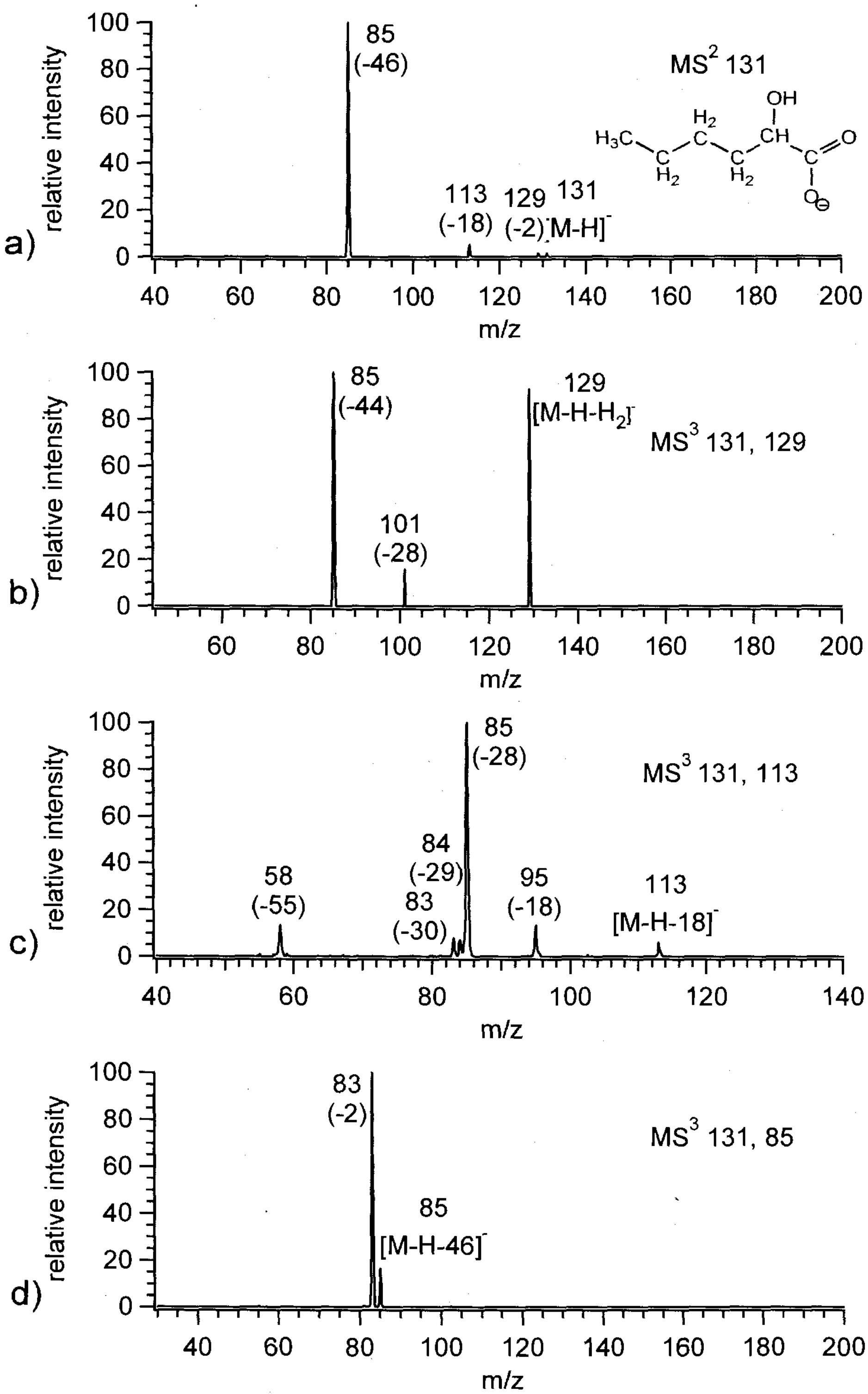
a)
MS² 131
85 (-46)
113 (-18)
129 (-2)
131 [M-H]⁻
b)
MS³ 131, 129
85 (-44)
101 (-28)
129 [M-H-H₂]⁻
c)
MS³ 131, 113
58 (-55)
83 (-30)
84 (-29)
85 (-28)
95 (-18)
113 [M-H-18]⁻
d)
MS³ 131, 85
83 (-2)
85 [M-H-46]⁻
relative intensity
m/z

e)

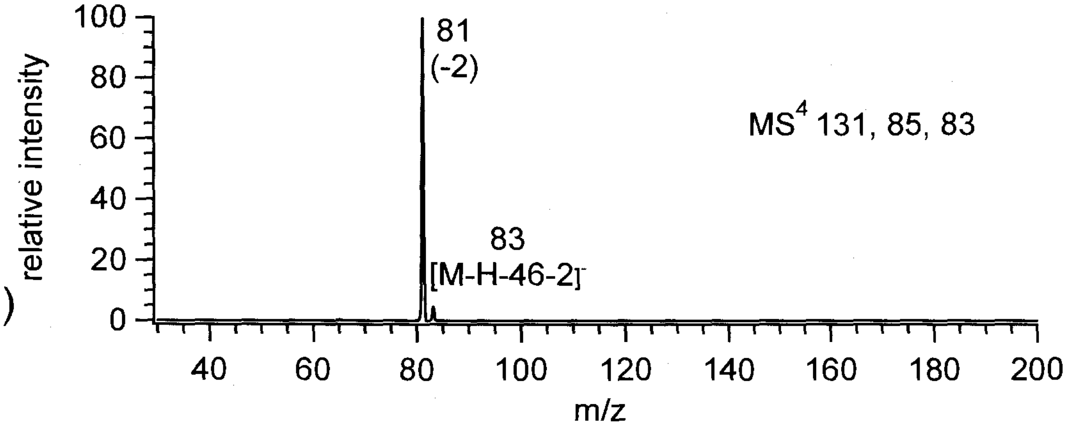

Figure 3.3: The mass spectra generated from MS^n analysis of 2-hydroxyhexanoate (*m/z* 131). Panel **a** is the MS^2 analysis of the parent ion ($[M-H]^-$), **b** the MS^3 analysis of the $[M-H-H_2]^-$ ion (*m/z* 129), **c** the MS^3 analysis of the $[M-H-18]^-$ ion (*m/z* 113), **d** the MS^3 analysis of the $[M-H-46]^-$ ion (*m/z* 85) and **e** the MS^4 analysis of the $[M-H-46-2]^-$ ion (*m/z* 83). The spectra were generated on a LCQ Ion Trap MS, operating in negative ion mode. NCE = 24 V.

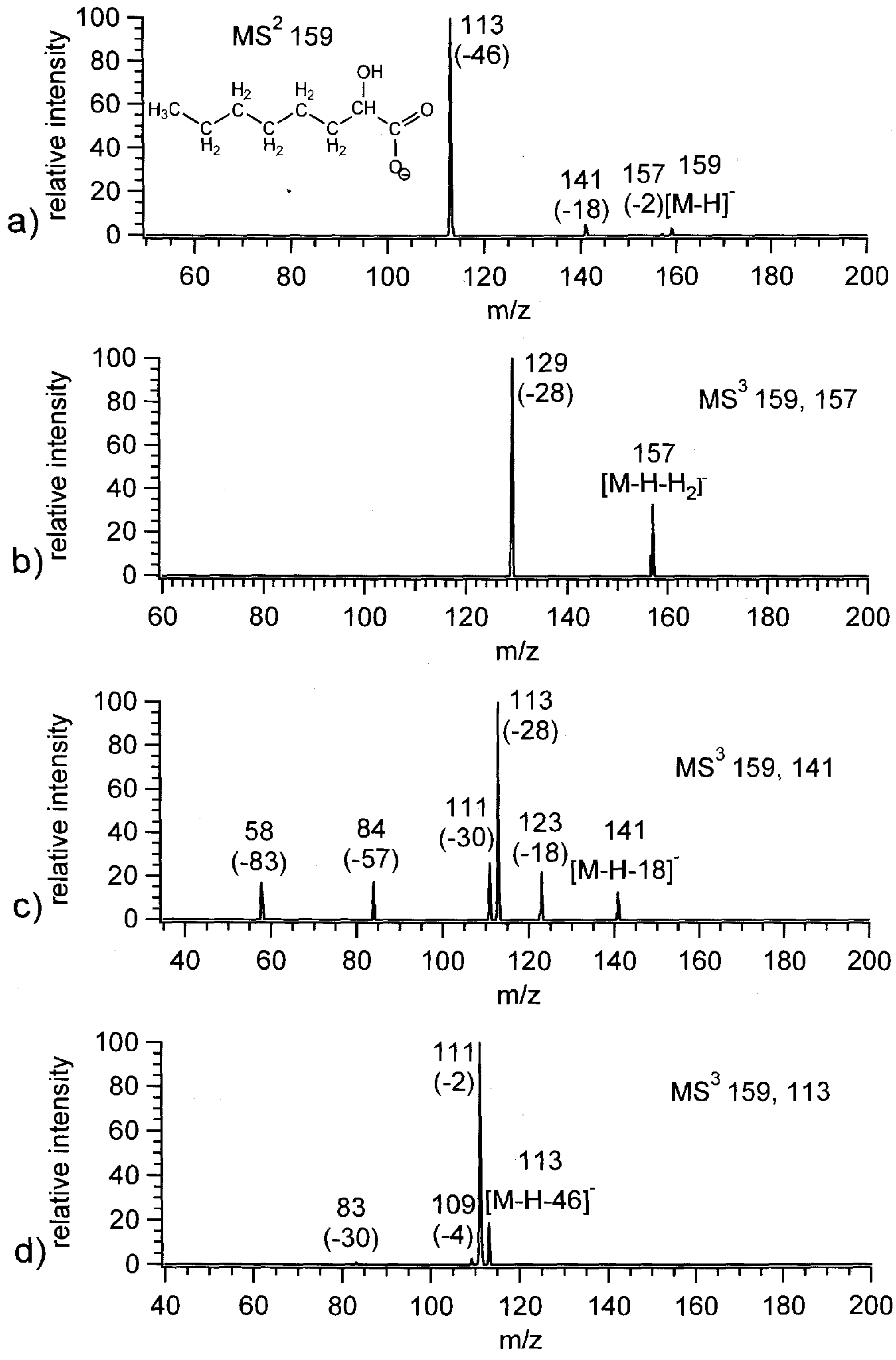
MS2 159
113
(-46)
141
(-18)
157
(-2)
159
[M-H]-
relative intensity
m/z
a)
MS3 159, 157
129
(-28)
157
[M-H-H2]-
b)
MS3 159, 141
113
(-28)
111
(-30)
58
(-83)
84
(-57)
123
(-18)
141
[M-H-18]-
c)
MS3 159, 113
111
(-2)
113
[M-H-46]-
109
(-4)
83
(-30)
d)

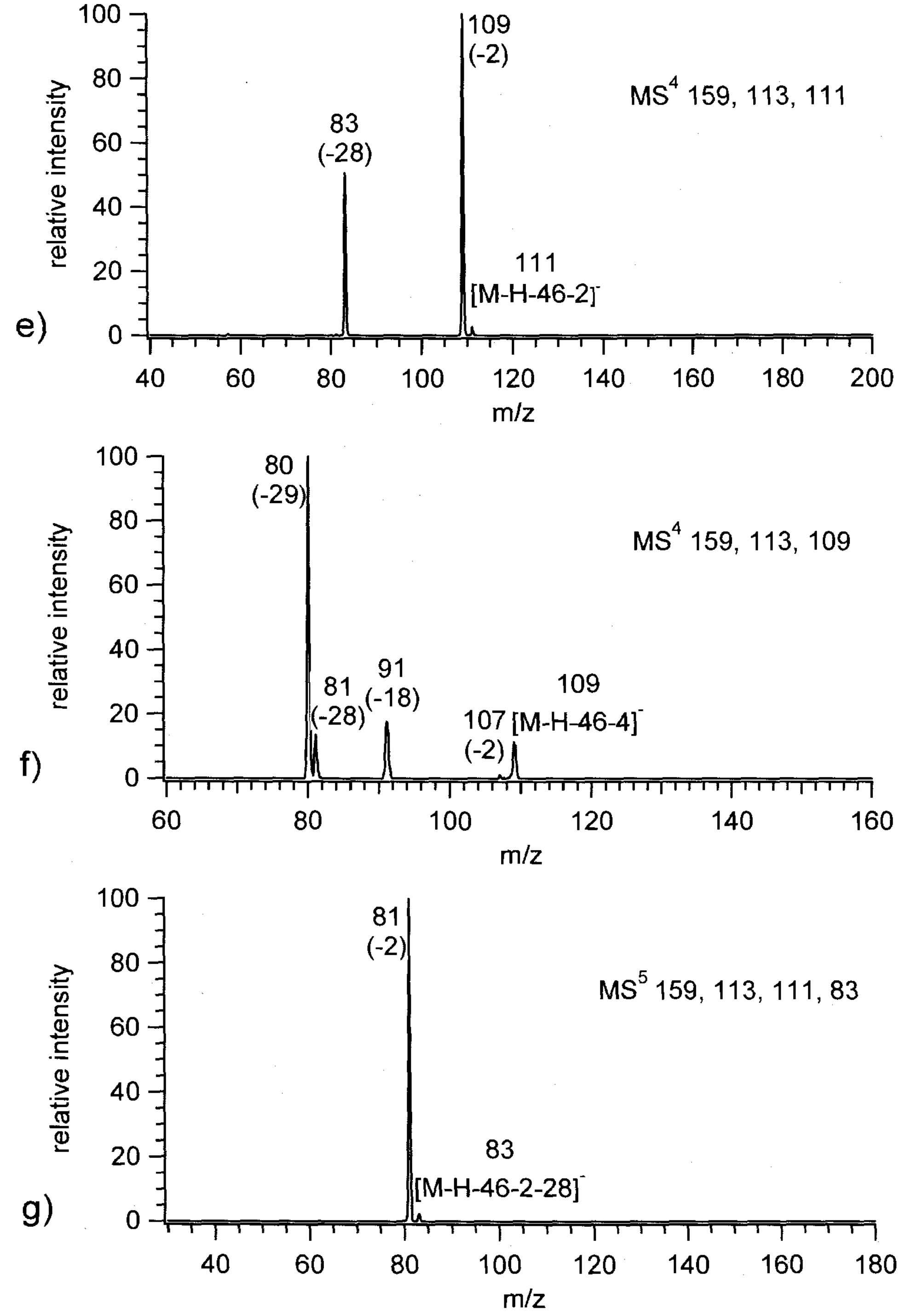

Figure 3.4: The mass spectra generated from MS^n analysis of 2-hydroxyoctanoate (*m/z* 159). Panel **a** is the MS^2 analysis of the parent ion ($[M\text{-}H]^-$), **b** the MS^3 analysis of the $[M\text{-}H\text{-}H_2]^-$ ion (*m/z* 157), **c** the MS^3 analysis of the $[M\text{-}H\text{-}18]^-$ ion (*m/z* 141), **d** the MS^3 analysis of the $[M\text{-}H\text{-}46]^-$ ion (*m/z* 113), **e** the MS^4 analysis of the $[M\text{-}H\text{-}46\text{-}2]^-$ ion (*m/z* 111), **f** the MS^5 analysis of the $[M\text{-}H\text{-}46\text{-}2\text{-}2]^-$ ion (*m/z* 109) and **g** the MS^5 analysis of the $[M\text{-}H\text{-}46\text{-}2\text{-}28]^-$ ion (*m/z* 83). The spectra were generated on a LCQ Ion Trap MS, operating in negative ion mode. NCE = 24 V.

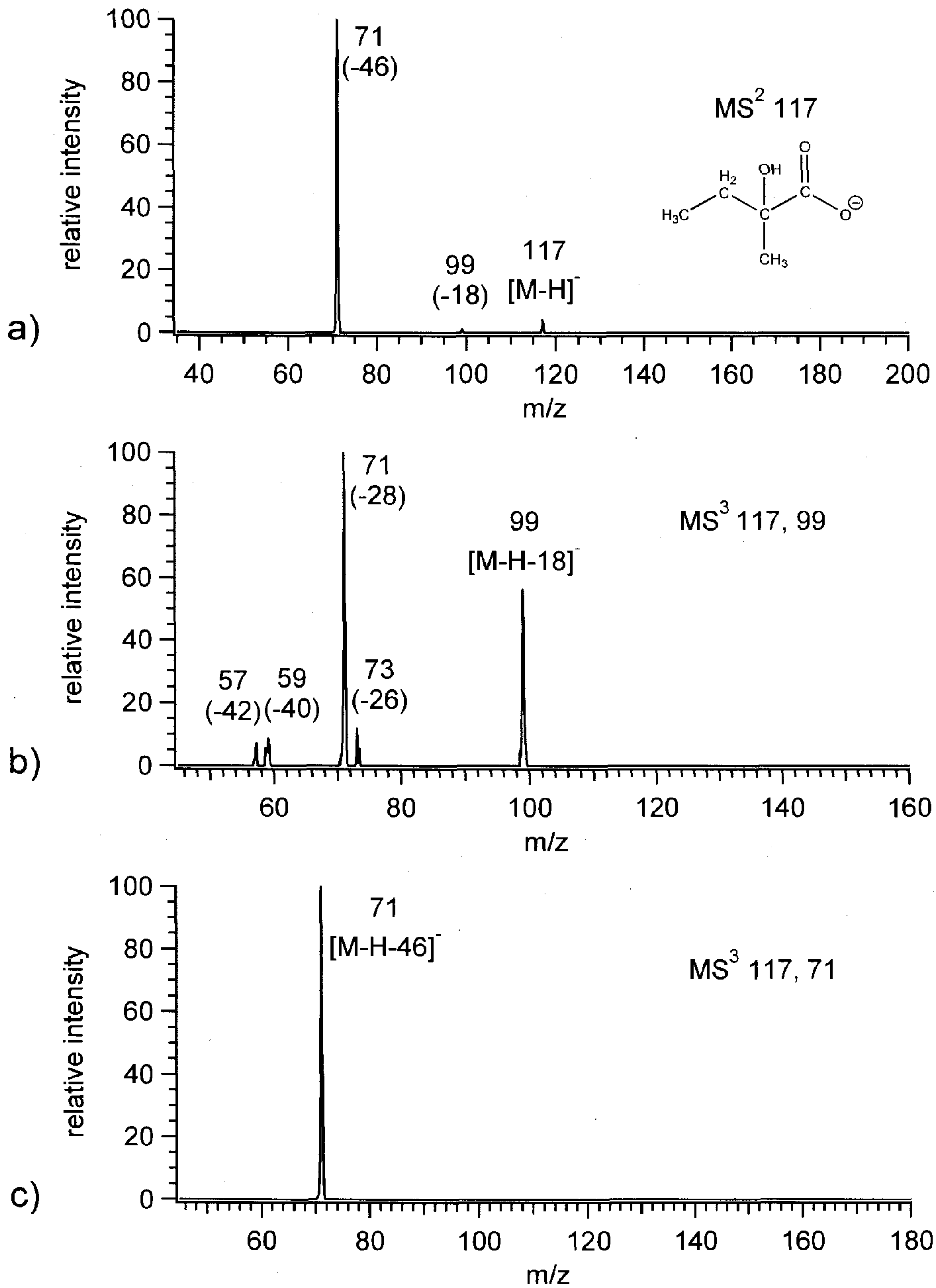

Figure 3.5: The mass spectra generated from MS^n analysis of 2-hydroxy-2-methylbutanoate (*m/z* 117). Panel **a** is the MS^2 analysis of the parent ion ($[M\text{-}H]^-$), **b** the MS^3 analysis of the $[M\text{-}H\text{-}18]^-$ ion (*m/z* 99) and **c** the MS^3 analysis of the $[M\text{-}H\text{-}46]^-$ ion (*m/z* 71). The spectra were generated on a LCQ Ion Trap MS, operating in negative ion mode. NCE = 24 V.

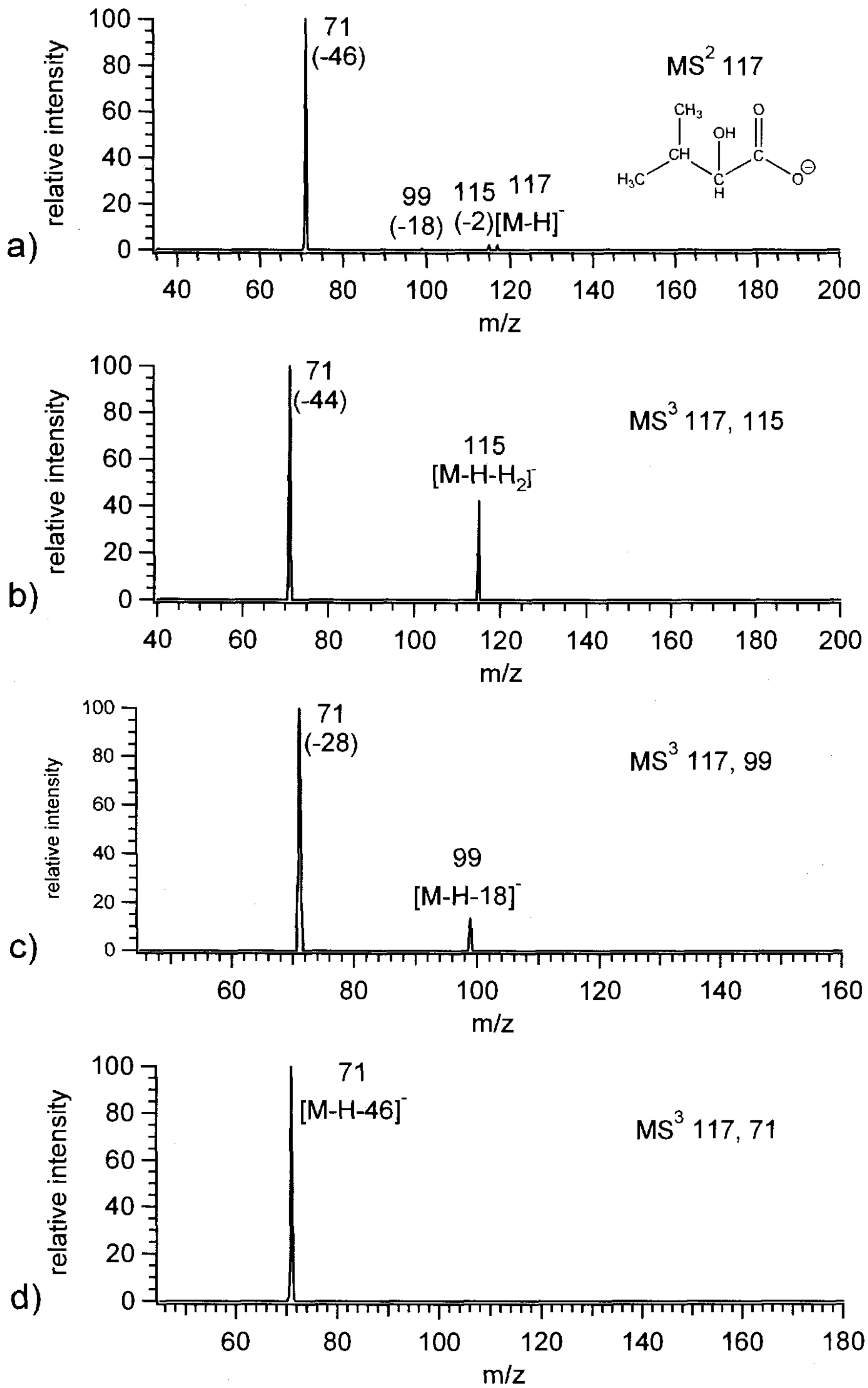

Figure 3.6: The mass spectra generated from MS^n analysis of 2-hydroxy-3-methylbutanoate (*m/z* 117). Panel **a** is the MS^2 analysis of the parent ion ([M-H]$^-$), **b** the MS^3 analysis of the [M-H-H$_2$]$^-$ ion (*m/z* 115), **c** the MS^3 analysis of the [M-H-18]$^-$ ion (*m/z* 99) and **d** the MS^3 analysis of the [M-H-46]$^-$ ion (*m/z* 71). The spectra were generated on a LCQ Ion Trap MS, operating in negative ion mode. NCE = 24 V.

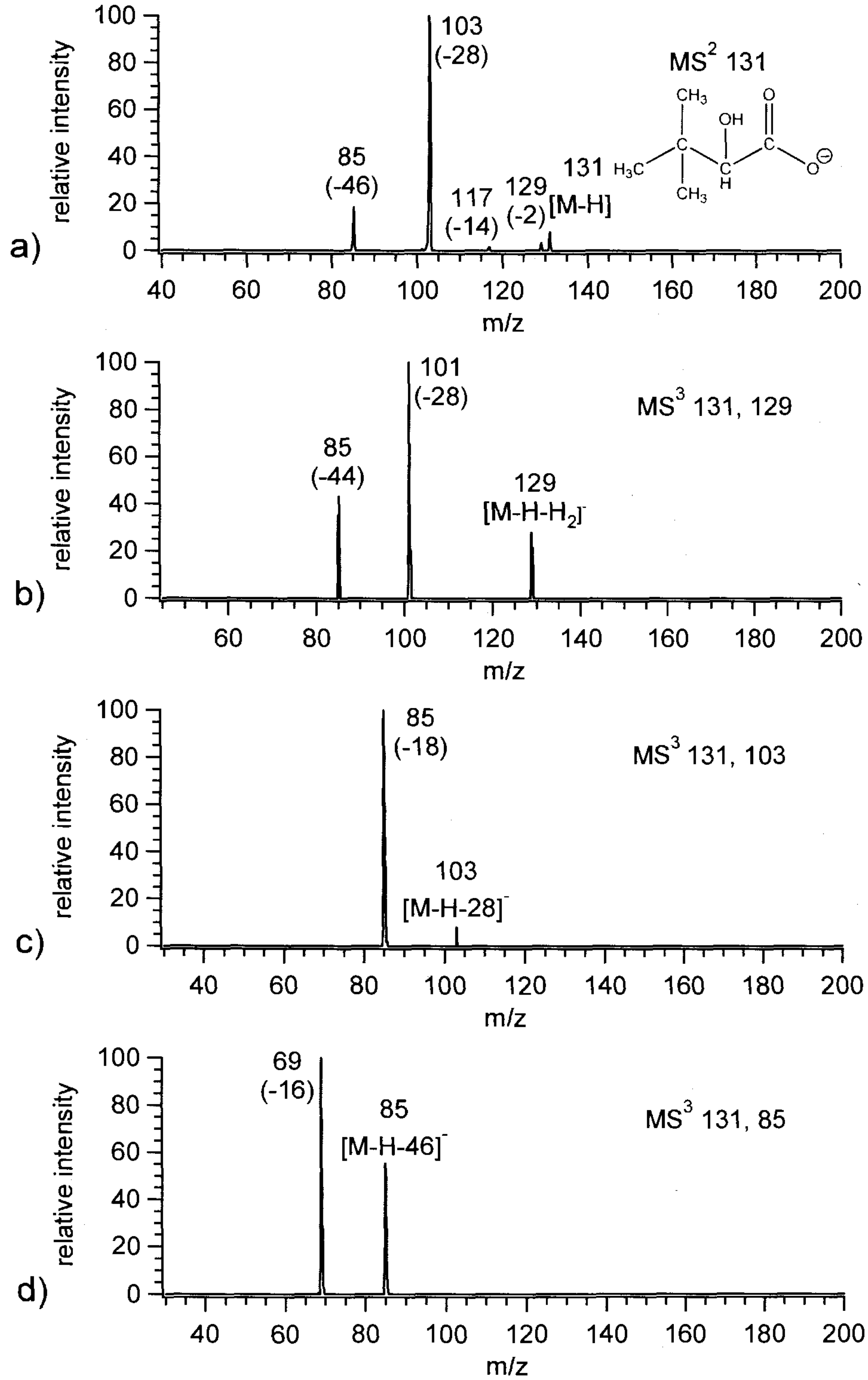

Figure 3.7: The mass spectra generated from MS^n analysis of 2-hydroxy-3,3-dimethylbutanoate (*m/z* 131). Panel **a** is the MS^2 analysis of the parent ion ([M-H]$^-$), **b** the MS^3 analysis of the [M-H-H$_2$]$^-$ ion (*m/z* 129), **c** the MS^3 analysis of the [M-H-28]$^-$ ion (*m/z* 103) and **d** the MS^3 analysis of the [M-H-46]$^-$ ion (*m/z* 85). The spectra were generated on a LCQ Ion Trap MS, operating in negative ion mode. NCE = 24 V.

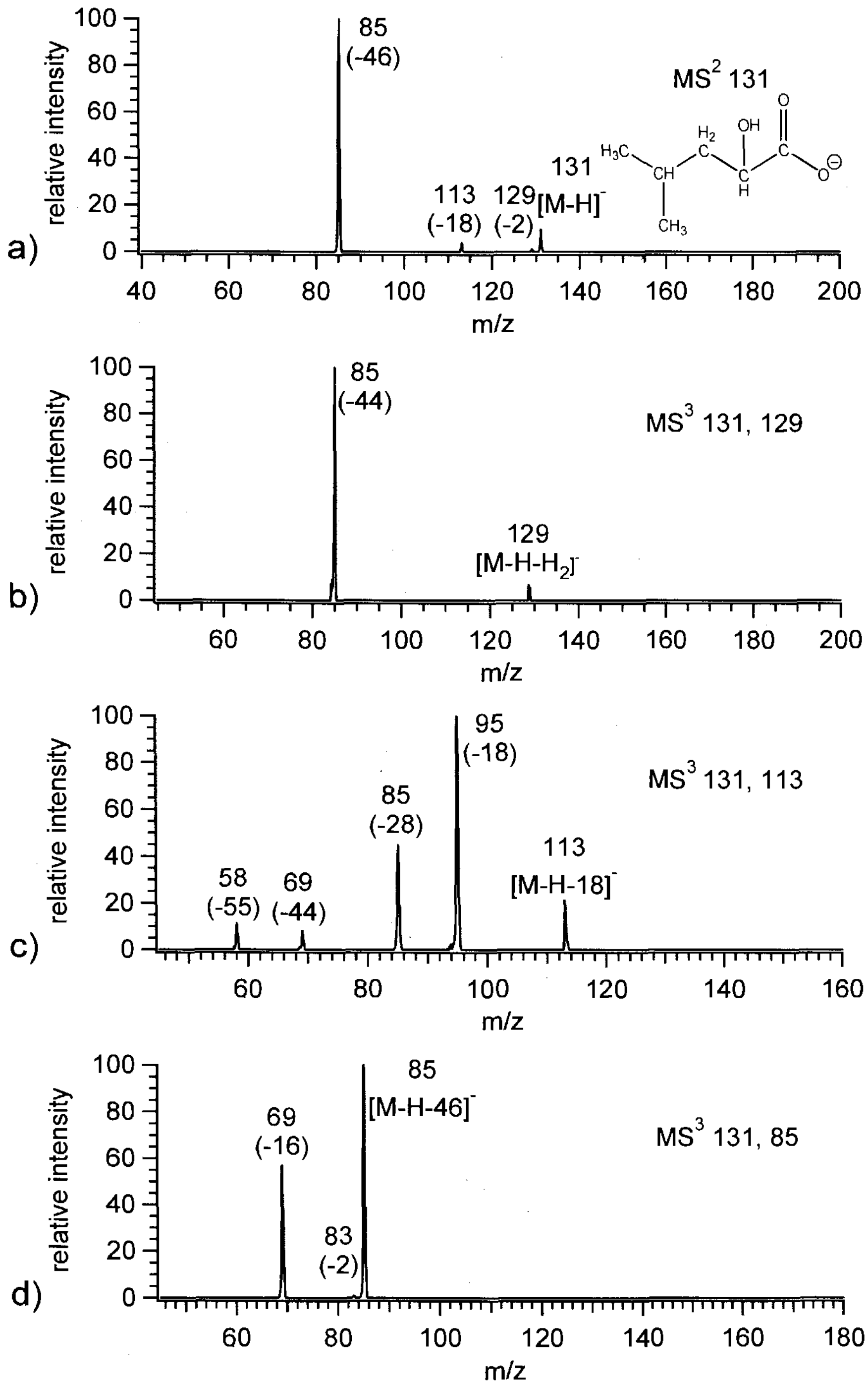

Figure 3.8: The mass spectra generated from MS^n analysis of 2-hydroxy-4-methylpentanoate (*m/z* 131). Panel **a** is the MS^2 analysis of the parent ion ($[M\text{-}H]^-$), **b** the MS^3 analysis of the $[M\text{-}H\text{-}H_2]^-$ ion (*m/z* 129), **c** the MS^3 analysis of the $[M\text{-}H\text{-}18]^-$ ion (*m/z* 113) and **d** the MS^3 analysis of the $[M\text{-}H\text{-}46]^-$ ion (*m/z* 85). The spectra were generated on a LCQ Ion Trap MS, operating in negative ion mode. NCE = 24 V.

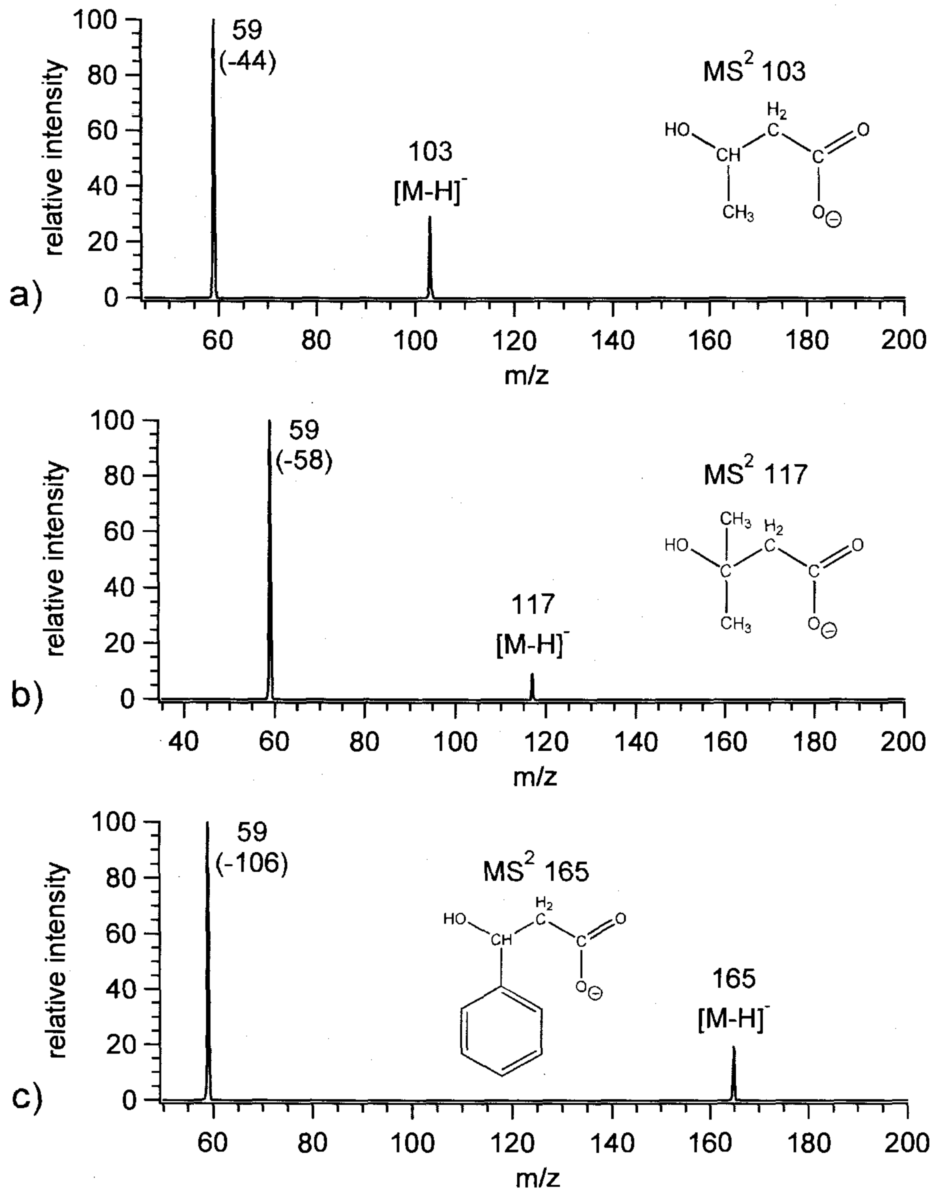

Figure 3.9: The MS^2 spectra generated from 3-hydroxycarboxylates. Panel **a** is the MS^2 spectrum of 3-hydroxybutanoate (*m/z* 103), **b** the MS^2 spectrum of 3-hydroxy-3-methylbutanoate (*m/z* 117) and **c** the MS^2 spectrum of 3-hydroxy-phenylpropanoate (*m/z* 165). The spectra were generated on a LCQ Ion Trap MS, operating in negative ion mode. NCE=24 V.

CHAPTER 4: FRAGMENTATION TREES FOR HYDROXYCARBOXYLATE ANIONS

Based on the spectral data obtained from the MS^n analysis of HAs^- (chapter *3*) fragmentation trees were constructed for each compound. The fragmentation trees are presented in this chapter starting with the $2\text{-}HA^-$ that has the shortest carbon-chain (2-hydroxypropanoate). The remainder of the $2\text{-}HAs^-$ is displayed based on increasing carbon-chain length (including those containing methyl branching) such that the fragmentation tree constructed for 2-hydroxyoctanoate (figure 4.8) is the last to be shown. The fragmentation trees for the $3\text{-}HAs^-$ are presented after the $2\text{-}HAs^-$ in figure 4.9.

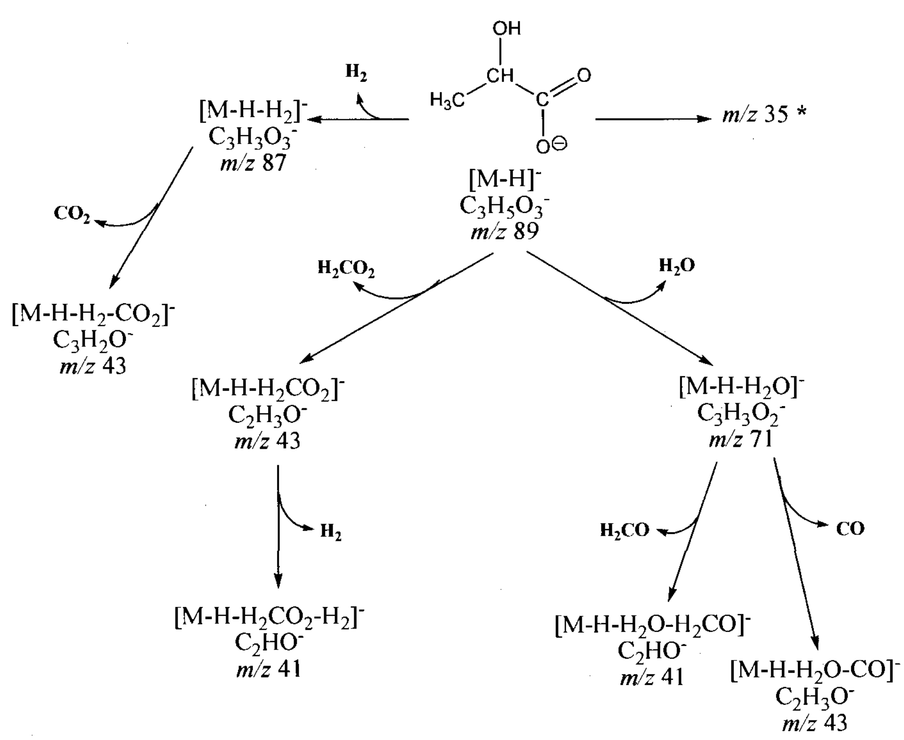

Figure 4.1: The fragmentation tree constructed from the MS^n analysis of 2-hydroxypropanoate (*m/z* 89). For each fragment ion generated via CID ([M-H-**X**]$^-$) the elemental composition is provided as well as the mass to charge ratio (*m/z*). The asterisks indicates the formation of a solvent adduct and is discussed in section *5.1.4*.

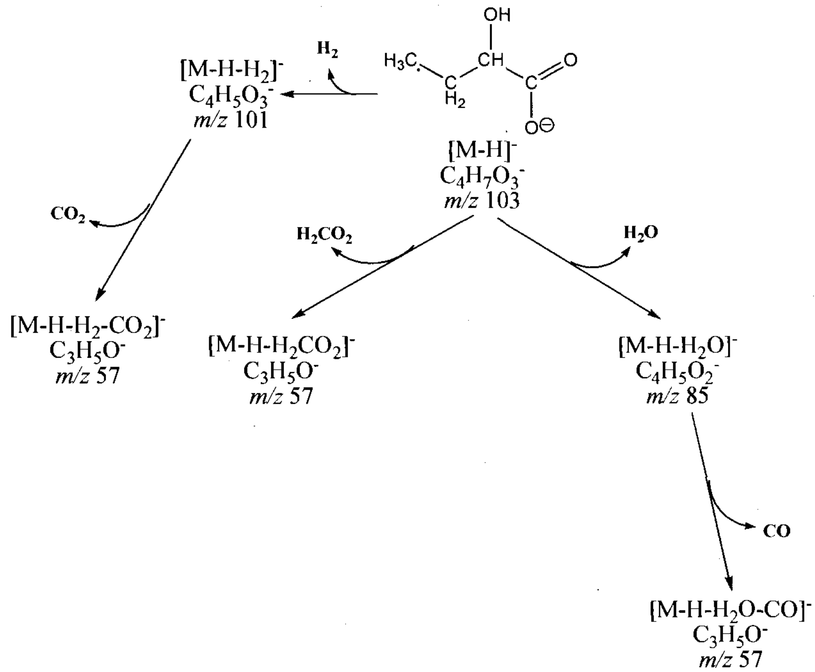

Figure 4.2: The fragmentation tree constructed from the MS^n analysis of 2-hydroxybutanoate (*m/z* 103). For each fragment ion generated via CID ([M-H-**X**]$^-$) the elemental composition is provided as well as the mass to charge ratio (*m/z*).

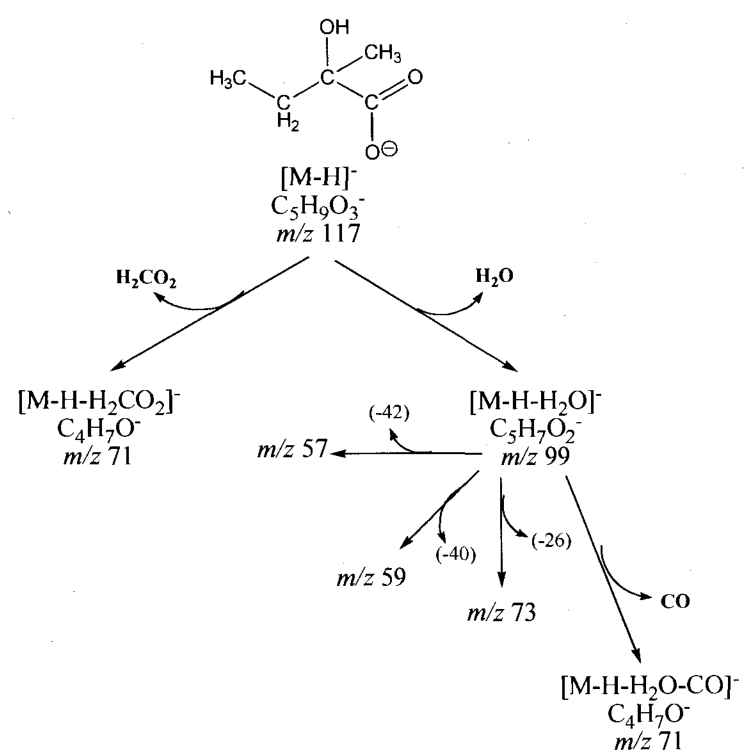

Figure 4.3: The fragmentation tree constructed from the MS^n analysis of 2-hydroxy-2-methylbutanoate (*m/z* 117). For each fragment ion generated via CID ([M-H-**X**]$^-$) the elemental composition is provided as well as the mass to charge ratio (*m/z*).

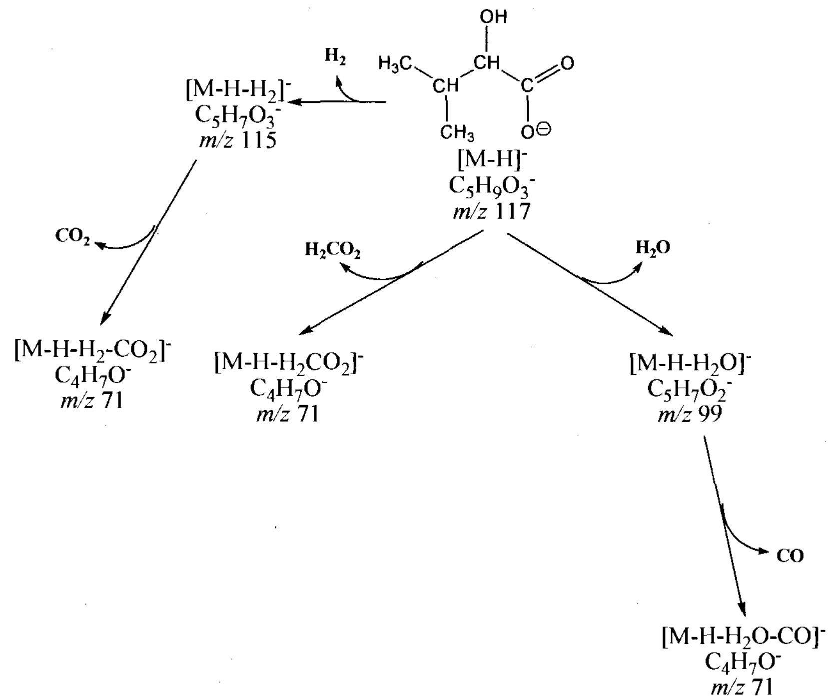

Figure 4.4: The fragmentation tree constructed from the MS^n analysis of 2-hydroxy-3-methylbutanoate (*m/z* 117). For each fragment ion generated via CID ([M-H-**X**]$^-$) the elemental composition is provided as well as the mass to charge ratio (*m/z*).

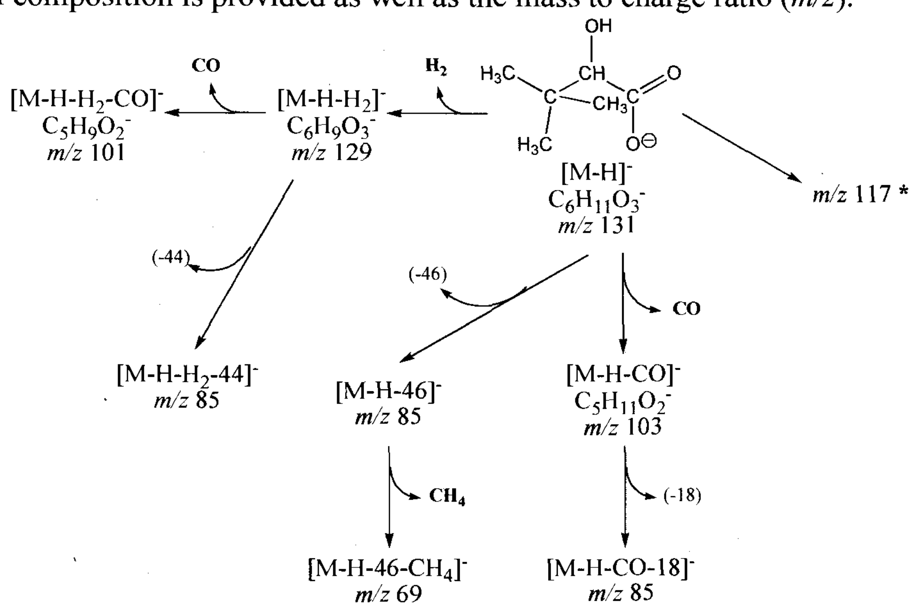

Figure 4.5: The fragmentation tree constructed from the MS^n analysis of 2-hydroxy-3,3-dimethylbutanoate (*m/z* 131). For each fragment ion, generated via CID ([M-H-**X**]$^-$), the mass to charge ratio (*m/z*) is provided as well as the elemental composition (if known). The asterisks indicates the formation of a solvent adduct and is discussed in section *5.1.5.2.*

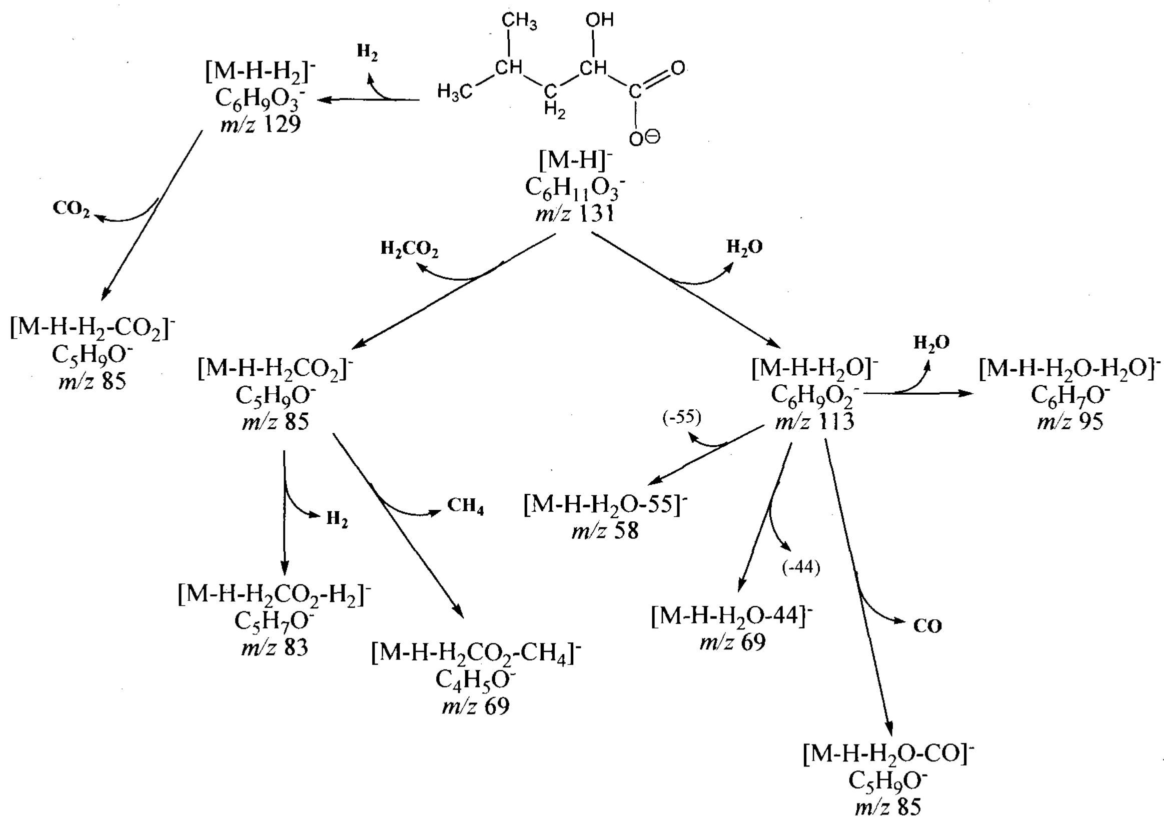

Figure 4.6: The fragmentation tree constructed from the MS^n analysis of 2-hydroxy-4-methylpentanoate (*m/z* 131). For each fragment ion, generated via CID ([M-H-**X**]$^-$), the mass to charge ratio (*m/z*) is provided as well as the elemental composition (if known).

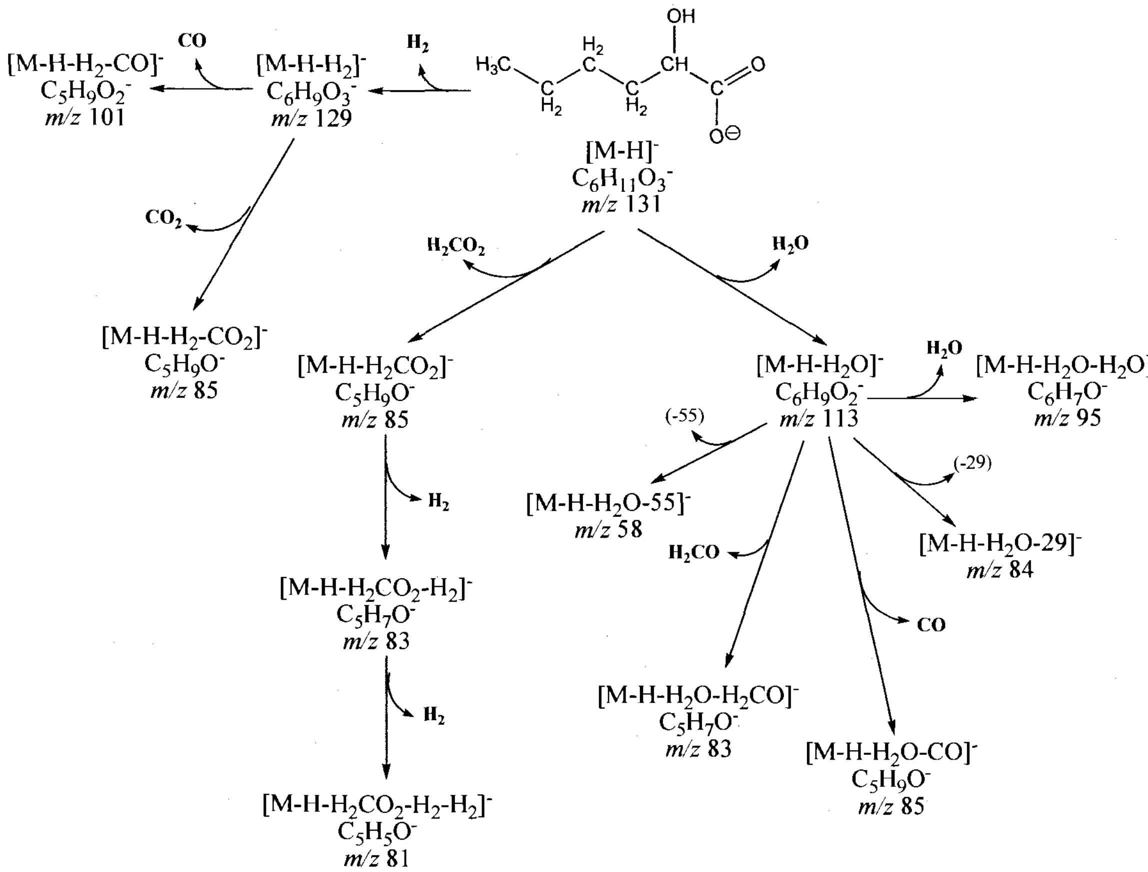

Figure 4.7: The fragmentation tree constructed from the MS^n analysis of 2-hydroxyhexanoate (*m/z* 131). For each fragment ion, generated via CID ([M-H-**X**]$^-$), the mass to charge ratio (*m/z*) is provided as well as the elemental composition (if known).

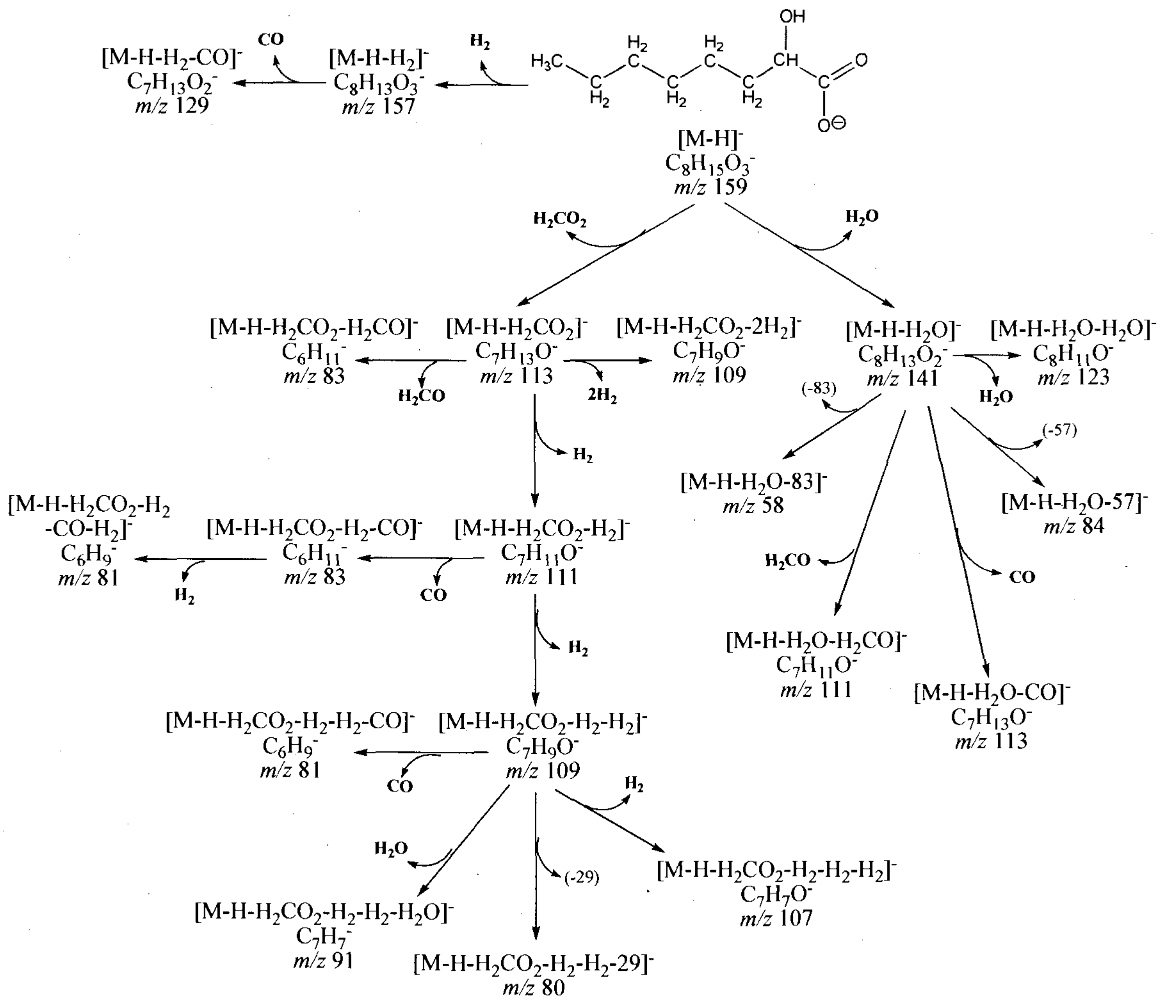

Figure 4.8: The fragmentation tree constructed from the MS^n analysis of 2-hydroxyoctanoate (*m/z* 159). For each fragment ion, generated via CID ([M-H-**X**]$^-$), the mass to charge ratio (*m/z*) is provided as well as the elemental composition (if known).

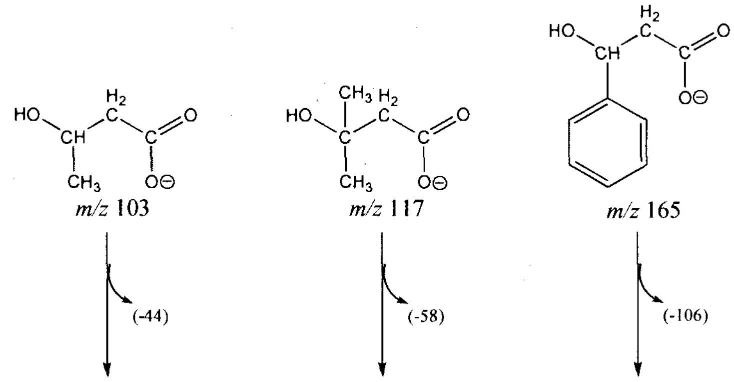

a) b) c)

Figure 4.9: The fragmentation trees constructed from the MS^n analysis of 3-hydroxycarboxylates. For each fragment ion, generated via CID ([M-H-**X**]$^-$), the mass to charge ratio (*m/z*) is provided. Figure **a** is the fragmentation tree for 3-hydroxybutanoate (*m/z* 103), **b** for 3-hydroxy-3-methylbutanoate (*m/z* 117) and **c** 3-hydroxy-3-phenylpropanoate (*m/z* 165).

CHAPTER 5: FRAGMENTATION PATTERNS OF HYDROXYCARBOXYLATES

5.1 MS^2 fragmentation patterns of hydroxycarboxylates

5.1.1 Overview of the MS^2 fragmentation patterns of 2-hydroxycarboxylates

The general fragmentation pattern of 2-HAs$^-$ results in the formation of three distinct characteristic CID product ions. The major CID product in the MS^2 spectrum is the [M-H-H_2CO_2]$^-$ ion, which is detected at a relative intensity (RI) of 100. The other two characteristic fragment ions are observed at low spectral intensities (RI ~ 5); they are the [M-H-H_2]$^-$ and [M-H-H_2O]$^-$ fragment ions. Detection of the [M-H-H_2CO_2]$^-$, [M-H-H_2]$^-$ and [M-H-H_2O]$^-$ ions in an MS^2 spectrum of an unknown compound may indicate the unknown is a 2-HA$^-$. However, it is important to note that through the analysis of these linear and branched 2-HAs$^-$, alkyl branching on carbon-2 inhibits the elimination of molecular hydrogen and thus the characteristic $[M-H-H_2]^-$ ions will be absent from the MS^2 spectrum. In addition, if the 2-HA$^-$ has a quaternary carbon in the carbon-3 position the elimination of water will be inhibited and therefore the $[M-H-H_2O]^-$ ions will not be observed in the spectrum. A quaternary carbon at the carbon-3 position will also inhibit the elimination of H_2CO_2 from the parent ion. Although a $[M-H-46]^-$ ion was detected following the fragmentation 2-hydroxy-3,3-dimethylbutanoate, its relative intensity was only 20 and perhaps in this case, the loss of 46 mass units is not due to H_2CO_2 elimination.

5.1.2 The loss of H_2CO_2 from 2-hydroxycarboxylates

In the MS^2 spectrum of 2-hydroxycarboxylates (top panel of figures 3.1-3.8) the major fragment ions generated result from the loss of 46 mass units. This mass loss is the elimination of H_2CO_2 from the parent ions, which is illustrated to the bottom left of the parent ion in the constructed fragmentation trees (figures 4.1-4.8). The loss of H_2CO_2 is observed with the greatest spectral intensity (relative intensity of 100) for all the linear and branched 2-HAs$^-$ (top panel of figures 3.1-3.6 and 3.8), with the exception of 2-hydroxy3,3-dimethylbutanoate (refer to spectrum in figure 3.7**a**). The 2-hydroxy-3,3-dimethylbutanoate generates $[M-H-46]^-$ product ions that are observed with a relative intensity (RI) of only 20. Therefore, based on the MS^2 spectrum generated from the various 2-HAs$^-$ (top panel of figures 3.1-3.8), it can be concluded that a quaternary carbon atom in the carbon-3 position will affect the feasibility of the H_2CO_2 elimination pathway.

As previously mentioned in section *1.6*, the smallest 2-HA$^-$ (2-hydroxyacetate) was extensively studied on an Ion-Trap mass spectrometer. Results of that study indicate that the major fragment ion generated was the $[M-H-H_2]^-$ ions. [47] Fragmentation of 2-hydroxyacetate (CH_2OHCOO^-) does not yield $[M-H-H_2CO_2]^-$ ions and thus it can be postulated that a 2-HA$^-$ must contain at least a three-carbon chain in order to achieve the H_2CO_2 elimination.

5.1.3 The loss of H_2 from 2-hydroxycarboxylates

The 2-HA$^-$ ions undergo H_2 elimination when fragmented via CID. The loss of molecular hydrogen from the $[M-H]^-$ ions is illustrated to the left of the parent ions in the fragmentation trees (figure 4.1-4.2, 4.4-4.8). These $[M-H-H_2]^-$ product ions were always observed with very low spectral intensities (RI of 5 or less) in the MS^2 spectrum of all the 2-HAs$^-$ examined (top panel of figures 3.1-3.4, 3.6-3.8), with the exception of 2-hydroxy-2-methylbutanoate (figure 3.5**a**) in which the peak correlating to the $[M-H-H_2]^-$ product ions was absent from the MS^2 spectrum. Based on the MS^2 spectra obtained from linear and branched 2-HAs$^-$, methyl branching at the α-carbon position inhibits the fragmentation pathway that eliminates molecular hydrogen from the parent ion.

The 2-hydroxyacetate anions (CH_2OHCOO^-) also generate the $[M-H-H_2]^-$ fragments upon CID. [47] Unlike the larger 2-HAs$^-$, the elimination of molecular hydrogen from the parent ion resulted in the major fragment ions, detected at a RI of 100 in the corresponding MS^2 spectrum. [47] Based on this previously established fragmentation behaviour of 2-hydroxyacetate and the current spectral data from the larger 2-HAs$^-$ it can be concluded that the elimination of H_2 does not require more than a two-carbon chain. In fact, the H_2 elimination is favoured for 2-hydroxyacetate because the H_2CO_2 elimination pathway is unavailable.

5.1.4 The loss of H_2O from 2-hydroxycarboxylates

A loss of 18 mass units from the parent ions was observed in the MS^2 spectrum for the linear and branched 2-HAs$^-$. The 18 mass units corresponds to the loss of H_2O and its elimination is illustrated in the fragmentation trees, to the bottom right of the parent ions (figure 4.1-4.4, 4.6-4.8). The elimination of water is always detected as a very low intensity peak (RI ~ 5) in the MS^2 spectrum of all linear and branched 2-HAs$^-$ (panel **a** of figures 3.1-3.6, 3.8), excluding that of 2-hydroxy-3,3-dimethylbutanoate (figure 3.7**a**). In compiling the MS^2 spectral information, a quaternary carbon in the carbon-3 position inhibits the loss of water from 2-HAs confirming that the hydrogen at carbon-3 is involved in the water loss.

It has also been established that 2-hydroxyacetate does not eliminate water. [47] Considering the larger 2-HAs$^-$ do, it can be concluded that a hydrogen atom on carbon-3 is required in the water loss pathway. Thus, explaining the absence of the $[M-H-H_2O]^-$ fragment in the MS^2 spectra of 2-hydroxyacetate and 2-hydroxy-3,3-dimethylbutanoate.

5.1.5 Detection of the m/z 35 fragment in the MS^2 spectrum of 2-hydroxypropanoate

The MS^2 spectrum of 2-hydroxypropanoate (figure 3.1**a**) shows a low intensity peak (RI <5) at *m/z* 35 that is not observed in the MS^2 spectrum of the other linear and branched 2-HAs$^-$. Rather than suggesting the parent ion lost a neutral fragment with a mass of 54, it is likely that the ion is the hydroxyl-water adduct previously observed for

2-hydroxyacetate.[47] This unique fragmentation pathway is illustrated to the right of the parent ion (2-hydroxypropanoate *m/z* 89) in the fragmentation tree of 2-hydroxypropanoate (refer to figure 4.1). Isolation of the *m/z* 35 ions for MS^3 analysis was attempted; however, the ions were fragile and could not be isolated, thus MS^3 data could not be obtained.

5.1.6 *Unique MS^2 fragment ions generated from 2-hydroxy-3,3-dimethylbutanoate*

2-Hydroxy-3,3-dimethylbutanoate (*m/z* 131) fragmented, via CID, and generated two product ions that were not liberated from the other 2-HAs$^-$ examined. It was the only 2-HA$^-$ examined that contained a quaternary carbon atom in the carbon-3 position and therefore, characteristic product ions were detected in the MS^2 spectrum (figure 3.7**a**) and discussed below.

5.1.6.1 *The loss of CO from the parent ion*

All other linear and branched 2-HAs$^-$ showed the elimination of H_2CO_2 from the parent ion to generate the major products. The 2-hydroxy-3,3-dimethylbutanoate ions resulted in CO elimination to generate the major product ion (*m/z* 103) which was detected with a RI of 100 (refer to spectrum in figure 3.7**a**). This fragmentation pathway is illustrated directly below the parent ion (*m/z* 131) in the fragmentation tree for 2-hydroxy-3,3-dimethylbutanoic acid. Based on the spectral data obtained from MS^2 analysis, it can be concluded that a quaternary carbon in the carbon-3 position had a negative affect on the typical major CID pathway (which is the loss of H_2CO_2) and dissociated to favour the loss of CO.

Once the $[M-H-CO]^-$ ions are generated from 2-hydroxy-3,3-dimethylbutanoic acid, CID reveals only one product ion in the MS^3 spectrum (figure 3.7**c**), detected at *m/z* 85 (RI 100). This loss of 18 mass units, which at first appears be the elimination of water, is illustrated directly below the *m/z* 103 ion in the fragmentation tree (figure 4.5). This *m/z* 85 ion ($[M-H-CO-18]^-$) may be structurally the same as the *m/z* 85 ion that was directly formed from the parent ion ($[M-H-46]^-$). However, as stated earlier the loss of 18 mass units may not necessarily be the loss of water (refer to reasoning in section *5.3.1*) and thus an elemental composition was not assigned to the neutral mass loss. Unfortunately, the $[M-H-CO-18]^-$ ions could not be fragmented in MS^4 analysis due to insufficient ion detection but their expected MS^4 spectrum would mirror the MS^3 spectrum of $[M-H-46]^-$, if the precursor ions were structurally the same.

5.1.6.2 The formation of the m/z 117 fragment ion

The final MS^2 fragment to be discussed is detected at *m/z* 117 (RI<5) (figure 3.7**a**). This CID pathway has been added to the fragmentation tree of 2-hydroxy-3,3-dimethylbutanoate (figure 4.5) to the bottom right of the parent ion. This low intensity fragment was 14 mass units smaller than the parent ion. Considering it is not possible to lose a neutral CH_2 fragment, it is reasonable to propose the *m/z* 117 ions to be solvent adducts of some fragment ions, much like the formation of the *m/z* 35 ion (hydroxyl ion-water complex) from 2-hydroxyacetate and 2-hydroxypropanoate (refer to section *5.1.5*). Ion solvent adducts have been documented in a number in MS^n studies for both positive and negative ions, especially with regards to water and methanol adducts. [49, 50]

5.1.7 Formation of the m/z 59 product ions in the MS^2 spectrum of 3-hydroxycarboxylates

Three different 3-HAs$^-$ were examined via tandem mass spectrometry. One linear (3-hydroxybutanoate (*m/z* 103)) and two branched compounds (3-hydroxy-3-methylbutanoate (*m/z* 117) and 3-hydroxy-3-phenylpropanoate (*m/z* 165)) were used to establish how the general fragmentation patterns of HAs differed when the hydroxyl group was positioned on carbon-3, rather than carbon-2. In the MS^2 spectrum of 3-HAs$^-$ (figure 3.9), a single product ion was observed with a relative intensity of 100. These product ions have a *m/z* of 59 and they are always generated regardless of branching at the carbon-3 position. Figure 4.9 displays the fragmentation trees of 3-HAs$^-$, each containing one CID pathway descending from the parent ions to generate the *m/z* 59 fragments. There are two possibilities for the elemental composition of these *m/z* 59 ions. They may be $C_2H_3O_2^-$ or $C_3H_7O^-$ and therefore these MS^2 products were not assigned an elemental composition in their fragmentation trees.

The formation of the characteristic *m/z* 59 fragment ions (via CID) may indicate that an unknown compound is a 3-HA$^-$. Unfortunately, by forming only one characteristic fragment ion (the *m/z* 59 ion) additional structural information regarding the parent ions cannot be obtained. Higher order fragmentation (MS^3) on the *m/z* 59 ions was attempted; however, second-generation fragment ions could not be detected.

5.2 MS^n fragmentation patterns stemming from the $[M\text{-}H\text{-}H_2CO_2]^-$ fragments of 2-hydroxycarboxylates

5.2.1 MS^3 of the $[M\text{-}H\text{-}H_2CO_2]^-$ ions derived from 2-hydroxycarboxylates

This section discusses the further fragmentation of the $[M\text{-}H\text{-}46]^-$ major fragment ions from the 2-HAs$^-$, with the exception of that from 2-hydroxy-3,3-dimethylbutanoate which will discussed separately (see below, section *5.3*). The $[M\text{-}H\text{-}H_2CO_2]^-$ ions from each of the 2-HAs$^-$ were isolated and further fragmented to generate MS^3 fragment ions which are observed in the MS^3 spectra displayed in figures 3.1**d**, 3.2**d**, 3.3**d**, 3.4**d**, 3.5**c**, 3.6**d** and 3.7**d**. The dissociation pathways originating from the $[M\text{-}H\text{-}H_2CO_2]^-$ ions are illustrated in the fragmentation trees (figures 4.1-4.8) to the right and descending from the corresponding $[M\text{-}H\text{-}H_2CO_2]^-$ ions. The results of the MS^3 analysis will be discussed below.

5.2.1.1 The loss of H_2 from $[M\text{-}H\text{-}H_2CO_2]^-$ ions

The common neutral mass loss observed from the $[M\text{-}H\text{-}H_2CO_2]^-$ ions was the elimination of molecular hydrogen. The loss of hydrogen was observed as the primary product ion from the fragments derived from 2-hydroxypropanoate (RI 15), 2-hydroxyhexanoate (RI 100) and 2-hydroxyoctanoate (RI 100). Detection of this $[M\text{-}H\text{-}H_2CO_2\text{-}H_2]^-$ fragment (*m/z* 83) was also observed in the MS^3 spectra of 2-hydroxy-4-methylpentanoate but at a relative intensity less than 5 (figure 3.8**d**). The low RI of the $[M\text{-}H\text{-}H_2CO_2\text{-}H_2]^-$ ions from 2-hydroxy-4-methylpentanoate will be addressed in section *5.2.1.2*.

The $[M-H-H_2CO_2]^-$ ions that were produced from a 2-HA$^-$ containing a four-carbon chain (2-hydroxybutanoate, 2-hydroxy-2-methylbutanoate and 2-hydroxy-3-methylbutanoate) did not show H_2 elimination, in fact they did not generate any MS^3 fragment ions (refer to spectra in figure 3.2**d**, 3.5**c** and 3.6**d** respectively). Based on the spectral information, it appears $[M-H-H_2CO_2]^-$ ions must be generated from 2-HAs$^-$ that contain more than a four-carbon chain to eliminate H_2. However, the $[M-H-H_2CO_2]^-$ ions from 2-hydroxypropanoate do not meet that criterion and yet still undergo H_2 elimination. Their $[M-H-H_2CO_2-H_2]^-$ ions are moderately detected at *m/z* 41 (refer to spectra in figure 3.1**d**). Considering the RI of the *m/z* 41 ions was only 15, compared to 100 for the larger analogous ions, perhaps an alternative H_2 elimination pathway may have occurred for the 2-hydroxypropanoate $[M-H-H_2CO_2]^-$ product ion.

By conducting the MS^3 analysis on the $[M-H-H_2CO_2]^-$ ions, important structural information was established. If the original parent ion contained at least a five-carbon chain then MS^3 analysis on the generated $[M-H-H_2CO_2]^-$ ions would show H_2 elimination. This can be used as a tool for distinguishing between 2-HA$^-$ isomers containing five carbon atoms. If the 2-HA$^-$ does not generate $[M-H-H_2CO_2-H_2]^-$ ions at the MS^3 stage, it can be concluded that the 2-HA$^-$ contains a four-carbon chain with methyl branching on either carbon-2 or carbon-3. If the 2-HA$^-$ does show the formation of $[M-H-H_2CO_2-H_2]^-$ ions then the 2-HA$^-$ would be 2-hydroxypentanoate.

5.2.1.2 Additional product ions generated from the $[M\text{-}H\text{-}H_2CO_2]^-$ ions of 2-hydroxy-4-methylpentanoic acid

As mentioned in section *5.2.1.1*, MS^3 analysis on the $[M\text{-}H\text{-}H_2CO_2]^-$ ions from 2-hydroxy-4-methylpentanoate resulted in the elimination of H_2. However, the detection of the $[M\text{-}H\text{-}H_2CO_2\text{-}H_2]^-$ product ions was low (RI less than 5). In the corresponding MS^3 spectrum (figure 3.8**d**), the major product ions were not from the loss of H_2 but rather the loss of methane (RI 100). The linear $[M\text{-}H\text{-}H_2CO_2]^-$ analogues did not undergo methane elimination (refer to spectra in figure 3.3**d** and 3.4**d**), thus the carbon-4 methyl group on the branched $[M\text{-}H]^-$ ions dictated the favourability between the two corresponding MS^3 fragmentation pathways.

5.2.1.3 Additional product ions generated from the $[M\text{-}H\text{-}H_2CO_2]^-$ ions of 2-hydroxyoctanoate

The MS^3 fragmentation behaviour of the largest 2-HA$^-$, 2-hydroxyoctanoate, showed additional dissociation pathways that were not observed with any of the smaller analogues. These pathways are illustrated in the fragmentation tree of 2-hydroxyoctanoate (figure 4.8) to the left of the *m/z* 113 ion ($[M\text{-}H\text{-}H_2CO_2]^-$) as well as below the *m/z* 113 ion. The pathway to the left of the *m/z* 113 ion displays the loss of H_2CO to form the MS^3 product ion of *m/z* 83. These *m/z* 83 ions were detected in the MS^3 spectrum (figure 3.4**d**) with a relative intensity just above zero. Due to their low intensity, they could not be further isolated and fragmented to generate MS^4 data. However, the formation of these *m/z* 83 ions are believed to be the result of an initial H_2 elimination (to generate the *m/z* 111 fragments) followed by a sequential loss of CO. Further explanation of this sequential loss will be addressed in section *5.2.2.2.*

By fragmenting the *m/z* 113 ions, product ions were detected in the MS^3 spectrum at *m/z* 109 (RI >5) (refer to spectrum in figure 3.4**d**). This correlated to the loss of $2H_2$ and is illustrated in the fragmentation tree of 2-hydroxyoctanoate (figure 4.8) below the *m/z* 113 ion, bypassing the *m/z* 111 pathway. The elimination of $2H_2$ is another example of a pathway believed to be sequential in neutral fragment eliminations. The initial loss of H_2 formed the MS^3 fragment of *m/z* 111 where a second elimination of H_2 results in the *m/z* 109 ions. Support of the sequential hydrogen loss will be address in section *5.2.2.1.*

5.2.2 MS^4 of the $[M\text{-}H\text{-}H_2CO_2\text{-}H_2]^-$ ions derived from larger 2-hydroxycarboxylates

The MS^4 $[M\text{-}H\text{-}H_2CO_2\text{-}H_2]^-$ product ions generated from 2-hydroxyhexanoate (*m/z* 83) and 2-hydroxyoctanoate (*m/z* 111) were the only $[M\text{-}H\text{-}H_2CO_2\text{-}H_2]^-$ ions that could be fragmented to generate an MS^4 spectrum. The MS^4 spectrum is displayed in panel **e** of figures 3.3 and 3.4 and is discussed below.

5.2.2.1 The loss of H_2 from the $[M\text{-}H\text{-}H_2CO_2\text{-}H_2]^-$ ions

The $[M\text{-}H\text{-}H_2CO_2\text{-}H_2]^-$ fragments from 2-hydroxyhexanoate (*m/z* 83) and 2-hydroxyoctanoate (*m/z* 111) both underwent H_2 elimination, generating $[M\text{-}H\text{-}H_2CO_2\text{-}H_2\text{-}H_2]^-$ product ions. These ions (*m/z* 81 and 109 respectively) were detected in the MS^4 spectrum with RI of 100 (panel **e** of figures 3.3 and 3.4) and illustrated directly below the $[M\text{-}H\text{-}H_2CO_2\text{-}H_2]^-$ ions in the corresponding fragmentation trees (figure 4.7 and 4.8). Based on the spectral data obtained from the various 2-HAs$^-$ examined, H_2 elimination from the $[M-H-H_2CO_2-H_2]^-$ ions can only occur if the parent ion contains a carbon-chain of at least six carbon atoms. The absence of the $[M-H-H_2CO_2-H_2-H_2]^-$ ions in the MS^4 spectrum of an unknown 2-HA^- could indicate the length of the carbon chain to be five.

In brief, the *m/z* 111 ions from 2-hydroxyoctanoate (the MS^4 product) were formed via H_2 elimination from *m/z* 113. Considering the *m/z* 111 ions undergo further H_2 elimination to form the *m/z* 109 ions, it can be postulated that the *m/z* 109 ions formed directly from the *m/z* 113 ions (via loss of $2H_2$) are structurally the same and formed through sequential H_2 eliminations. This is most likely due to the energy applied to fragment the *m/z* 113 ions. The normalized collision energy used was 24 V and this energy appears to be high enough to cause the *m/z* 111 fragments (in figure 3.4**d**) to begin losing another molecule of hydrogen.

5.2.2.2 Additional product ions generated from the $[M-H-H_2CO_2-H_2]^-$ ions of 2-hydroxyoctanoate

In the MS^4 spectrum of 2-hydroxyoctanoate (figure 3.4**e**) the $[M-H-H_2CO_2-H_2]^-$ ions (*m/z* 111) eliminated CO to generate *m/z* 83 ions, detected with a RI of 50. The pathway illustrating the loss of CO is presented to the left of the *m/z* 111 ion in the fragmentation tree of 2-hydroxyoctanoate (figure 4.8).

The preceding MS^3 fragment with a *m/z* 113 also generated a *m/z* 83 fragment ion via H_2CO elimination (refer to parallel pathway above the CO elimination in the fragmentation tree in figure 4.8). It can be postulated that these two *m/z* 83 ions are structurally the same for similar reasons mentioned in section *5.2.2.1* regarding the sequential loss of $2H_2$ to form the *m/z* 109 ions. Since the *m/z* 113 ions lost H_2 to generate the *m/z* 111 ions, and the *m/z* 111 ions lose CO to form *m/z* 83 ions, direct detection of the *m/z* 83 ions in the MS^3 spectrum of the *m/z* 113 ions (figure 3.4**d**) implies the collisional energy applied (NCE 24 V) is high enough to initiate the sequential loss of CO from the major *m/z* 111 product ions.

The *m/z* 83 ions formed, from the fragmentation of the *m/z* 111 ions, were isolated and fragmented to generate a MS^5 spectrum (refer to figure 3.4**g**). There was only one ion detected at *m/z* 81, having a RI of 100. The loss of H_2 from the $[M\text{-}H\text{-}H_2CO_2\text{-}H_2\text{-}H_2\text{-}CO]^-$ ion is illustrated in the fragmentation tree 2-hydroxyoctanoate (figure 4.8) to the left of the *m/z* 83 ion. Additional fragmentation of the *m/z* 81 ions was attempted but was unsuccessful.

5.2.3 MS^5 of the $[M\text{-}H\text{-}H_2CO_2\text{-}H_2\text{-}H_2]^-$ ions (m/z 109) derived from 2-hydroxyoctanoate

The MS^5 spectrum of the *m/z* 109 ion showed the formation of four different product ions (figure 3.4**f**). None of these product ions could be further fragmented to generate MS^6 data, therefore their description and placement on the fragmentation tree completed the MS^n findings, stemming from the $[M\text{-}H\text{-}H_2CO_2]^-$ ions (major MS^2 product).

The most intense peak in the MS^5 spectrum has a RI of 100 and is detected at *m/z* 80. This indicates the *m/z* 109 ion lost 29 mass units, identifying for the first time radical cleavage reactions. The radical reaction is illustrated on the fragmentation tree (figure 4.8) directly below the *m/z* 109 ion.

A small peak was observed in the MS^5 spectrum (figure 3.4**f**) just above the base line at *m/z* 107. The loss of H_2 from the *m/z* 109 fragment is positioned to the bottom right of the *m/z* 109 ion in the fragmentation tree (figure 4.8).

The two remaining product ions were moderately detected (RI 15-20) at *m/z* 81 (loss of CO) and *m/z* 91 (loss of H_2O). Their placement on the fragmentation tree (figure 4.8) is to the left and bottom left of the *m/z* 109 ion, respectively.

5.3 MS^3 fragmentation patterns stemming from the $[M-H-46]^-$ fragments of 2-hydroxy-3,3-dimethylbutanoate

5.3.1 The loss of methane from the $[M-H-46]^-$ ion of 2-hydroxy-3,3-dimethylbutanoate

The MS^3 spectrum generated from the moderately intense $[M-H-46]^-$ ions is displayed in panel **d** of figure 3.7. The MS^3 CID product ion was detected with a relative intensity of 100 at *m/z* 69, indicating the elimination of methane. The pathway attributed to loss of methane is illustrated in the fragmentation tree of 2-hydroxy-3,3-dimethylbutanoate (figure 4.5) directly below the *m/z* 85 ion. Attempts to further fragment the *m/z* 85 ions were unsuccessful and therefore MS^4 data could not be obtained.

In briefly recapping the MS^3 findings of the other branched 2-HAs$^-$ and the linear 2-HAs$^-$, it was evident that 2-HAs$^-$ containing a four-carbon chain (regardless of branching) did not generate MS^3 fragments from their corresponding $[M-H-H_2CO_2]^-$ products (refer to spectra in figures 3.2**d**, 3.5**c** and 3.6**d**). Considering 2-hydroxy-3,3-dimethylbutanoate has a four-carbon chain, the $[M-H-46]^-$ ions should not generate MS^3

fragments, if in fact the $[M-H-46]^-$ ions are $[M-H-H_2CO_2]^-$ ions. Observing the loss of methane in the MS^3 spectrum (figure 3.7**d**) strongly suggests the $[M-H-46]^-$ ions are not formed via H_2CO_2 elimination.

5.4 MS^3 fragmentation patterns stemming from the $[M-H-H_2]^-$ fragments of 2-hydroxycarboxylates

As mentioned in section *5.1.3*, all deprotonated 2-HAs$^-$ eliminate H_2 to generate the MS^2 minor fragment $[M-H-H_2]^-$, except for 2-hydroxy-2-methylbutanoate. For the compounds that did generate this minor product ion, their ions were individually isolated and fragmented to produce MS^3 spectra (refer to panel **b** in figures 3.1-3.4 and 3.6-3.8). The results of the MS^3 analysis show an elimination of CO_2 and/or CO and will be discussed below; however, the results from the $[M-H-H_2]^-$ ion of 2-hydroxy-3,3-dimethylbutanoate will be discussed separately in section *5.4.3*.

5.4.1 The loss of CO_2 from the $[M-H-H_2]^-$ ions of 2-hydroxycarboxylates

The $[M-H-H_2]^-$ ions that were formed, from 2-HAs$^-$ containing up to five carbons in their carbon-chain (linear or branched), showed only one product ion in their MS^3 spectra. The product ions were formed through CO_2 elimination and were all detected with a RI of 100 (refer to panel **b** in figures 3.1, 3.2, 3.6 and 3.8). The MS^3 spectrum from the $[M-H-H_2]^-$ ions of 2-hydroxyhexanoate (figure 3.3**b**) showed two product ions; however, the major product ion generated (RI 100) was also due to the loss of CO_2. The pathway illustrating the loss of CO_2 from the $[M\text{-}H\text{-}H_2]^-$ ions is illustrated in the fragmentation trees (figure 4.1, 4.2, 4.4, 4.6, 4.7) to the bottom left of the $[M\text{-}H\text{-}H_2]^-$ ions.

The largest 2-HA$^-$ examined (2-hydroxyoctanoate) did not show a spectral peak representing $[M\text{-}H\text{-}H_2\text{-}CO_2]^-$ ions in its MS^3 spectrum (figure 3.4**b**). The smallest 2-HA$^-$ (2-hydroxyacetate) has already been studied in detail and MS^3 analysis on its $[M\text{-}H\text{-}H_2]^-$ ions do not produce ions formed via CO_2 elimination. [47] Based on the MS^3 results of 2-HAs (containing 2-8 carbon atoms in its carbon chain) it can be concluded that $[M\text{-}H\text{-}H_2]^-$ ions will fragment to lose CO_2, provided its carbon chain is 3-6 carbons in length. Whether or not a 2-HA$^-$ with a 7-carbon chain will lose CO_2 at the MS^3 stage can only be determined experimentally; however, once it contains an eight-carbon chain the loss of CO_2 does not occur.

5.4.2 The loss of CO from the $[M\text{-}H\text{-}H_2]^-$ ions of 2-hydroxycarboxylates

In the MS^3 spectrum of the largest compound, 2-hydroxyoctanoate, the only fragments generated were detected at *m/z* 129 (figure 3.4**b**). This identifies CO elimination from the $[M\text{-}H\text{-}H_2]^-$ ions. The second largest compound analyzed was 2-hydroxyhexanoate whose $[M\text{-}H\text{-}H_2]^-$ ions also lost CO to generate ions detected at *m/z* 101; however, they were not the major CID fragments (RI is ~ 20) (refer to figure 3.3**b**). The MS^3 elimination of CO is unique to the larger 2-HAs$^-$ and is illustrated in the fragmentation trees (figure 4.7, 4.8) directly to the left of the $[M\text{-}H\text{-}H_2]^-$ ions.

Based on the MS^3 spectral data, the elimination of CO and CO_2 from the $[M\text{-}H\text{-}H_2]^-$ ions are two competing CID reactions. The favourability of one compared to the other appears to be governed by the length of the ion's carbon chain. As stated in section

5.4.1, the loss of CO_2 is favoured in $[M-H-H_2]^-$ ions containing up to a six-carbon chain. However, at a carbon chain of six atoms the elimination of CO begins to proceed and takes over as the only CID reaction once the carbon chain reaches eight carbons in length. The loss of CO from a seven-carbon chained $[M-H-H_2]^-$ ion may or may not be accompanied by the loss of CO_2. Analysis on a 2-HA with a seven-carbon chain would be required to determine the maximum chain length that still allows for the loss of CO_2 to proceed at the MS^3 stage.

5.4.3 MS^3 fragmentation patterns of the $[M-H-H_2]^-$ ions from 2-hydroxy-3,3-dimethylbutanoate

In the MS^3 spectrum of 2-hydroxy-3,3-dimethylbutanoate (figure 3.7**b**) there are two CID products detected at *m/z* 101 (RI 100) and *m/z* 85 (RI 45). The major fragments (*m/z* 101) were generated through a loss of CO. The pathway that forms these $[M-H-H_2-CO]^-$ ions is illustrated in the fragmentation tree (figure 4.5) directly to the left of the *m/z* 129 ion ($[M-H-H_2]^-$). The minor fragments were generated through the loss of 44 mass units, possibly a CO_2 elimination, and this pathway is illustrated on the fragmentation tree (figure 4.5) to the bottom left of the *m/z* 129 ion.

Based on the MS^3 fragmentation patterns of the other linear and branched $[M-H-H_2]^-$ ions, the only fragmentation pathway that should be occurring is the loss of CO_2 (refer to section *5.4.1* and *5.4.2*). The $[M-H-H_2]^-$ ions from 2-hydroxy-3,3-dimethylbutanoate would have a branched four-carbon chain and therefore, not long enough to proceed through the CO elimination pathway (requires at least a six-carbon chain). However, the spectrum shows a predominant loss of CO and a moderate loss of

44 mass units. Perhaps, in this case the quaternary C-3 carbon atom (in the parent ion) is adversely affecting the $[M-H-H_2]^-$ ion's ability to eliminate CO_2 and by default proceeds to lose CO. Based on this spectral observation, it appears a hydrogen at carbon-3 is required for the CO_2 elimination pathway. The fact that the $[M-H-H_2-44]^-$ MS^3 product ions were not detected with the greatest spectral intensity could also indicate that the loss of 44 is not CO_2. Maybe the loss of 44 is the result of a sequential CO loss (28 mass units) followed by a CH_4 loss (16 mass units). Unfortunately, the *m/z* 101 ions could not be further fragmented to produce MS^4 data, due inadequate detection.

5.5 MS^3 fragmentation patterns stemming from the $[M-H-H_2O]^-$ fragments of 2-hydroxycarboxylates

As mentioned in section *5.1.4*, all 2-HAs^- eliminated H_2O to generate the MS^2 minor fragment $[M-H-H_2O]^-$, except for 2-hydroxy-3,3-dimethylbutanoate. For the compounds that generated this minor product ion, their ions were individually isolated and fragmented to produce MS^3 spectra (refer to panel **c** in figures 3.1-3.4, figure 3.5**b**, 3.6**c** and 3.8**c**). The results of the MS^3 analysis show an elimination of CO and quite often the elimination of H_2CO. However, the results from the longer $[M-H-H_2]^-$ ions showed extensive fragmentation and therefore discussed in the later part of this section (*5.5.3-5.5.6*). The $[M-H-H_2O]^-$ ion from 2-hydroxy-2-methylbutanoate generated a unique MS^3 spectrum and as a result is discussed separately in section *5.5.7*. Although attempted, it is important to note that none of the MS^3 product ions that were generated produced MS^4 data.

5.5.1 The loss of CO from the [M-H-H_2O]$^-$ fragments of 2-hydroxycarboxylates

Collision induced dissociation of all [M-H-H_2O]$^-$ ions, including those generated from 2-hydroxy-2-methylbutanoate, resulted in CO eliminations. These [M-H-H_2O-CO]$^-$ product ions were detected as the most intense peak (RI 100) in the MS^3 spectra displayed in panel **c** of figures 3.1-3.4, 3.5**b**, 3.6**c** (all linear and methyl branched 2-hydroxybutanoates). The [M-H-H_2O-CO]$^-$ products, stemming from 2-hydroxy-4-methylpentanoate, were also detected in the MS^3 spectrum (figure 3.8**c**) but at a RI of 50. The elimination of CO from the [M-H-H_2O]$^-$ MS^2 products is illustrated in the fragmentation trees descending from the [M-H-H_2O]$^-$ ions (figures 4.1-4.4, 4.6-4.8).

This MS^3 product ion ([M-H-H_2O-CO]$^-$) was the only ion detected in the MS^3 spectrum of 2-HAs containing a four-carbon chain (excluding that of 2-hydroxy-2-methylbutanoate, refer to section *5.5.7*). Therefore, detection of only the [M-H-H_2O-CO]$^-$ ions at the MS^3 stage would strongly suggest the parent ion is a 2-hydroxybutanoate anion (with/without branching) when analyzing an unknown 2-HA$^-$.

Since the MS^3 spectra of the [M-H-H_2O]$^-$ ions from 2-HAs$^-$ containing a four-carbon chain did not show any additional product ions, it is believed that the [M-H-H_2O-CO]$^-$ ions are structurally the same as the MS^2 [M-H-H_2CO_2]$^-$ ions. As stated in section *5.2.1.1*, the [M-H-H_2CO_2]$^-$ ions from 2-HAs$^-$ containing a linear or branched four-carbon chain do not generate product ions upon CID. Therefore, it is possible that the [M-H-H_2CO_2]$^-$ ions are formed through a sequential loss of H_2O and CO.

5.5.2 The loss of H_2CO from the $[M-H-H_2O]^-$ fragments of 2-hydroxycarboxylates

The loss of H_2CO from the $[M-H-H_2O]^-$ ions was observed from 2-hydroxypropanoate and the linear 2-HAs⁻ containing at least a six-carbon chain (refer to spectrum in panel **c** of figure 3.1, 3.3 and 3.4). Detection of these $[M-H-H_2O-H_2CO]^-$ ions resulted in low spectral intensity peaks at *m/z* 41 for 2-hydroxypropanoate (RI 15), *m/z* 83 for 2-hydroxyhexanoate (RI 10) and moderately intense at *m/z* 111 for 2-hydroxyoctanoate (RI 25). The elimination of H_2CO is illustrated in the fragmentation trees (figures 4.1, 4.6-4.8) descending from the $[M-H-H_2O]^-$ ion and to the left of the CO eliminations; however, it is likely the loss of CO is followed by H_2 elimination to yield the $[M-H-H_2O-H_2CO]^-$ products.

Referring back to the MS^3 spectra of the $[M-H-H_2CO_2]^-$ ions from 2-hydroxypropanoate (figure 3.1**d**), 2-hydroxyhexanoate (figure 3.3**d**) and 2-hydroxyoctanoate (figure 3.4**d**), all three ions showed the elimination of H_2 to generate $[M-H-H_2CO_2-H_2]^-$ products. It is likely these $[M-H-H_2CO_2-H_2]^-$ ions are structurally the same as $[M-H-H_2O-H_2CO]^-$ ions for two reasons. As stated earlier (section *5.5.1*), it is likely that the $[M-H-H_2CO_2]^-$ ions are structurally the same as the $[M-H-H_2O-CO]^-$ ions; therefore, an additional H_2 elimination could result in $[M-H-H_2CO_2-H_2]^-$ ions being structurally the same as $[M-H-H_2O-H_2CO]^-$ ions. Secondly, The fact that the $[M-H-H_2O-H_2CO]^-$ ions were not generated from 2-HAs⁻ that have a four-carbon chain suggests the loss of CO is followed by a sequential loss of H_2 (from the $[M-H-H_2O]^-$) and that the structure of $[M-H-H_2O-H_2CO]^-$ ions may be the same as $[M-H-H_2CO_2-H_2]^-$ ions (also not generated from four-carbon chained 2-HAs⁻).

5.5.3 The loss of H_2O from the $[M\text{-}H\text{-}H_2O]^-$ fragments of 2-hydroxycarboxylates

A second loss of H_2O was observed from the 2-HAs$^-$ containing at least a five-carbon chain (linear or branched). In the MS^3 spectrum of 2-hydroxyhexanoate (figure 3.3**c**) and 2-hydroxyoctanoate (figure 3.4**c**), the $[M\text{-}H\text{-}H_2O]^-$ ions eliminate H_2O to form $[M\text{-}H\text{-}H_2O\text{-}H_2O]^-$ fragments which were detected with RIs between 15 and 20. The formation of the $[M\text{-}H\text{-}H_2O\text{-}H_2O]^-$ ions from 2-hydroxy-4-methylpentanoate was more favourable in comparison, as their RI was 100 (figure 3.8**c**). The elimination of water from the $[M\text{-}H\text{-}H_2O]^-$ ions have been illustrated in the fragmentation trees (figure 4.6-4.8) directly to the right of the $[M\text{-}H\text{-}H_2O]^-$ ions.

Based on the MS^3 data obtained from this study, it can be concluded that the generation of the $[M\text{-}H\text{-}H_2O\text{-}H_2O]^-$ ions requires the parent ions to have a minimum of five carbons in its carbon chain. In addition, methyl branching in the carbon-four position appears to increase the favourability of this CID pathway.

5.5.4 The formation of the m/z 58 distonic radical from 2-hydroxycarboxylates

The $[M\text{-}H\text{-}H_2O]^-$ ions were the only MS^2 product ions that undergo radical cleavage via CID. In the MS^3 spectrum 2-hydroxyhexanoate (figure 3.3**c**), 2-hydroxyoctanoate (figure 3.4**c**) and 2-hydroxy-4-methylbutanoate (figure 3.8**c**) the $[M\text{-}H\text{-}H_2O]^-$ ions eliminated a neutral radical to generate the *m/z* 58 distonic radical anions (RI 10-15). The radical reaction forming the *m/z* 58 ions is illustrated in the fragmentations trees (figure 4.6-4.8) to the left of the $[M\text{-}H\text{-}H_2O]^-$ ions.

Based on the spectral data, MS^3 fragmentation of the $[M\text{-}H\text{-}H_2O]^-$ ions generated the *m/z* 58 distonic radical anions provided the $[M\text{-}H\text{-}H_2O]^-$ ions have a minimum of a five-carbon chain, as this MS^3 product ion was not formed from 2-HAs^- containing four (or less) carbon atoms in its carbon chain (refer to spectra in figure 3.1**c**, 3.2**c**, 3.5**b** and 3.6**c**).

5.5.5 The formation of the m/z 84 distonic radical from 2-hydroxycarboxylates

The $[M\text{-}H\text{-}H_2O]^-$ ions also undergo an alternative radical cleavage reaction via CID. In the MS^3 spectrum of 2-hydroxyhexanoate (figure 3.3**c**) and 2-hydroxyoctanoate (figure 3.4**c**) the $[M\text{-}H\text{-}H_2O]^-$ ions show the elimination a different neutral radical to generate *m/z* 84 distonic radical anions (RI 5 and 15, respectively). The radical reaction forming the *m/z* 84 ions is illustrated on the fragmentations trees (figure 4.7 and 4.8) to the bottom right of the $[M\text{-}H\text{-}H_2O]^-$ ions.

Based on the spectral data, MS^3 fragmentation of the $[M\text{-}H\text{-}H_2O]^-$ ions will generate the *m/z* 84 distonic radical anions provided the $[M\text{-}H\text{-}H_2O]^-$ ions have a minimum of a six-carbon chain, as this MS^3 product ion (*m/z* 84) is not formed from 2-HAs^- containing five (or less) carbon atoms in its carbon chain (refer to spectra in figure 3.1**c**, 3.2**c**, 3.5**b,** 3.6**c** and 3.8**c**).

5.5.6 The unique loss of 44 mass units from the $[M\text{-}H\text{-}H_2O]^-$ fragment ion of 2-hydroxy-4-methylpentanoate

There is one MS^3 product ion that was only generated from the $[M\text{-}H\text{-}H_2O]^-$ ions of 2-hydroxy-4-methylpentanoate. This product ion has a *m/z* of 69 (RI 10), therefore formed through the elimination of 44 mass units (refer to spectra in figure 3.8**c**). The elimination of 44 mass units from the $[M\text{-}H\text{-}H_2O]^-$ ion (*m/z* 113) is illustrated on the fragmentation tree of 2-hydroxy-4-methylpentanoate (figure 4.6) descending to the left of the $[M-H-H_2O]^-$ ion.

The loss of 44 could be a CO_2 elimination; however, that would likely result in an unstable carboanion (as all oxygen atoms would have been eliminated). Based on the low spectral intensity of the *m/z* 69 ion, it is more reasonable to suggest that the $[M-H-H_2O]^-$ ion loses CO (already addressed in section *5.5.1*) followed by a loss of CH_4 (28 + 16 = 44 mass units). Although the *m/z* 85 ions ($[M-H-H_2O-CO]^-$) could not be fragmented to generate MS^4 fragments (due to insufficient detection), it is likely the elimination of CH_4 would have been observed in their MS^4 spectrum. This is because, as stated in section *5.5.1*, the structures of the $[M-H-H_2O-CO]^-$ ions are likely the same as the $[M-H-H_2CO_2]^-$ ions; and the $[M-H-H_2CO_2]^-$ ions from 2-hydroxy-4-methylpentanoate readily eliminate CH_4 via CID (refer to MS^3 spectrum in figure 3.8**d**).

5.5.7 Additional MS^3 fragmentation unique to the $[M-H-H_2O]^-$ fragment ion of 2-hydroxy-2-methylbutanoate

The $[M-H-H_2O]^-$ fragments from 2-hydroxy-2-methylbutanoate (*m/z* 99) generated three distinct MS^3 fragment ions. The fragments have a *m/z* of 73 (RI 15), 59 (RI 10) and 57 (RI 8) (refer to spectrum in figure 3.5**b**). Formation of the *m/z* 73 product ion is illustrated directly below the $[M-H-H_2O]^-$ ion (*m/z* 99) in the fragmentation tree (figure 4.3). The pathway that forms the *m/z* 59 ions is found descending to the left of the *m/z* 99 ion and directly to the left of the *m/z* 99 ion is the pathway that forms the *m/z* 57 ions (refer to fragmentation tree in figure 4.3).

Neutral mass loss assignments were more difficult regarding to the formation of the *m/z* 73, 59 and 57 ions. The *m/z* 73 ion is 26 mass units smaller than the $[M\text{-}H\text{-}H_2O]^-$ ion. This could correlate to a loss of ethyne (C_2H_2). There is a difference of 40 mass units between the $[M\text{-}H\text{-}H_2O]^-$ ion and its *m/z* 59 product. This elimination may be the loss of C_3H_4 (cyclopropene, $H_2C{=}C{=}CH_2$ or $HC{\equiv}C\text{-}CH_3$) or C_2O. The *m/z* 57 ion has a mass 42 units smaller than the $[M\text{-}H\text{-}H_2O]^-$ ion. This could be the elimination of C_3H_6 (cyclopropane or $H_2C{=}CH\text{-}CH_3$) or H_2C_2O ($H_2C{=}C{=}O$, $HC{\equiv}C\text{-}OH$ or oxirene (unsaturated three-membered ring)).

There is also the possibility of a product ion that readily forms bonds with solvent molecules. Ion solvent adducts have been documented in a number in MS^n studies for both positive and negative ions, especially with regards to water and methanol adducts.[49, 50] In addition, it has been well documented that a ketene functional group will readily incorporate solvent molecules into its structure.[52-55] As a result, solvent adduct formation cannot be ruled out when looking to explain formation of the *m/z* 59, 73 and 71 ions from the $[M\text{-}H\text{-}H_2O]^-$ ions of 2-hydroxy-2-methylbutanoate (figure 3.5**b**). For example, if the $[M\text{-}H\text{-}H_2O]^-$ ion dissociated to yield MS^3 products with a *m/z* 41 then the incorporation of H_2O (18 mass units) or methanol (32 mass units) via solvent adduct would result in ions detected at *m/z* 59 and 73, respectively. Alternatively, the $[M\text{-}H\text{-}H_2O]^-$ ion may generate *m/z* 39 fragments that form water or methanol adducts, thus be detected in the MS^3 spectrum at *m/z* 57 and 71. Considering there are a number of possibilities for assigning the neutral mass eliminations yielding the *m/z* 73, 59 and 57 product ions, their assignments within the fragmentation tree remain numerical rather than elemental (figure 4.3).

CHAPTER 6: HYDROGEN-DEUTERIUM EXCHANGE (HDX) STUDIES ON HYDROXYCARBOXYLATES

Hydrogen-deuterium exchange (HDX) is a simple way of D-labeling of compounds containing functional group(s) that can be involved in the process of a proton transfer in solution. Neutral hydroxycarboxylic acids (HAs) contain two functional groups (OH and COOH) that can exchange their protons with protons present in aqueous solution.[56] It is important to note that if HAs are dissolved in D_2O (source of D^+ in solution) [57], OH and COOH groups will participate in HDX. [56] As a result of the HDX process, HAs will accommodate (to some extent) D-labeled OD and COOD groups in their structure. Such a conversion of HA to its D-labeled analogue is useful in MS studies of their dissociation reactions. Although a deuteron from a COOD group is lost during electrospray ionization, the deuterium of the deuteroxyl group provides additional information with respect to all fragmentation reactions involving this particular atom. DO-labeled hydroxycarboxylates are detected at an *m/z* one unit higher than the unlabeled species, thus they can be independently examined in tandem mass spectrometry experiments.

Three of the linear 2-HAs (2-hydroxyacetic acid, 2-hydroxybutanoic acid and 2-hydroxyhexanoic acid), two of the branched 2-HAs (2-hydroxy-2-methylbutanoic acid and 2-hydroxy-3,3-dimethylbutanoic acid) and all three 3-HA compounds were selected for HDX. The mass spectrum from each of the HDX HAs^- is displayed in figures 6.1 (linear 2-HAs), 6.3 (branched 2-HAs) and 6.5 (3-HAs). Each spectrum clearly showed successful D-labeling as the D-exchanged parent ions (even *m/z*) generally had greater relative intensities than those of the non-exchanged HAs⁻ (odd *m/z*).

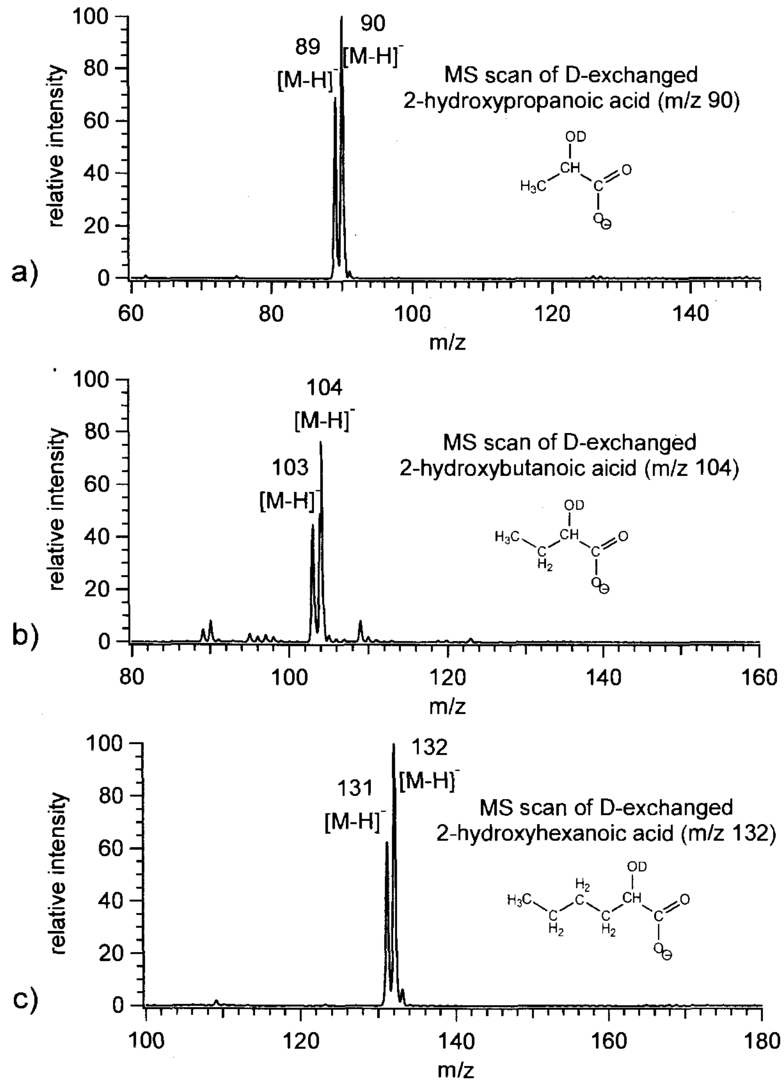

Figure 6.1: The MS scan of hydrogen-deuterium exchanged linear 2-hydroxycarboxylates. The MS spectrum of **a**) 2-hydroxyacetate (*m/z* 90) **b**) 2-hydroxybutanoate (*m/z* 104) and **c**) 2-hydroxyhexanoate (*m/z* 132) show the deuterium atom has replaced a hydrogen within the structure of the parent ion. The ions detected at *m/z* 89 (panel **a**), *m/z* 103 (panel **b**) and *m/z* 131 (panel **c**) are the parent ions that did not incorporate the deuterium.

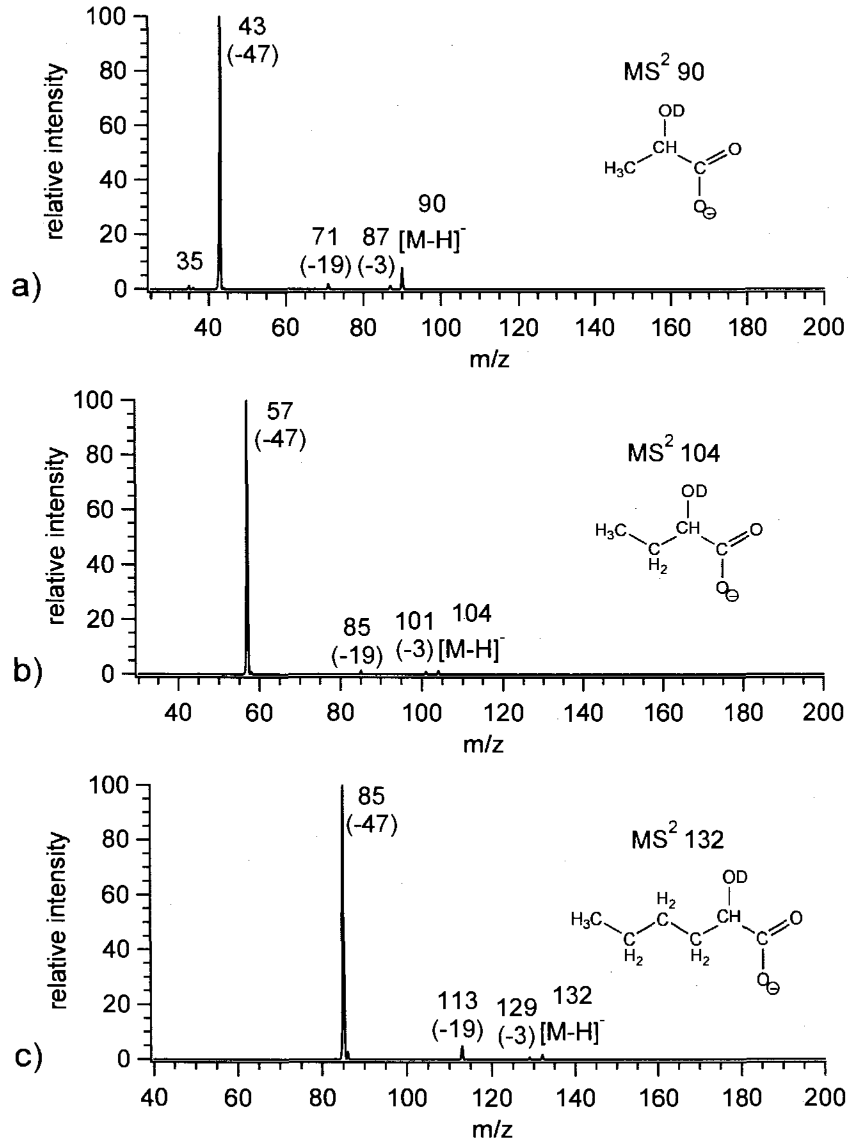

Figure 6.2: The MS^2 spectrum of HDX linear 2-hydroxycarboxylates. Panel **a** displays the MS^2 spectrum of 2-hydroxyacetate (*m/z* 90), **b** the spectrum of 2-hydroxybutanoate (*m/z* 104) and **c** the spectrum of 2-hydroxyhexanoate (*m/z* 132). The spectra were generated on a LCQ Ion Trap MS, operating in negative ion mode. NCE = 24 V.

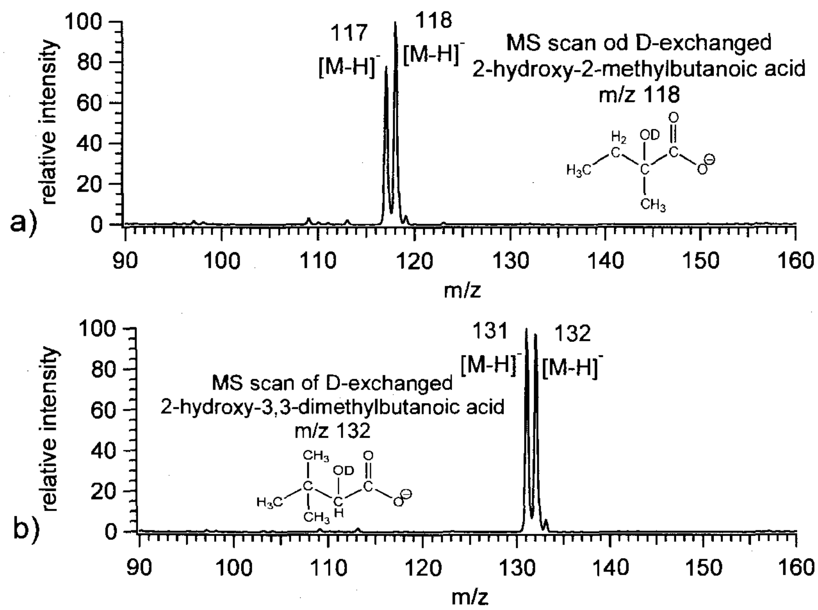

Figure 6.3: The MS scan of hydrogen-deuterium exchanged branched 2-hydroxycarboxylates. The MS spectrum of **a**) 2-hydroxy-2-methylbutanoate (*m/z* 118) and **b**) 2-hydroxy-3,3-dimethylbutanoate (*m/z* 132) show the deuterium atom has replaced a hydrogen within the structure of the parent ion. The ions detected at *m/z* 117 (panel **a**), and *m/z* 131 (panel **b**) are the parent ions that did not incorporate the deuterium.

6.1 HDX findings from Deuterium labeled 2-hydroxycarboxylates

DO-labeled molecular ions of investigated HAs were analyzed in gas phase by tandem mass spectrometry, following the hydrogen-deuterium exchange (HDX) of corresponding HAs in solution. The MS^2 analysis on the HDX 2-HAs^- was conducted to gain additional information regarding the fragmentation behaviour that leads to the formation of the three typical MS^2 products: $[M\text{-}H\text{-}H_2CO_2]^-$, $[M\text{-}H\text{-}H_2O]^-$ and $[M\text{-}H\text{-}H_2]^-$. Ion trap isolation and fragmentation of DO-labeled parent $[M\text{-}H]^-$ ions of 2-hydroxypropanoate (*m/z* 90), 2-hydroxybutanoate (*m/z* 104) and 2-hydroxyhexanoate (*m/z* 132) showed dissociation products that were detected 3, 19 and 47 units smaller than the parent ions (figure 6.2). These fragment ions correlate to the loss of HD, HOD and

$HDCO_2$ from the $[M-H]^-$ ion, respectively. Fragmentation of the DO-labeled 2-hydroxy-2-methylbutanoate (*m/z* 118) generated MS^2 product ions that were 19 and 47 mass units smaller than the parent ion (figure 6.4**a**) and DO-labeled 2-hydroxy-3,3-dimethylbutanoate (*m/z* 132) produced a product ion 3 mass units smaller (figure 6.4**b**).

Based on the HDX spectral data, it is clear that the hydroxyl group on the carbon-2 atom is involved in loss of H_2, H_2CO_2 and H_2O because the deuterium label was lost in the form of HD, $HDCO_2$ and HOD (refer to spectra in figure 6.2 and 6.4**b**).

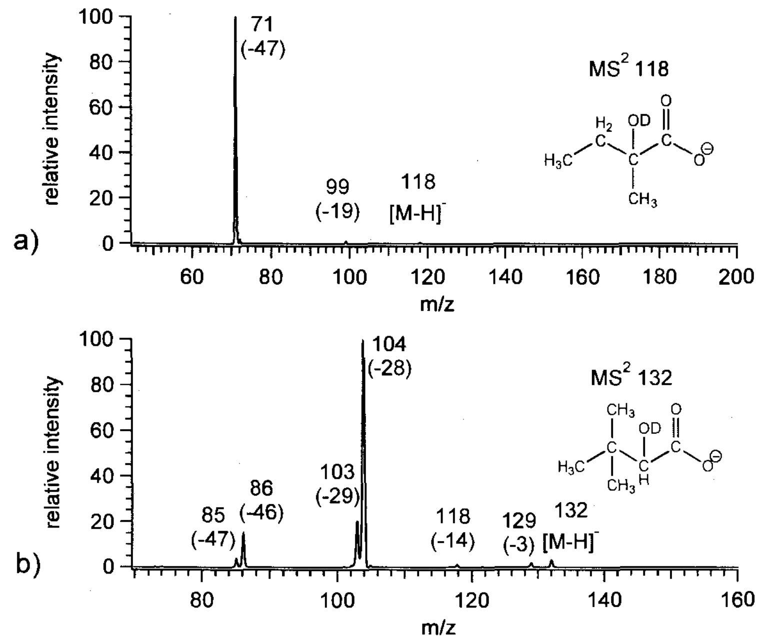

Figure 6.4: The MS^2 spectrum of HDX branched 2-hydroxycarboxylates. Panel **a** displays the MS^2 spectrum of 2-hydroxy-2-methylbutanoate (*m/z* 118) and **b** the spectrum of 2-hydroxy-3,3-dimethylbutanoate (*m/z* 132). The spectra were generated on a LCQ Ion Trap MS, operating in negative ion mode. NCE = 24 V.

6.2 Evidence of deuterium hydrogen back-exchange

Interestingly, a peak at *m/z* 103 is detected in the MS^2 spectrum of 2-deuteroxy-3,3-dimethylbutanoate (refer to spectra in figure 6.4**b**). The spectral intensity of this *m/z* 103 peak is approximately 1/5 of that of the *m/z* 104 peak. Unlike the HDX studies conducted for the other 2-hydroxycarboxylates (figures 6.2 and 6.4**a**), the fragmentation of 2-deuteroxy-3,3-dimethylbutanoate has generated fragment ions that retain the deuterium label in a product ion (the $[M\text{-}H\text{-}CO]^-$ fragments at *m/z* 104). It is likely that gas-phase interactions of the *m/z* 104 ions with water molecules, that are present in the trap, are responsible for the detection of the *m/z* 103 fragments via deuterium hydrogen back-exchange. It has been well documented in protein/peptide analysis, that the HDX (in solution) is accompanied by a significant degree of back-exchange in gas phase.[58-60] Analysis of the HDX peptides, using ESI-MS, has been reported to show deuterium hydrogen back-exchange levels varying from 10 percent to 50 percent.[58]

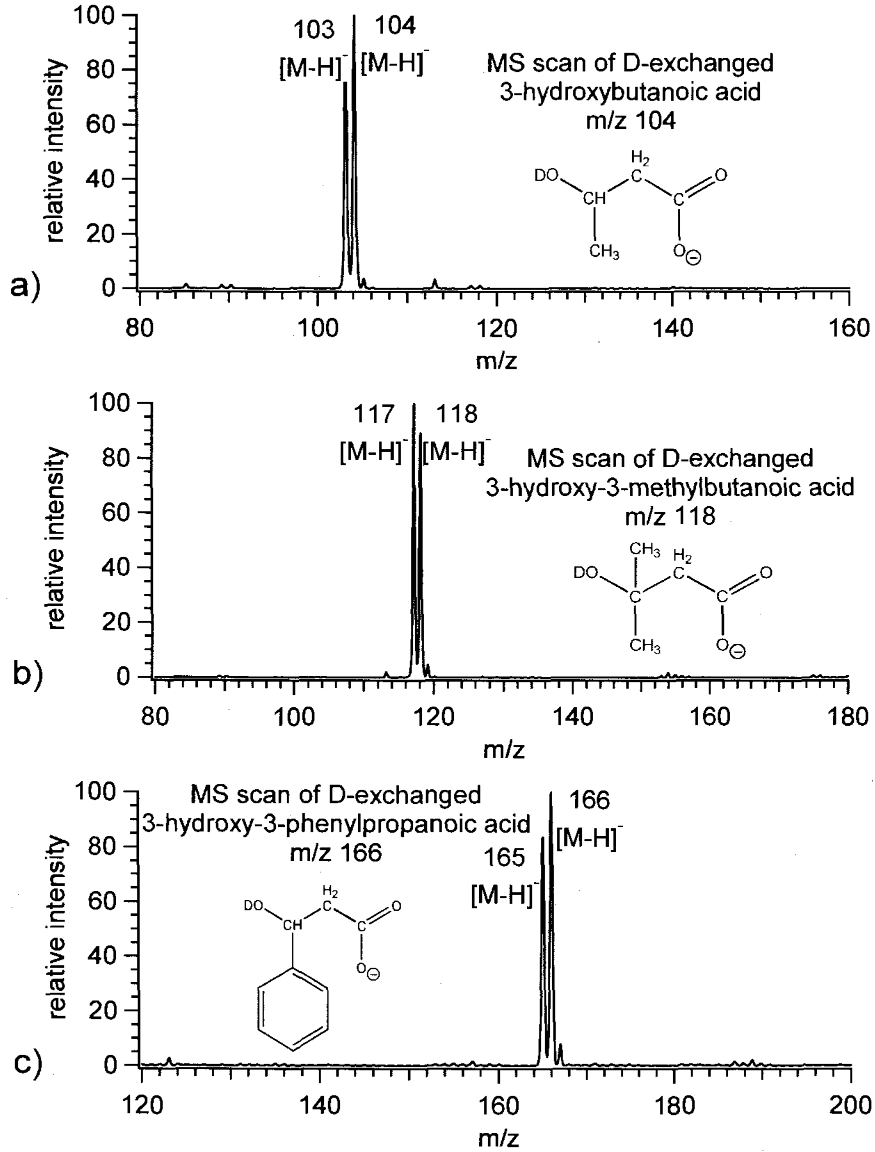

Figure 6.5: The MS scan of hydrogen-deuterium exchanged 3-hydroxycarboxylates. The MS spectrum of **a**) 3-hydroxybutanoate (*m/z* 104) **b**) 3-hydroxy-3-methylbutanoate (*m/z* 118) and **c**) 3-hydroxy-3-phenylpropanoate (*m/z* 166) show the deuterium atom has replaced a hydrogen within the structure of the parent ion. The ions detected at *m/z* 103 (panel **a**), *m/z* 117 (panel **b**) and *m/z* 165 (panel **c**) are the parent ions that did not incorporate the deuterium.

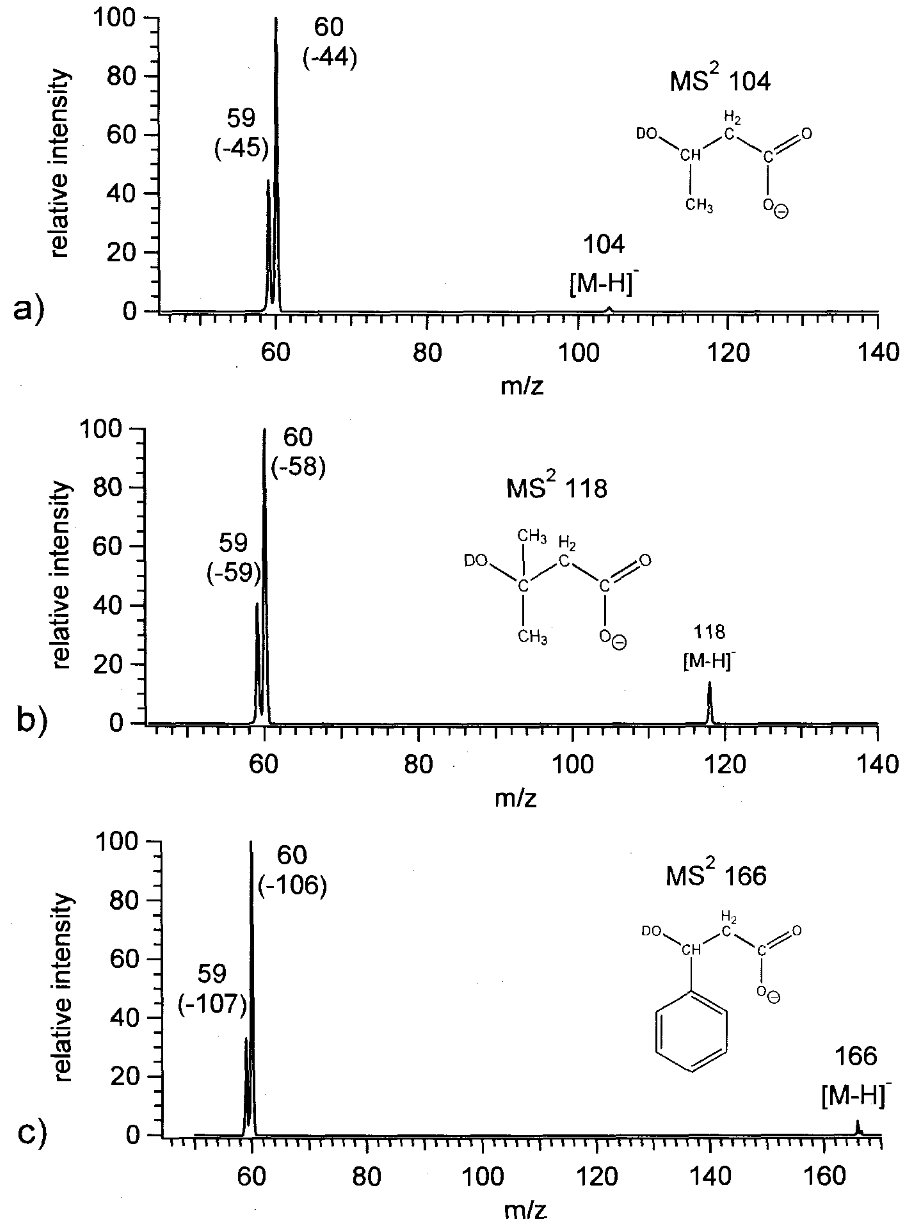

Figure 6.6: The MS^2 spectrum of HDX 3-hydroxycarboxylates. Panel **a** displays the MS^2 spectrum of 3-hydroxybutanoate (*m/z* 104), **b** the spectrum of 3-hydroxy-3-methylbutanoate (*m/z* 118) and **c** the spectrum of 3-hydroxy-3-phenylpropanoate (*m/z* 166). The spectra were generated on a LCQ Ion Trap MS, operating in negative ion mode. NCE = 24 V.

6.3 HDX findings from Deuterium labeled 3-hydroxycarboxylates

The D-labeled 3-hydroxycarboxylates were individually isolated and fragmented and their MS^2 spectra are presented in figure 6.6. 3-deuteroxybutanoate (figure 6.6**a**), 3-deuteroxy-3-methylbutanoate (figure 6.6**b**) and 3-deuteroxy-3-phenylpropanoate (figure 6.6**c**) all generate a *m/z* 60 product ion as the major fragment (RI 100). All three D-labeled parent ions also generated a *m/z* 59 fragment ion (RI 35-45). Based on the spectral data of a limited number of 3-HAs, the major CID pathway retains the hydroxyl hydrogen because the deuterium label remained on the MS^2 product ions.

The fact that a *m/z* 59 product ion was detected in all three spectra suggests there is an alternative fragmentation pathway (minor in comparison) in which the hydroxyl hydrogen is lost from the anion to generate *m/z* 59 fragments. Another possibility for the detection of the *m/z* 59 ions is deuterium back-exchange of the *m/z* 60 products. While in the gas-phase, interactions of the *m/z* 60 ions with water molecules present in the trap may be responsible for the removal of the deuterium label to result in the detection of the *m/z* 59 fragments, much like the *m/z* 103 ions detected in the MS^2 spectrum of 2-deuteroxy-3,3-dimethylbutanoate (refer to section *6.2*). Unfortunately, the HDX studies did not provide enough evidence to identify the structure or composition of the *m/z* 59 fragments; however, a structure and CID will be proposed for these products in the following chapter (*Proposed structures of fragment ions generated from hydroxycarboxylates*).

CHAPTER 7: PROPOSED STRUCTURES OF FRAGMENT IONS GENERATED FROM HYDROXYCARBOXYLATES

Structures for many of the MS^2 fragments and some of the MS^3 fragments can be proposed. The spectral data, already displayed in chapter *3*, gives important structural information regarding the atoms involved in the neutral mass elimination. Additional information regarding the neutral mass losses was obtained by conducting hydrogen-deuterium exchange (HDX) studies on the various 2-hydroxycarboxylates (previously presented). The information obtained from the HDX studies will be addressed throughout this chapter as it pertains to individual CID pathways. In addition to the HDX data, the available literature will be used to propose the various structures as well as construct possible fragmentation pathways that yield these product ions. It is important to note that the literature regarding the CID behaviour of hydroxycarboxylates is limited, thus many of the MS^n ions detected in the MS^n spectra will not be addressed throughout this chapter. The MS^2 product ions that will be discussed are the $[M\text{-}H\text{-}H_2CO_2]^-$, $[M\text{-}H\text{-}H_2O]^-$ and $[M\text{-}H\text{-}H_2]^-$ ions (*7.1*, *7.2* and *7.4*) from 2-HAs and the *m/z* 59 ions from 3-HAs (*7.5*). The $[M\text{-}H\text{-}H_2CO_2\text{-}H_2]^-$, and $[M\text{-}H\text{-}H_2CO_2\text{-}CH_4]^-$ ions will be the only MS^3 products described below (section *7.3*).

Prior to discussing the structure of the individual ions, the various classes of fragmentation processes will be revisited. Even electron organic anions will fragment by (i) reactions that are initiated by a proton transfer, (ii) rearrangement reactions including nucleophilic attack, charge and skeletal rearrangements, (iii) homolytic cleavage to form a stable radical anion and (iv) initial formation of an anion complex (such as with an neutral molecule) which may be followed elimination reactions. [44] While proposing the particular CID pathways, these four classes will be considered along with reported literature to propose the most feasible reactions that generate the MS^n products.

7.1 Proposed origins of the H_2O elimination from 2-HAs

The first pathway to be discussed is the elimination of water to yield the minor $[M-H-H_2O]^-$ products. This is because the elimination of water will be incorporated into the proposed CID pathway that generates the major MS^2 fragments, $[M-H-H_2CO_2]^-$, which is discussed in section *7.2*.

Based on the spectral data presented in chapter *3*, all 2-HAs⁻ eliminated water with the exception of 2-hydroxy-3,3-dimethylbutanoate (figure 3.7**a**), therefore the hydrogen atom on the β-carbon is involved in the loss of water. The other hydrogen atom, the hydroxyl hydrogen, was established through HDX studies and previously proposed in the literature. [13, 61, 62]

The oxygen atom involved is believed to be from the carboxyl group, according to Kerwin *et al.* They were looking at the fragmentation behaviour of 2-OH fatty acids and proposed the hydroxyl hydrogen is transferred to the carboxyl group. Following the transfer, they speculated that the loss of water must have occurred through a hydroxyl ion-neutral complex without providing a reaction mechanism. [13] Although Kerwin *et al.* have proposed the carboxyl oxygen, computational studies on small 2-HAs suggest the hydroxyl oxygen atom involved instead. [61, 62] Taking this into consideration, a CID pathway can be proposed involving the hydroxyl group and the β-hydrogen (see below).

7.1.1 Proposed CID pathway and structure of the [M-H-H_2O]$^-$ fragment ion from 2-HAs

The water elimination is likely initiated by a nucleophilic attack on the α-carbon (see Scheme **1**). As the oxygen-carbon bond forms, the hydroxyl group will form a bond with the β-hydrogen. The result would be the elimination of water and formation of an α-lactone intermediate anion. Redistribution of the negative charge will open the three-member ring forming a more stable alk-2-enoate product.

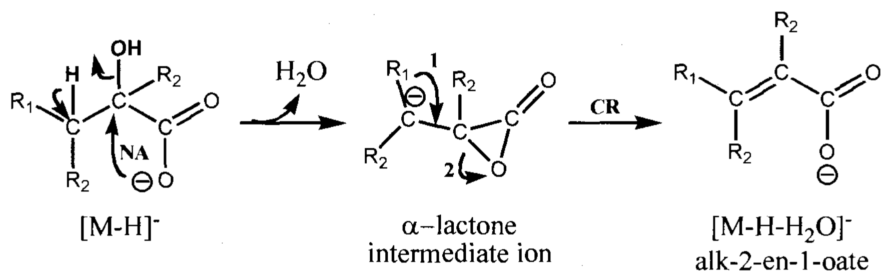

Scheme 1: Proposed water loss pathway for 2-hydroxycarboxylates. The atoms in bold font indicate those that comprise the mass elimination. Arrows indicate the movement of the electron density. NA = nucleophilic attack, CR = negative charge redistribution. R_1 = alkyl group (linear or branched) and R_2 = H or CH_4.

The reaction outlined in scheme **1** is supported with literature. Initiation via nucleophilic attack [44] on the α-carbon has already been described with regards to CID pathways of 2-hydroxyacetate. [47] The α-lactone intermediate anion is also supported through computational means [61, 62] and applied to the fragmentation of 2-hydroxyacetate.[47] Scheme **1** is supported with the spectral data (presented in chapter *3*) as it can account for the absence of the [M-H-H_2O]$^-$ fragment from 2-hydroxy-3,3-dimethylbutanoate (figure 3.7**a**).

7.2 Proposed origin of the H_2CO_2 elimination from 2-HAs

In order to propose a structure for the [M-H-H_2CO_2]$^-$ fragments the atoms involved in the mass loss must be first identified. Based on the HDX data (chapter *6*) it was established that the hydroxyl hydrogen in involved in the loss of H_2CO_2. The spectral data in chapter *3* has established that the hydrogen atom on the α-carbon is not involved in the loss of H_2CO_2 as the [M-H-H_2CO_2]$^-$ fragment was generated from 2-hydroxy-2-methylbutanoate (figure 3.5**a**). Instead, it is likely the other hydrogen atom involved is on the β-carbon, despite the moderately intense [M-H-46]$^-$ ion observed in the MS^2 spectrum of 2-hydroxy-3,3-dimethylbutanoate (figure 3.7**a**). The probable carbon source is carbon-1 and the oxygen source includes the hydroxyl oxygen and one carboxyl oxygen.

There have been a limited number of studies on the fragmentation of 2-HAs/2-hydroxy fatty acids, to which they attribute the loss of 46 to an elimination of H_2CO_2. [63-65] However, the origins of this fragment typically are not addressed. There are a few publications that look into the atoms involved in the H_2CO_2 loss and they also propose the hydroxyl hydrogen, β-hydrogen and carbon-1. However, they suggested the oxygen atoms involved are both from the carboxyl group. [12, 45] A separate study on 2-OH fatty acids proposed that the hydroxyl oxygen and one carboxyl oxygen comprise the H_2CO_2 elimination yet does not propose a CID pathway. [13] Taking this into consideration, a feasible CID pathway can be proposed involving the hydroxyl group, β-hydrogen, carbon-1 and one carboxyl oxygen (see scheme **3**).

7.2.1 The proposed CID pathway that generates the [M-H-H_2CO_2]$^-$ ions

Before proposing the mechanism for the loss of H_2CO_2, it is important to explain the CID pathway already proposed by Bandu *et al.* and Bialecki *et al.* (presented in scheme **2** [12, 45]) and why it is not in agreement with the spectral data displayed in chapter *3*. The authors of both publications examined various 2-HAs$^-$ using a triple quadrupole mass spectrometer. Based on the MS^2 spectrum generated, they propose the elimination of H_2CO_2 is carried out according to the reaction outlined in scheme **2**. A proton transfer from the hydroxyl group onto the carboxyl group initiates the heterolytic process. Redistribution of the charge releases a formic acid carboanion (*m/z* 45), which forms an ion-neutral complex with the remaining aldehyde. The *m/z* 45 ion then abstracts a proton off the β-carbon to form a resonance stable enolate (scheme **2**). [12, 45] Support for their proposed reaction is based on the detection of an *m/z* 45 ion (RI 20-50) in the corresponding MS^2 spectrum.

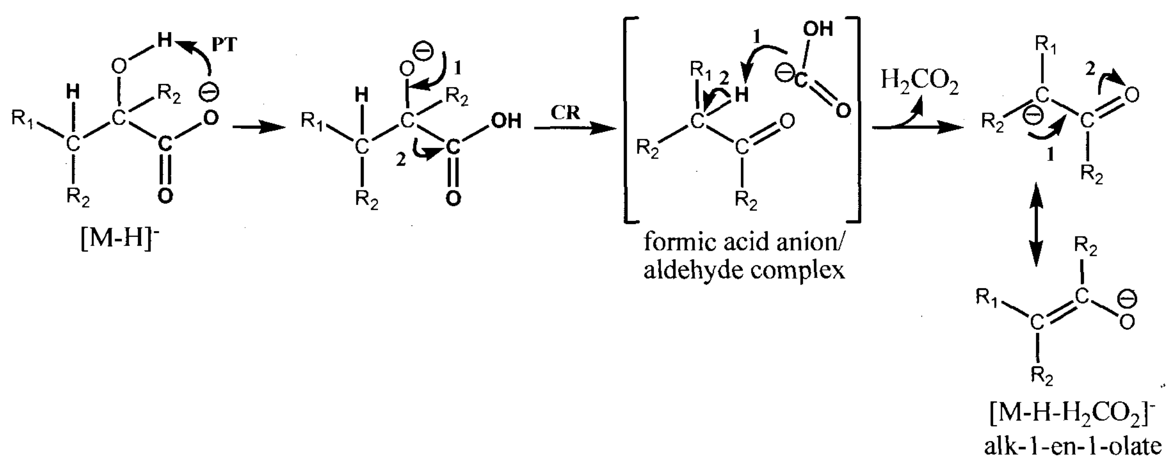

Scheme 2: The proposed CID reaction eliminating H_2CO_2 from 2-HAs$^-$ via formic acid anion (*m/z* 45)/aldehyde complex. [12, 45] The atoms in bold font indicate those that comprise the mass elimination. Arrows indicate the movement of the electron density. PT = proton transfer, CR = negative charge redistribution. R_1 = alkyl group (linear or branched) and R_2 = H or CH_4.

Unlike the MS^2 spectrum generated in the Bandu *et al.* and Bialecki *et al.* studies, [12, 45] the *m/z* 45 ion was absent in the MS^2 spectrum obtained in this study (refer to Figure 3.1**a**-3.6**a** and 3.8**a**). As a result, a feasible CID pathway is outlined in scheme **3** that incorporates a two-step elimination of water, followed by a loss of CO. The CID pathway is initiated by a nucleophilic attack on the α-carbon. A water molecule is lost by the α-hydroxyl group bonding to a β-hydrogen, which generates an α-lactone intermediate (just like in scheme **1**). Redistribution to the negative charge, to carbon-1, allows for the elimination of CO to form the same resonance stable enolate (scheme **3**) as the product ion in scheme **2**.

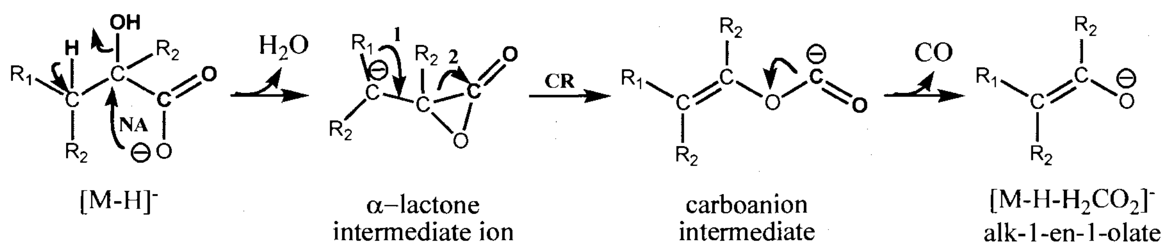

Scheme 3: The proposed CID pathway that eliminates H_2CO_2 via nucleophilic attack. The loss of water and CO generate a resonance stable alk-1-en-1-olate without forming an *m/z* 45 intermediate ion. The atoms in bold font indicate those that comprise the mass elimination. Arrows indicate the movement of the electron density. NA = nucleophilic attack, CR = negative charge redistribution. R_1 = alkyl group (linear or branched) and R_2 = H or CH_4.

The reaction outlined in scheme **3** is supported with literature. Initiation via nucleophilic attack [44] on the α-carbon has already been described with regards to CID pathways of 2-hydroxyacetate. [47] Elimination of CO from the α-lactone intermediate anion, following the loss of water, is also supported through computational means. [61, 62] In addition, the carboanion intermediate that resulted from opening the three-member ring has already been proposed to lose CO in the fragmentation study of 2-

hydroxyacetate. [47] Regardless, the reaction mechanisms illustrated in Scheme **2** and **3** both suggest the final product to be an alk-1-en-1-olate and that the $[M-H-46]^-$ fragment from 2-hydroxy-3,3-dimethylbutanoate (figure 3.7**a**) is not $[M-H-H_2CO_2]^-$ because the β-carbon does not have the required β-hydrogen atom.

7.3 Proposed origin of H_2 elimination from the $[M-H-H_2CO_2]^-$ fragment ions from 2-HAs

Based on the CID pathways proposed in scheme **2** and scheme **3**, it is likely that the $[M-H-H_2CO_2]^-$ ions are alk-1-en-1-olates. This is further supported through literature as enolates readily lose H_2 via CID. [44, 66-68] I believe the origin of the H_2 comes from the hydrogen atoms on carbon-3 and carbon-4 as this would increase the conjugation of the $[M-H-H_2CO_2-H_2]^-$ product ions, thus increase their stability. [69] In the past, cycloalkenolates have been analyzed through tandem mass spectrometry their elimination of H_2 is believed to come from their 3,4-positions. [66, 68] As a result, a pathway can be proposed for the loss of H_2 from the alk-1-en-1-olates (see below scheme **4**).

7.3.1 The proposed CID pathway and structure of the $[M-H-H_2CO_2-H_2]^-$ ions

The literature regarding the loss of H_2 from cycloalk-1-en-1-olates does not show a reaction mechanism, just a final cycloalk-1,3-dien-1-olate ion as the fragment. [66, 68] The proposed reaction mechanism in scheme **4** accounts for the 3,4-positioning loss of H_2 via redistribution of the negative charge towards carbon-3. This would result in a concerted loss of H_2 followed by charge redistribution back to the terminal oxygen atom. The final product would be a conjugated alk-1,3-dien-1-olate as the $[M-H-H_2CO_2-H_2]^-$ MS^3 product ions.

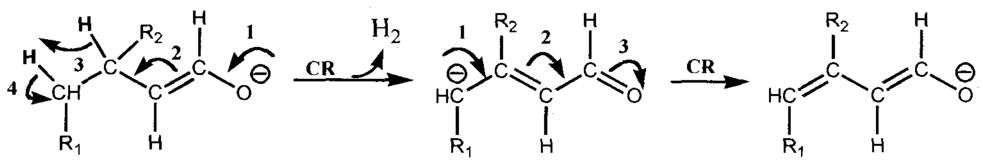

Scheme 4: The proposed CID pathway eliminating H_2 from the [M-H-H_2CO_2]$^-$ ions via negative charge redistribution. The loss of H_2 generates a stable conjugated alk-1,3-dien-1-olate. The atoms in bold font indicate those that comprise the mass elimination. Arrows indicate the movement of the electron density. CR = negative charge redistribution. R_1 = alkyl group or H and R_2 = H or CH_4.

The alk-1-en-1-olate ions, from 2-hydroxybutanoates (linear or branched), would not have a carbon-4 and thus could not eliminate H_2 from the 3,4-positions. Perhaps this is why the [M-H-H_2CO_2-H_2]$^-$ ions are not generated at the MS^3 stage (refer to spectra in figure 3.2**d**, 3.5**c** and 3.6**d**). However, the alk-1-en-1-olate ions from 2-hydroxypropanoate do not have a third or fourth carbon yet still show the [M-H-H_2CO_2-H_2]$^-$ ions in the MS^3 spectrum (figure 3.1**d**). Based on this spectral observation, an alternative pathway must be occurring for the [M-H-H_2CO_2]$^-$ ions of 2-hydroxypropanoate to achieve the loss of hydrogen that is not feasible for the analogous 2-hydroxybutanoate fragments (linear or branched).

7.3.2 Proposed origin of the CH_4 elimination from [M-H-H_2CO_2]$^-$ fragment ions formed via MS^3 analysis of 2-hydroxy-4-methylpentanoate

The [M-H-H_2CO_2]$^-$ ion from 2-hydroxy-4-methylpentanoate is believed to be 3-methylbut-1-en-1-olate based on the product ions formed in scheme **2** and scheme **3.** I believe the origin of the CH_4 comes from the methyl group on carbon-3 and the hydrogen atom carbon-4. This would increase the conjugation of the [M-H-H_2CO_2-CH_4]$^-$ product ions, thus increase their stability. [69] In the past, 3-methylcycloalkenolates have been analyzed through tandem mass spectrometry their elimination of CH_4 is believed to come from their 3,4-positions. [66, 68] As a result, a pathway can be proposed for the loss of CH_4 from the 3-methylbut-1-en-1-olate (see below scheme **5**).

7.3.3 The proposed CID pathway and structure of the $[M\text{-}H\text{-}H_2CO_2\text{-}CH_4]^-$ ions

The literature regarding the loss of CH_4 from a 3-methylcycloalk-1-en-1-olate does not show a reaction mechanism, just a linear cycloalk-1,3-dien-1-olate ion as the product ion. [66, 68] The proposed reaction mechanism in scheme **4** (H_2 elimination) has been applied to the 3-methylbut-1-en-1-olate ion; however, the reaction mechanism was modified to incorporate the loss of the 3-methyl group via negative charge redistribution (see scheme **5**). This would result in a concerted loss of CH_4 followed by charge redistribution back to the terminal oxygen atom. The final product would be a conjugated linear alk-1,3-dien-1-olate as the $[M\text{-}H\text{-}H_2CO_2\text{-}CH_4]^-$ MS^3 product ions.

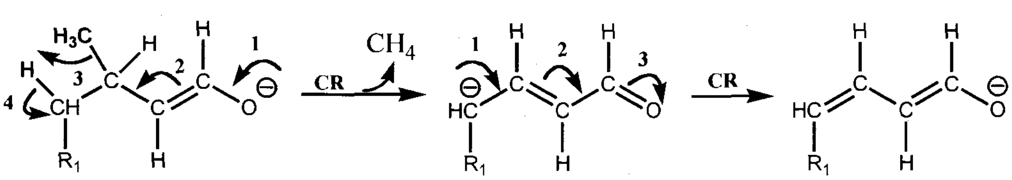

$[M\text{-}H\text{-}H_2CO_2]^-$
alk-1-en-1-olate

$[M\text{-}H\text{-}H_2CO_2\text{-}H_2]^-$
alk-1,3-dien-1-olate

Scheme 5: The proposed CID pathway eliminating CH_4 from the $[M\text{-}H\text{-}H_2CO_2]^-$ ions via negative charge redistribution. The loss of CH_4 generates a stable conjugated alk-1,3-dien-1-olate. The atoms in bold font indicate those that comprise the mass elimination. Arrows indicate the movement of the electron density. CR = negative charge redistribution. R_1 = alkyl group or H.

7.4 The proposed origin of the H_2 elimination from 2-HAs

Based on the spectral data presented in chapter *3*, all 2-hydroxycarboxylates eliminated molecular hydrogen with the exception of 2-hydroxy-2-methylbutanoate (figure 3.5**a**), therefore the hydrogen atom on the α-carbon is involved in the loss of H_2. The other hydrogen atom, the hydroxyl hydrogen, was established through HDX studies as the analogous HD loss was observed (refer to spectrum in figure 6.2 and 6.4**b**). Previous studies on 2-hydroxyacetate [47] and dihydroxycarboxylates have observed the loss of H_2 and also propose the origin of hydrogen to be the hydroxyl hydrogen and the hydrogen atom bonded to the carbon bearing the hydroxyl group. [64, 70, 71] As a result, a CID pathway can be proposed for the loss of H_2 incorporating both hydrogen atoms (see scheme **6** below).

7.4.1 The proposed CID pathway and structure of the [M-H-H₂]⁻ ions

Previous studies on dihydroxycarboxylates have led the authors to propose the loss of H_2 to occur via homolytic cleavage; [64, 70, 71] however, if this were the case then the spectra presented in chapter *3* would show peaks correlating to $[M\text{-}H\text{-}H\bullet]^-$ ions along with the $[M\text{-}H\text{-}H_2]^-$ ions. The $[M\text{-}H\text{-}H\bullet]^-$ radical anions were not observed in the corresponding MS^2 spectrum and thus an alternative CID pathway has been proposed (scheme **6**).

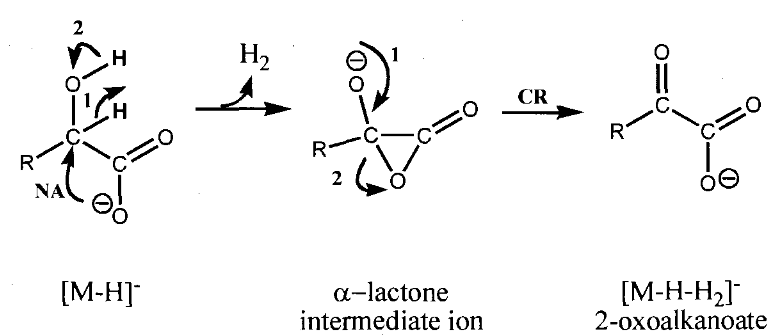

Scheme 6: The proposed CID pathway eliminating H_2 from 2-hydroxycarboxylates via nucleophilic attack. The elimination of H_2 generates 2-oxoalkanoates as the $[M\text{-}H\text{-}H_2]^-$ products. The atoms in bold font indicate those that comprise the mass elimination. Arrows indicate the movement of the electron density. NA = nucleophilic attack, CR = negative charge redistribution. R = alkyl group (linear or branched).

The proposed elimination of H_2 from 2-hydroxycarboxylates (scheme **6**) is initiated by a nucleophilic attack on the α-carbon. This would cause the α-carbon-hydrogen bond to break and form a bond with the hydrogen atom on the hydroxyl group. The concerted loss of H_2 would form an α-lactone intermediate ion. Redistribution of the negative charge opens the three-member ring to yield 2-oxoalkanoates as the $[M\text{-}H\text{-}H_2]^-$ fragments (scheme **6**). This pathway is supported with computational calculations (regarding the α-lactone intermediate) [61, 62] and has already been applied to the formation of the $[M\text{-}H\text{-}H_2]^-$ ions from 2-hydroxyacetate. [47]

7.5 Proposed elemental composition of the m/z 59 fragment ions generated from 3-HAs

The possible elemental compositions for the *m/z* 59 product ions, from 3-hydroxycarboxylates, are either $C_2H_3O_2^-$ or $C_3H_7O^-$. Based on the MS^2 spectra presented in chapter *3* (figure 3.9) it is clear that a hydrogen on carbon-3 is not involved in the formation of the *m/z* 59 ion since 3-hydroxy-3-methylbutanoate generated this fragment (refer to spectrum in figure 3.9**b**). In addition, the MS^2 spectrum from 3-hydroxy-phenylpropanoate has determined a carbon-4 atom is not required to generate the *m/z* 59 ions (figure 3.9**c**) as it only has a three-carbon chain. It was determined through HDX studies that the hydroxy hydrogen is incorporated in to the *m/z* 59 ion as the D-labeled parent ions generated *m/z* 60 fragments (refer to figure 6.6). As stated earlier in section *6.3*, deuterium back-exchange of the *m/z* 60 ions is suspected (accounting for the *m/z* 59 ions) and therefore the hydroxyl hydrogen/deuterium would be bonded to an oxygen atom.

The m/z 59 ions have been observed in the MS^2 spectrum of complex 3-hydroxy acids (multiple functional groups and aromatic rings) [72, 73] and suspected to be acetate ($C_2H_3O_2^-$). Unfortunately, CID pathways yielding the acetate ion were not proposed. Therefore, a CID pathway has been proposed for the 3-HAs that result in m/z 59 ions with the elemental composition of $C_2H_3O_2^-$ (see scheme **8**). The pathway will form the product ion comprised of the hydroxyl hydrogen, both hydrogen atoms on carbon-2, carbon-2 and the carboxyl moiety.

7.5.1 Possible fragmentation pathways that lead to the formation of the m/z 59 ions

The CID pathway that forms the m/z 59 ions, from 3-hydroxycarboxylates, is illustrated in scheme **8** and resembles the McLafferty rearrangement. The McLafferty rearrangement has typically been described with radical cations [74-76] but has been proposed for even electron cations as well (metal cationized esters). [77] In a McLafferty rearrangement, the γ-hydrogen (hydrogen atom bonded to the atom in the γ position) is transferred through a six-membered cyclic transition state onto a formerly unsaturated group. This is followed by subsequent bond cleavage between the atoms in the α and β-positions. [76] An example of the McLafferty rearrangement is presented in scheme **7** using radical cations of carbonyl systems. Once the hydrogen is transferred to the carbonyl group (γ-hydrogen rearrangement), electron redistribution results in the loss of an alkene via homolytic cleavage of the α,β-bond (scheme **7**). A similar even electron reaction can be applied to the 3-hydroxycarboxylates to account for the formation of the m/z 59 products (see scheme **8**).

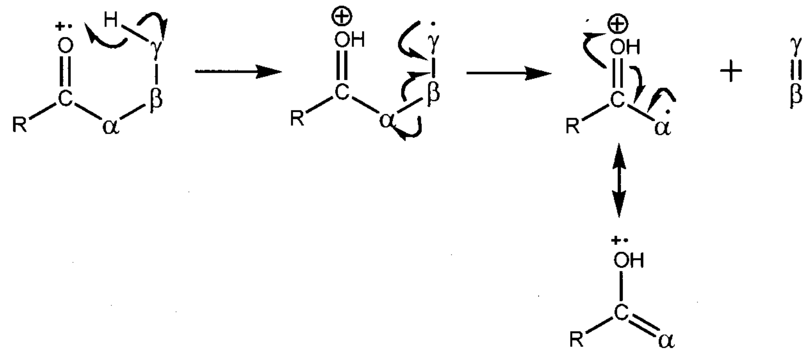

Scheme 7: An example of the McLafferty rearrangement using carbonyl radical cations. The arrows indicate the movement of one electron. The Greek symbols indicate the atom's position with respect to carbon-1. [75]

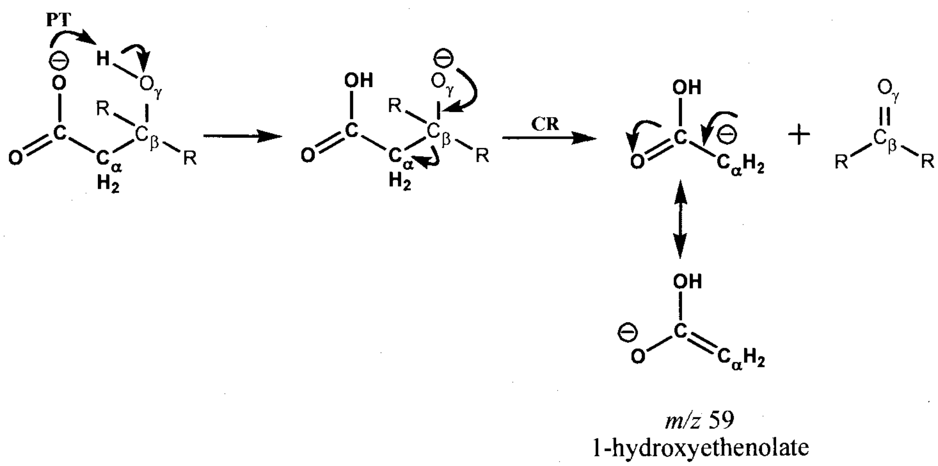

Scheme 8: The proposed McLafferty-type rearrangement of 3-hydroxycarboxylates that generates the *m/z* 59 fragments. The Greek symbols indicate the atom's position with respect to carbon-1. The atoms in bold font indicate those that comprise the *m/z* 59 ion. Arrows indicate the movement of the electron density. PT = proton transfer, CR = negative charge redistribution. R = alkyl group, phenyl group or hydrogen atom.

The proposed CID pathway that forms the *m/z* 59 fragments (scheme **8**) is initiated with a proton transfer off the hydroxyl group. Subsequent redistribution of the negative charge will eliminate a neutral ketone/aldehyde to generate resonance stable 1-hydroxyethenolate (*m/z* 59). The initial proton transfer in scheme **8** is analogous to the γ-hydrogen rearrangement in McLafferty reactions. The elimination of a ketone/aldehyde (scheme **8)** is achieved through heterolytic cleavage of the α,β-bond, whereas the comparable cleavage of this bond in the McLafferty reaction (scheme **7**) is homolytic. This reaction complies with MS^2 spectra presented in figure 3.9 (chapter *3*) as it can account for the detection of the *m/z* 59 ions regardless of branching on carbon-3. This reaction also accounts for the *m/z* 59 ions in the HDX MS^2 spectra because the product ion (1-hydroxyethenolate) could undergo deuterium back-exchange of 1-deuteroxy group. Additional support to this CID pathway comes from a previous proposal of this McLafferty-type dissociation pathway towards 3-aminocarboxylates, some amino acids and 3-hydroxybutanoate. [74]

CHAPTER 8: CONCLUSIONS AND FUTURE WORK

By conducting controlled CID experiments, using negative mode ESI-QIT-MS, a better understanding of the gas phase dissociation chemistry of aliphatic HAs^- was obtained. This knowledge allowed for fragmentation profiles to be ascertained for both 2- and 3-HAs^-. There is a distinct difference in the fragmentation behaviour between HAs^- depending on location of the hydroxyl group (carbon-2 versus carbon-3). Regardless of methyl branching or a phenyl group on carbon-3, fragmentation of 3-HAs^- result in the formation of a single fragment ion with a *m/z* 59. Incorporation of the HDX studies on 3-HAs has show the fragment ions retain the deuterium label, to yield *m/z* 60 fragments (RI 100). However, HDX studies also suggest the deuterium is bonded to an oxygen atom as the spectra shows (in figure 6.6) evidence of deuterium back-exchange, revealing a less intense *m/z* 59 peak. This indicates these *m/z* 59 ions are likely 1-hydroxyethenolates, based on the proposed fragmentation pathway illustrated in scheme **8**.

The gas phase chemistry of 2-HAs$^-$ is more complex than 3-HAs$^-$ and their spectral complexity increases as the length of the aliphatic chain increases. The general CID behaviour has been established, at the MS^2 stage, for 2-HAs$^-$. With the exception of 2-hydroxyacetate, fragmentation of 2-HAs$^-$ results in the formation of [M-H-H_2CO_2]$^-$, [M-H-H_2O]$^-$ and [M-H-H_2]$^-$ fragments when using a QIT for the tandem MS analysis.

The major fragment generated from 2-HAs$^-$ was the [M-H-H_2CO_2]$^-$ ion. By incorporating HDX studies the hydroxyl hydrogen was identified as one of the hydrogen atoms involved in this mass loss. Literature identified the other hydrogen as that on the β-carbon. [45] The results in this current study agree, however a moderately intense [M-H-46]$^-$ ion was observed in the MS^2 spectrum of 2-hydroxy-3,3-dimethylbutanoate (refer to figure 3.7**a**). This study was unable to identify the composition of this mass elimination and therefore, tandem MS analysis on an isotopically labeled analogue of this 3,3-dimethyl 2-HA$^-$ (which are not commercially available) would need to be conducted. For example, oxygen isotopes (^{18}O) in the carboxyl moiety as well as the hydroxy moiety would be able to establish whether or not two oxygen atoms are involved in this mass loss. If the loss of 46 is the loss of H_2CO_2, then the ^{18}O labeled compound would show a peak correlating to a [M-H-50]$^-$ ion in the MS^2 spectrum. As speculated earlier, the loss of 46 mass units may be the sequential loss of CO followed by a concerted loss of CH_4 and H_2. By tandem MS analysis on an ^{18}O labeled species, the MS^2 spectrum would show a moderately intense peak correlating to [M-H-48]$^-$ ions, instead of the presumptive [M-H-50]$^-$ ions. Similarly, if the six carbon atoms in 2-hydroxy-3,3-dimethylbutanoate were carbon isotopes (^{13}C) the loss of 47 mass units would determine the loss to be H_2CO_2, whereas the loss of 48 would identify CO followed by a concerted CH_4 and H_2 as the neutral elimination. Excluding the $[M-H-46]^-$ ion from the 3,3-dimethyl 2-HA^-, a feasible structure has been proposed for the $[M-H-H_2CO_2]^-$ ions. Although the pathway to which it is formed has yet to be concluded (scheme **2** vs. scheme **3**), it is likely these ions are alk-1-en-1-olates.

The other two peaks typically observed in the MS^2 spectrum of 2-HAs^- correlate to the $[M-H-H_2O]^-$ and $[M-H-H_2]^-$ ions, both of which are observed with low spectral intensities (RI<5). In both cases, the complimentary HDX studies identified the hydroxyl hydrogen as part of the mass elimination. The second hydrogen in the loss of H_2 is that on the α-carbon, which was determined with the analysis of 2-hydroxy-2-methylbutanoate (see figure 3.5**a**). Methyl branching at carbon-2 inhibited H_2 elimination, thus identifying the carbon-2 hydrogen as part of this mass loss. The structure of the $[M-H-H_2]^-$ fragment would be a 2-oxoalkanoate if the pathway proposed in scheme **6** is correct.

The second hydrogen comprising the water loss was determined to be one on carbon-3. This was established through the analysis of 2-hydroxy-3,3-dimethylbutanoate as its MS^2 spectrum (figure 3.7**a**) does not show a peak correlating to the $[M-H-H_2O]^-$ ion. It is likely the hydroxyl oxygen accounts for the oxygen atom in the water loss; however, the current study could not conclude its involvement. Again, tandem MS analysis on an ^{18}O analogue (either located in the hydroxyl moiety or the carboxyl group) can determine which oxygen atom is involved. Provided the CID pathway illustrated in scheme **1** is correct, the structure of the $[M-H-H_2O]^-$ fragments are alk-2-en-1-oates.

When looking to identify unknown compounds, tandem mass spectrometry at the MS^2 stage can provide clues to assist with structural elucidation. Based on the results of this current fragmentation study, observation of the three characteristic fragment ions (intense $[M-H-H_2CO_2]^-$, minor $[M-H-H_2O]^-$ and $[M-H-H_2]^-$) in the MS^2 spectrum would strongly suggest the unknown to be a 2-HA$^-$. The MS^2 stage can also establish methyl branching to a degree, as branching at particular carbon atoms will result in the absence of one of these characteristic fragments. Unfortunately, some isomers could not be distinguished from one another (such as 2-hydroxyhexanoate and 2-hydroxy-4-methylpentanoate) with MS^2 analysis.

This current study is an excellent example of how the QIT MS is the preferred mass analyzer to use when looking at fragmentation profiles. By conducting higher order tandem mass spectrometry, 2-HA$^-$ isomers can be distinguished from one another when MS^2 analysis alone could not. The MS^3 analysis of the $[M-H-H_2CO_2]^-$ ions is one example that can establish whether the carbon chain (of the parent 2-HA$^-$) is four carbons in length or greater. If the 2-HA$^-$ has a carbon chain at least five carbons in length, their $[M-H-H_2CO_2]^-$ ions will show a prominent loss of H_2 in their corresponding MS^3 spectrum. However, if the parent 2-HA$^-$ ion has only a four carbon-chain then the corresponding MS^3 spectrum will not show the $[M-H-H_2CO_2-H_2]^-$ products, or any other product ions (figure 3.2**a** and 3.6**a**). This finding would allow 2-hydroxypentanoate to be distinguished from a methyl branched 2-hydroxybutanoate.

Another example deals with 2-hydroxyhexanoate and 2-hydroxy-4-methylpentanoate. Their corresponding MS^2 spectra look identical (see figure 3.3**a** and 3.8**a**); however, it is the variations in their MS^3 spectra that allow them to be distinguished from one another. As mentioned, a predominant loss of H_2 occurs when fragmenting the $[M-H-H_2CO_2]^-$ ions. However, this corresponding fragment was detected with low spectral intensity in the MS^3 spectrum of 2-hydroxy-4-methylpentanoate. Instead, a favourable loss of methane was observed (figure 3.8**d**). Therefore, if an unknown 2-HA$^-$ has methyl branching at the carbon-4 position, the branching can be identified because the MS^3 spectrum will reveal a prominent loss of methane instead of H_2.

One last example of how MS^3 analysis can offer structural information of unknown 2-HAs$^-$ is by fragmenting the $[M-H-H_2O]^-$ ions. Typically, upon CID, there is a predominant CO elimination but extensive fragmentation accompanies the loss of CO for the ions containing more than a four-carbon chain. Also, by looking at the radical reactions that are observed in the MS^3 spectrum, ions with at least six carbons in their carbon chain can be distinguished from ions with a five-carbon chain. The former generates two distonic radical anions (at *m/z* 58 and 84, see figure 3.3**c** and 3.4**c**) and the later only generates one (the *m/z* 58 ion, see figure 3.8**c**).

The current study has illustrated how analysis of a class of compounds on QIT MS is not only capable of identifying fragmentation trends but identifying CID pathways that can be used to distinguish between isomeric compounds. The current study limited its analysis to aliphatic saturated 2-HAs and 3-HAs. This study did not include halogenated HAs. Future work could be conducted in the same manor to determine how halide substituants may change the general fragmentation behaviour of these organic acids. Although one of the 3-HAs studied (3-hydroxy-3-phenylpropanoic acid) contained an aromatic substituant, none of the 2-HAs studied did. The addition of an aromatic group to the 2-HAs would most likely result in extensive MS^n analysis as it would stabilize the MS^n fragments formed (providing the aromatic group was not eliminated as a neutral). However, without experimental data this can only be speculated. This study also omitted 2-HAs containing more than one hydroxyl and carboxylic group, thus the variations in CID patterns remain to be explored.

By understanding the gas phase chemistry of HAs, and their fragment ions, the knowledge can be applied to other ESI-MS^2 studies to help identify non-target HAs. The information gained in this study could be used as a basic profile that can be expanded up on following detailed comprehensive analyses of other HAs and similar compounds (that may contain halides, phenyl or additional carboxyl/hydroxyl groups). Expanding the CID profiles would be beneficial as it would generate a structural elucidation tool that can be used for identification purposes.

Since hydroxycarboxylic acids (HAs) were found to be abundant contaminants in drinking water, [14] future research into developing an LC/MS/MS method for the quantification of target HAs (such as 2-hydroxyacetic acid) and the identification of other non-target HAs in water samples (through the use of fragmentation profiles) should be explored. A combination of an efficient liquid separation technique with mass spectrometry detection would be required for such analysis due to the high complexity of water samples. Ideally, this method would use nano-flow capillary ultra-high performance liquid chromatography (UPLC), nanospray ionization (nESI), and a high resolution mass analyzer such as the quadrupole-time-of-flight-mass spectrometry (Q-TOF-MS). [16] Once a UPLC-nESI-Q-TOF MS method is established and optimized (using commercially available standards) water samples can then be analyzed with this LC-MS/MS system.

Although 2-hydroxyacetic acid and other non-halogenated HAs are not currently considered contaminants of concern, [78-80] future water research may change this perspective. 2-hydroxyacetic acid was found to be present at high ppm concentration, in a sample of Canadian chlorinated drinking water. [14] Establishing the source of contamination may be significant as they are thought to be disinfection byproducts. Development of such a method could be applied to a range of water samples (pre and post-disinfection, and even source water) to determine the abundance of HA contamination in Ontario; correlations between HA concentrations and the content of natural organic matter in drinking water; as well as correlations between water disinfection regimes and HA contamination.

9. REFERENCES

1. Datta, R.; Henry, M. *J. Chem. Technol. Biotechnol.* **2006**, *81*, 1119-1129.
2. Kitzmiller, W.; Visscher, M.; MacLennan, S.; Butterfield, J.; Fuhrman, E.; Doughty, D.; Dawes, N. *Aesthet. Surg. J.* **2003**, *23*, 339-344.
3. Anh, K.; Park, K.; Jung, K.; Jung, H.; Lee, S.; Chung, S.; Yang, K.; Yun, Y.; Pyo, H.; Park, Y.; Yun, Y.; Kim, D.; Park, S.; Hong, J. *Cancer Lett.* **2002**, *186*, 125.
4. Furukawa, F.; Yamamoto, Y. *J. Dermatol.* **2006**, *33*, 655-661.
5. Ng, L.; Lafontaine, P.; Harnois, J. *J. Chromatogr. A.* **2000**, *873*, 29-38.
6. Miwa, H. *J. Chromatogr. A* **2000**, *881*, 365-385.
7. Carballo, R.; Covelo, B.; Vázquez-López, E. *Z. Anorg. Allg. Chem.* **2002**, *628*, 468-472.
8. Smith, G.; Reddy, A.; Byriel, K.; Kennard, C. *Aust. J. Chem.* **1994**, *47*, 1179-1183.
9. Cuin, A.; Massabni, A.; Leite, C.; Sato, D.; Neves, A.; Szpoganicz, B.; Silva, M.; Bortoluzzi, A. *J. Inorg. Biochem.* **2007**, *101*, 291-296.
10. King, J.; Winters, C.; Stickler, D. *Méd. Mal. Infect.* **1992**, 614-620.
11. Mathews, C.; Van Holde, K.; Ahern, K. *Biochemistry*, 3rd Ed. NY; Addison Wesley Longman, Inc., 2000, 648-651.
12. Bandu, M.; Grubbs, T.; Kater, M.; Desaire, H. *Int. J. Mass Spectrom.* **2006**, *251*, 40-46.
13. Kerwin, J.; Torvik, J. *Anal. Biochem.* **1996**, *237*, 56-64.
14. Sultan, J.; Gabryelski, W. *Anal. Chem.* **2006**, *78*, 2905-2917.

15. De Laat, J.; Bawa, M.; Dore, M. *Environ. Technol.* **1995**, *16*, 1035-1048.

16. Gross, J. *Mass Spectrometry – A Textbook.* NY; Springer, 2004. Pg 145-164, 193-218.

17. Dass, C. *Principles and Practice of Biological Mass Spectrometry.* NY; John Wiley & Sons, Inc., 2001. Pg. 11-14, 146-148.

18. Ford, Q.; Burns, J.; Ferry, J. *J. Chromatogr. A.* **2007**, *1145*, 241-245.

19. Liebich, H.; Gesele, E.; Wahl, H.; Wirth, C.; Wöll, J.; Husek, P. *J. Chromatogr.* **1992**, *626*, 289-293.

20. Oehlenschläger, J.; Hintze, U.; Gercken, G. *J. Chromatogr.* **1975**, *110*, 53-62.

21. Richardson, S.; Ternes, T. *Anal. Chem.* **2005**, *77*, 3807-3838.

22. Zwiener, C.; Richardson, S. *Trends Anal. Chem.* **2005**, *24*, 613-621.

23. Hernández, F.; Sancho, J.; Pozo, O. *Anal. Bioanal. Chem.* **2005**, *382*, 934-946.

24. Kuksis, A.; Myher, J. *J. Chromatogr. B.* **1995**, *671*, 35-70.

25. Harris, D. *Quantitative Chemical Analysis,* 6th ed. NY; W. H Freeman and Company, 2003. Pg 532-534.

26. Cech, N.; Enke, C. *Mass Spectrom. Rev.* **2001**, *20*, 362-387.

27. Tang, K.; Smith, R. *Int. J. Mass Spectrom.* **1999**, *185/186/187*, 97-105.

28. El-Aneed, A.; Cohen, A.; Banoub, J. *Appl. Spectrosc. Rev.* **2009**, *44*, 210-230.

29. Volmer, D.; Sleno, L. *Spectrosc.* **2005**, *20*, 20-26.

30. March, E.; Todd, J. *Quadrupole Ion Trap Mass Spectrometry*, 2nd Ed. NJ, John Wiley & Sons, Inc. 2005. Pg 1-3.

31. Werner, E.; Heilier, J.; Ducruix, C.; Ezan, E.; Junot, C. *J. Chromatogr. B* **2008**, *871*, 143-163.

32. Pérez, S.; Barceló, D. *Trends* **2007**, *26*, 494-314.

33. Soler, C.; Hamilton, B.; Furey, A.; James, K.; Mañes, J.; Picó, Y. *Rapid Commun. Mass Spectrom.* **2006**, *20*, 2151-2164.

34. Paul, G.; Winnik, W.; Hughes, N.; Schweingruber, H.; Heller, R.; Schoen, A. *Rapid Commun. Mass Spectrom.* **2003**, *17*, 561-568.

35. Petrovic, M.; Barceló, D. *Trends*, **2007**, *26*, 486-493.

36. O'Hair, R. *Chem. Comm.* **2006**, *14*, 1469-1481.

37. March, R. *J. Mass Spectrom.* **1997**, *32*, 351-369.

38. www.chm.bris.ac.uk/ms/theory/qit-massspec.html. Date accessed: March 28, 2009.

39. Badman, E.; Chrisman, P.; McLuckey, S. *Anal. Chem.* **2002**, *74*, 6237-6243.

40. Gonert, S. *Mass Spectrom, Rev.* **2005**, *24*, 100-120.

41. Nourse, B.; Hettich, R.; Buchanan, M. *J. Am. Soc. Mass Spectrom.* **1993**, *4*, 296-305.

42. Somogyi, Á.; Pasilis, S.; Pemberton, J. *Int. J. Mass Spectrom.* **2007**, *265*, 281-294.

43. Ferguson, P.; Pan, J.; Wilson, D.; Dempsey, B.; Lajoie, G.; Shilton, B.; Konermann, L. *Anal. Chem.* **2007**, *79*, 153-160.

44. Bowie, J. *Mass Spectrom. Rev.* **1990**, *9*, 349-379.

45. Bialecki, J.; Axe, F.; Attygalle, A. *J. Mass Spectrom.* **2008**, *44*, 252-259.

46. Bandu, M.; Watkins, K.; Bretthauer, M.; Moore, C.; Desaire, H. *Anal. Chem.* **2004**, *76*, 1746-1753.

47. Baker, M.; Gabryelski, W. *Int. J. Mass Spectrom.* **2007**, *262*, 128-135.

48. Tuytten, R.; Lemiere, F.; Van Dongen, W.; Esmans, E.; Witters, E.; Herrebout, W.; Van Der Veken, B.; Dudley, E.; Newton, R. *J. Am. Chem. Soc.* **2005**, *16*, 1291-1304.

49. Grujic, S.; Vasiljevic, T.; Lausevic, M.; Ast, T. *Rapid Commun. Mass Spectrom.* **2008**, *22*, 67-74.

50. Giancotti, V.; Medana, C.; Aigotti, R.; Pazzi, M.; Baiocchi, C. *J. Pharma. Biomed. Anal.* **2008**, *48*, 462-466.

51. Attygalle, A.; Kharbatia, N.; Bialecki, J.; Ruzicka, J.; Svatos, A.; Stuaber, E. *Rapid Commun. Mass Spectrom.* **2006**, *20*, 2265-2270.

52. Lyashchuk, S.; Skrypnik, Y. *React. Kinet. Catal. Lett.* **1994**, *52*, 453-459.

53. Kim, C.; Lee, K.; Chen, J.; Lee, H.; Lee, B.; Kim, C. *Bull. Korean. Chem. Soc.* **2008**, *29*, 1335-1343.

54. Nguyen, M.; Raspoet, G. *Can. J. Chem.* **1999**, *77*, 817-829.

55. Sultan, J. *Int. J. Mass Spectrom.* **2008**, *273*, 58-68.

56. Ferguson, P.; Pan, J.; Wilson, D.; Dempsey, B.; Lajoie, G.; Shilton, B.; Konermann, L. *Anal. Chem.* **2007**, *79*, 153-160.

57. Chipuk, J.; Brodbelt, J. *Int. J. Mass Spectrom.* **2007**, *267*, 98-108.

58. Wang, L; Pan, H.; Smith, D. *Mol. Cell. Proteomics* **2002**, *1*, 132-138.

59. Wu, Y.; Kaveti, S.; Engen, J. *Anal. Chem.* **2006**, *78*, 1719-1723.

60. Emmit, R.; Kazazic, S.; Marshall, A.; Chen, W.; Shi, S.; Bolaños, B.; Greig, M. *Anal. Chem.* **2006**, *78*, 7058-7060.

61. Domingo, L.; Andrés, J.; Moliner, V.; Safont, V. *J. Am. Chem. Soc.* **1997**, *199*, 6415-6422.

62. Domingo, L.; Picher, M.; Safont, V.; Andrés, J.; Chuchani, G. *J. Phys. Chem.* **1999**, *103*, 3935-3943.

63. Tomer, K.; Jensen, N.; Gross, M. *Anal. Chem.* **1986**, *58*, 2429-2433.

64. Moe, M.; Strøm, M.; Jensen, E.; Claeys, M. *Rapid Commun. Mass Spectrom.*, **2004**, *18*, 1731-1740.

65. Gross, M. *Int. J. Mass Spectrom.* **2000**, *200*, 611-624.

66. Ahmad, M.; Kass, S. *Aust. J. Chem.* **2003**, *56*, 453-458.

67. Raftery, M.; Bowie, J. **1987**, *79*, 267-286.

68. Chowdhury, S.; Harrison, A. *J. Am. Chem. Soc.* **1988**, *110*, 7345-7349.

69. Solomon, G.; Fryhle, C. *Organic Chemsitry.* 7th Ed. NY; John Wiley & Sons, Inc., 2002. Pg 572-590.

70. Moe, M. *Rapid Commun. Mass Spectrom.* **2005**, *19*, 859-862.

71. Moe, M.; Jensen, E. *Eur. J. Mass Spectrom.* **2004**, *10*, 47-55.

72. Qin, X. *J. Mass Spectrom.* **2003**, *38*, 677-685.

73. Kocijan, A.; Grahek, R.; Zupancic-Kralj, L. *Acta. Chim. Slov.* **2006**, *53*, 464-468.

74. Grossert, J.; Cook, M.; White, R. *Rapid Commun, Mass Specrtom.* **2006**, *20*, 1511-1516.

75. Stringer, M.;Underwood, D.; Bowie, J. *Org. Mass Spectrom.* **1992**, *27*, 270-276.

76. Zollinger, M.; Seibl, J. *Org. Mass Specrtom.* **1985**, *11*, 649-661.

77. Anbalagan, V.; Patel, J.; Niyakorn, G.; Stipdonk, M. *Rapid Commun. Mass Specrtom.* **2003**, *17*, 291-300.

78. www.e-laws.gov.on.ca/DBLaws/Regs/English/030169_e.htm. Date Accessed: March 28 2009.

79. www.epa.gov/safewater/regs.html. Date Accessed: March 27 2009.

80. www.epa.gov/safewater/ccl/ccl2.html. Date Accessed: March 27 2009.